January 2021

Predicting The Geometrical Disassembly Feasibility Of Mechanical Assemblies In Design Phase

Header Alrufaifi
Wayne State University

PREDICTING THE GEOMETRICAL DISASSEMBLY FEASIBILITY OF MECHANICAL ASSEMBLIES IN DESIGN PHASE

by

HEADER M. ALRUFAIFI

DISSERTATION

Submitted to the Graduate School

of Wayne State University,

Detroit, Michigan

in partial fulfillment of the requirements

for the degree of

DOCTOR OF PHILOSOPHY

2021

MAJOR: INDUSTRIAL ENGINEERING

Approved By:

_____

Advisor Date

_____

_____

_____

DEDICATION

To my parents and wonderful family

ACKNOWLEDGEMENTS

First, I would like to express my deepest gratitude to my dissertation advisor Dr. Jeremy Rickli for his guidance, ideas, and support and provide me with a chance to work as a graduate research assistant and as a graduate teacher assistance in the Industrial and Systems Engineering (ISE) department. I value his guidance, as well as his efficiency and responsiveness in reviewing my work. I would also like to extend my thanks and appreciation to Dr. Kyoung-yun Joseph Kim, Dr. Ana Djuric, and Dr. Murat Yildirim who have served as my dissertation committee members, for their valuable comments and constructive suggestions on this work. I would also like to thank the Higher Committee for Education Development (HCED) and the Government of Iraq for providing financial support throughout my study.

I would like to convey my appreciation to my friends Bubnish Kumar and Joao Prioli for their support in programming the collision test tool.

My journey in pursuit of this research program would not have been possible without the sacrifice and constant prayers from my family especially my mother, my wife, Rusul Almagsoosi, and our wonderful sons, Musa and Yahya. They are the driving factor in my life and work, and the road will be less exciting without them.

I ask Allah to bless us all, to whom I owe the wisdom, courage, and resolve to complete this study.

TABLE OF CONTENTS

LIST OF TABLES

LIST OF FIGURES

CHAPTER 1: INTRODUCTION

1.1 BACKGROUND AND MOTIVATION

Most manufacturing companies have historically appeared to be powered by revenue without taking due account of energy consumption, pollutant emissions, and material conservation [1]. Where a few decades ago, the products were designed mainly to answer the customer requirements and the possibilities of the manufacturers without considering the environmental aspects and those of recycling during the design process. However, with the implementation of new European and International standards and recommendations of environmental legislation (e.g. European Directive 2000/53/EC) [2], the problem of dismantling and products recycling is increasingly important. Therefore, considering the environmental aspects during the design process should be a viable aim in the modern manufacturing industry, and the advanced manufacturing industry must focus on environmental friendliness, sustainable energy, and reusing material usage. Thus, today's designers need new tools allowing them in the early stage of assembly's life (i.e. design phase) generating, evaluating, and verifying the feasibility of disassembling an assembly, determining disassembly sequence feasible in geometrical aspects , and predicting the change happens in the geometrical disassemble feasibility in the assembly's lifetime due to corrosion.

Preservation of the environment and the planet's resources is a significant concern. Awareness of the substantial environmental impact of production has led to research on using value recovery processes (i.e. remanufacturing, recycling, rebuilt, reuse, and maintenance) to retain the benefits of the End–of–Life (EOL) products and reduce waste. For example, remanufacturing can save energy, production cost and raw materials as well as providing high-value components quickly for production [3]. Remanufacturing as a value recovery process provides an economically and

environmentally sound way to achieve this by closing the material's use cycle and forming a closed-loop manufacturing system [4]. The essence of remanufacturing is to renew an End-Of-Life (EOL) product through appropriate recovery techniques instead of disposing of it through landfill or incineration [5]. Landfill and incineration can harm the environment, causing air pollution and soil contamination. Design for recycling, reusing and remanufacturing of an EOL product invariably starts with taking it apart to recover an assembly's components. Also, the practice of all these operations faces the same issue, i.e., product disassembly [6]. However, the disassembly process represents the first step in many value recovery processes [7]; therefore, primarily, the importance of disassembling research comes from that point. Also, only after disassembly, the product in the EOL stage of its life can be reutilized or remanufactured [8].

The world's environment's sustainability is under risk. This is mainly due to a dramatic increase in the world's population (calculated at 6 billion in 2008 and expected to rise to 12 billion by 2050) combined with rapid economic growth and change and life-style aspirations for much of the world's population. This is based on the use of manufactured consumer products and their availability [9]. Unfortunately, economic enabling for a growing number of nations around the world would result in totally unacceptable overuse of natural resources and even higher contamination of the atmosphere unless steps are taken to at least curb or reverse this trend [10].

Motor vehicles, electronics, screens, mobile phones, and flat-panel TVs some kind of products that seem to provide minimal life spans and are most frequently disposed of to landfill while they still have at least some degree of usability from many of their parts and materials. Waste like this is entirely unsustainable, especially in the context of rapidly developing nations and growing populations. In fact, the Earth does not provide enough space and power to handle waste, nor does it have secure landfill

sites to sustain such activities. Also, the problem is exacerbated by the use of extremely toxic materials in many of these products to the environment and presents a significant threat to future generations as the use of industrially manufactured products is growing. Therefore, it is becoming imperative that through modern manufacturing practices existing manufactured products and their parts should be reused or recycled.

Manufacturers operating in a highly competitive business environment feel they need to cut costs, and by doing so, conventional wisdom has led them to think they have to design products that provide very limited life spans with little or no opportunity for reuse and recycling of any of their parts and materials. Much of this belief stems from some very poor philosophies of product design which do not allow the disassembly of products and thus encourage the recovery of valuable materials and components.

1.1.1 The Importance of Disassembly

Used items are isolated for reuse to obtain the desired parts and subassemblies. This process is known as Disassembly, and it is characterized as a systematic method of separating a product or other subassemblies into its constituent parts. Both Wiendahl et al. [11] and Mok [12] affirm the importance of disassembly as an aid to environmental protection in the reuse of materials and pieces. Salomonski, & Zussman, [13] and Gupta & Gungor [14] have shown that disassembly is an economically important method in remanufacturing because it reduces the cost of goods by selectively removing the necessary parts and recycling materials. Disassembly [what of disassembly minimizes the costs of disassembly] has also proven to be the best way to minimize the costs of disassembly operations and reap the value of the reused components.

Disassembly is a crucial issue in mechanical, industrial, and manufacturing engineering as the disassembly process represents the first step in many value recovery

processes (e.g., reuse, remanufacturing, and maintenance processes) [15]. Due to the economic and environmental benefits it brings, the importance of disassembly has grown over the years. The disassembly process is primarily aimed at the recovery of valuable materials and components from the end of life (EOL) and disposed of goods that otherwise go to sites and pollute the water bodies and the atmosphere. It also helps to save the world's resources and lowers the need for fresh materials [16, 17].

Regulations such as the European and International standards and recommendations of environmental legislation (e.g., European Directive 2000/53/EC) [2] are regulated to heal ecological concerns that arise from the limited space remaining for landfill sites and the potential pollution of the environment as a result of disposing of waste in these areas. Therefore, these regulations oblige manufacturers to comply with environmental laws on the treatment of waste material before they have been dumped by anticipating the need to implement processes for disassembling their products [18].

Also, the disassembly method is crucial to remanufacture, which is essential for materials and separation of components. Remanufacturing is the most effective and efficient way to save energy and material resources because the goal is to maximize reuse and reduce waste disposal [19]. The importance of disassembly at this vital recovery process (i.e., the remanufacturing process) is that the disassembly is regarded as a crucial mechanism in the economic rehabilitation of goods by factoring in a potential selective separation between the desired components and materials [15, 20].

Using disassembly technologies will significantly benefit the manufacturing industry as well as the climate. This mutual benefit was reflected in a growing amount of disassembly technology research that has been carried out in universities, other institutions, and businesses since the late 1980s. This interest illustrated by Ilgin and

Gupta [21] is a critical review of Environmentally Conscious Manufacturing and Product Recovery (ECMPR) research development. This survey included 540 published references classified into four fields, namely, remanufacturing and disassembly of environmentally conscious product design, reverse and closed-loop supply chains.

Zhou et al. [1] did an essential survey on disassembly sequence planning methods. They have analyzed and summarized the characteristics of the different DSP methods from the viewpoint of disassembly mode, modeling, and planning methods, as well as the future trend of the DSP to identify gaps in existing research. Their survey addressed 159 published references that have published since 2000.

With Shape Memory Materials (SMMs) with carbon nanotubes, Carrell, Zhang, and Li [22] reviewed current end-of-life options for electronics and future automatic disassembly options. Yang et al. [23] also presented a review on disassembly technology research and development, disassembly planning and equipment for PCB printed circuit boards Four different disassembly methods were used for various purposes, namely selective disassembly, simultaneous disassembly for material recycling, simultaneous disassembly, partial disassembly, reuse.

1.1.2 Classifications of Disassembling

Destructive Disassembly (DD) is the process where the geometry of one or more parts in an assembly modified during the disassembly process due to the cutting operations [24]. During the destructive disassembly, a part of an assembly or a component of a product destructed through the disassembly process to disassemble a selected element (component) and get it in an intact form. Destructive disassembly (DD) is usually employed when Non-Destructive disassembly (NDD) is not possible, or when only the raw materials of the components need to be recycled.[30]

Basically, the parts that have low value for remanufacturing or refurbishing (rebuilding) processer are destroyed to disassemble a product partially or completely. Bolts, screws, rivets are typically the first nominated for destructing in a disassembly process (complete, or partial). Pak and Sodhi [25] addressed the destructive process for joining elements. They have developed equations describing the waves of stress arising from the impact of a one-dimensional bar attached to an elastic medium. As a cost-effective method for destructive disassembly of joining components, the mechanical effect has been suggested. By studying the characteristics of elastic waves caused by the impact, their research analyzes the process of disassembly of impact. Elastic waves are modeled in a one-dimensional bar that transfers the energy of the impact to a protruding bolt head mounted in an infinite elastic medium or structure. Stress wave equations are presented between the two ends of the bar for each period when they bounce back and forth. The maximum stress is determined when the wave front is reflected in the second or later period. They approved that the higher stress could be applied to shear off the bolt head with the same amount of energy invested as in the impact of a single wave. The results can be used to design effective destructive disassembly procedures and new remanufacturing tools, resulting in increased efficiency in disassembly and reduced recycling costs.

The destructive disassembly is more common to use for recycling materials. It is surprising from an economic point of view for many that destructive disassembly is economically preferred to non-destructive disassembly. This is because destructive disassembly is much more economical than its non-destructive equivalent, where it is needed to devote man-hours to separating and sorting sub-assemblies [26] .

Non-destructive disassembly is a process that breaks down assemblies into sub-assemblies and subsequently into intact parts [26]. The Non-destructive disassembly

also can be categorized into two types: Complete Non-destructive disassembly, and Incomplete Non-destructive disassembly (partially or selectively) .

Zhong et al. [27] build their study on determining a complete non-destructive disassembly sequence. They used a graph (a part-fastener graph) to identify the components of the assembly into two groups of functional components and fasteners; developed an interference matrix to evaluate the removable component. They used an algorithm called Dijkstra's algorithm as a base to propose a complete non-destructive disassembly sequence planning of functional components. The interference matrix is developed to determine the removable component, and a disassembly sequence planning of functional components is proposed based on Dijkstra's algorithm; the disassembly sequence planning including fasteners is presented based on particle swarm optimization. They tested their methodology by using a regional jet's nose landing gear system as an object of analysis .

To determine the optimal disassembly series, Mircheski et al. [28] provided a mathematical model of the non-destructive disassembly method. Their method for disassembly sequence preparation has been developed based on a component-fastener relation graph and AND / OR logic operations. Assessment of the disassembly sequence and achieving optimum disassembly sequence is a feature of the expense and revenue of disassembly. An example is analyzed to present the applicability of the methodology in the early stages of product development to determine the optimum disassembly sequence. In the programming software, Visual Basic for Application (VBA), which runs directly on virtual 3D assembly models in a CAD system platform, the methodology developed in their research is implemented.

Rickli and Camelio [29] addressed determining the optimal or near optimal partial disassembly sequence without destruct any component of an assembly. A mathematical

method is used to test sequences of disassembly based on profit standard deviation and probability of profit as well as the estimated profit commonly used. They tested their approach on an example case study to investigate the impact of uncertain quality on the optimal or near-optimal sequence of disassembly, expected profit, deviation of profit standard and probability of profit .

Complete disassembly is a sequence of tasks that start with a fully assembled assembly and end up with all parts disconnected. Yeh et al. [30], Xia et al. [31], Alshibli M. et al. [32], Kheder et al. [33] have addressed this type of disassembly in their work. Yeh [30] proposed a solution procedure for the End of life EOL to get complete disassembly sequence plan to disassemble a mechanical product with divining the disassembly direction at the six principle directions. He tried to find the optimal disassembly sequence by utilizing a modified Simplified Swarm Optimization. My work for my second objective at this proposal is original and there are significant differences between the methodology proposed by me and the method by Yeh [30] published in their papers in 2011, and 2012. Yeh [30] used a modified simplified swarm optimization in their procedure to find optimal disassembly sequence based on predefined disassembly precedence requirements as shown in Figure 1. While in my work, my proposed methodology starts with checking the mating relationships between components after each decision of removing a component, where disassemble one component of a product affects the type of relations between the rest of the other parts. More details on my proposed method for answering the second objective at this proposal available at the proposed methodology section.

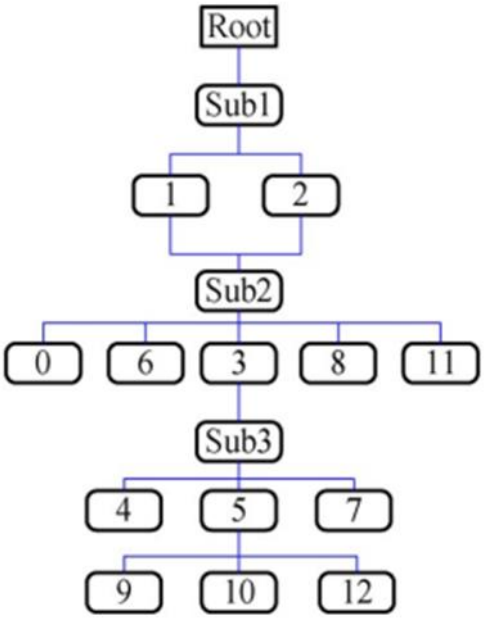

Figure 1.1: Structure of EOL product used at Yeh. [30]

Xia et al. [31] proposed using a cloud-based approach for determining the disassembly planning of Electrical and Electronic Equipment. Their method proposed that when the disassembler wants to determine the disassembly sequence for a product, he requests the information services to get information support. When the required services are found, the relevant information providers will provide the services. After that, the disassembler will need to request the disassembly modeling, evaluation and optimization services to help to make optimized or near optimized disassemble planning. The relevant services will be recalled when they are found. Alshibli et al. [32] improved a genetic algorithm model that proposed by ElSayed et al. [34] by employing Tabu search (i.e. metaheuristic algorithm) to find the optimal solution in terms of minimizing the travel distance in case of using robotic arm to disassemble a product, minimizing the number of changes required for disassembly methods, and minimizing of the number of robotic arm travels. Alshibli's proposed algorithm aimed to decrease the uncertainty in the disassembly process by using a sensory system and an online real-time Tabu Search module to minimize the traveling distance of a robotic arm, the

robotic arm travels, and the number of disassembly method changes. Their Tabu Search algorithm uses the information coming from the sensory system to determine the optimal disassembly sequence for present disassembly level. Where the sensory system captures product images after every removal, providing the Tabu Search algorithm with accurate online real-time data. This loop continues until all the components demanded for recycling and reuse are removed .

Kheder et al. [33] used a genetic algorithm as a base for their proposed optimizing disassembly method for preventive maintenance. They considered many norms like the change in disassembly directions and part volume tools changes to identify the feasible disassembly sequence. The principle six Cartesian directions are specified in determining the disassembly directions. They have considered the changes in disassembly directions and disassembly tools, maintenance index and component size, a genetic algorithm with the other preservative crossover was proposed to find the optimum feasible rear axle disassembly sequence. However, their method requires forming an initial population which is a feasible disassembly sequence for using the Genetic Algorithm manually. They have used SOLIDWORKS API (Application Programming Interface) to determine the direction that the disassembly operation must be performed. It is not obvious how they check the disassemble feasibility at least in geometrical feasibility terms other than using SOLIDWORKS API to determine the feasible disassembly directions. New determination of the mating relationships between components are required after removing one part of an assembly because when removing a component from a product this will change the feasible disassembly direction for the rest of the other parts. Hui et al. [35] addressed determining feasible optimal disassembly sequence problem. They have compiled using the Genetic Algorithm with disassembly feasibility information graph (DFIG) to construct feasible

optimal disassembly sequence. The genetic algorithm has been used as a guidance to construct the DFIG. By using disassembly planning tool based on CAD platform, they disassemble feasibility for the tested assembly's parts. However, they haven't explained the mechanism that they followed to check the disassemble feasibility for the components of the assembly where they have used a tool in the CAD platform to check the disassemble feasibility .

Complete disassembly is typically costly due to performing the disassembly process manually. Smith et al. [36] have researched the development of a new partial disassembly sequence planning process, contrary to a full disassembly. They reported that most previous partial disassembly sequence planning methods did not use life cycle effect analysis techniques to conduct cost-benefit analyses to find an optimal disassembly stop point. Eco-indicator 99 is used in their research to examine the partial disassembly process impacts on the environment. Their proposed method takes into account partial order, partial disassembly direction, number of reorientations and number of tool changes to find an optimized disassembly plan and an optimized disassembly stop point. The results of the study show that, compared to traditional disassembly methods, the proposed partial disassembly sequence planning method can be used to reduce environmental costs and increase economic benefits. Their study results also show that the method can help designers to redesign the products, make the high economic (recycling) benefits components more accessible, and reduce the cost of disassembly.

Partial disassembly is the optimum order of disassembly operations to an ideal disassembly rate which decreases returns if exceeded [29]. The partial disassembly does not require the complete breakdown of the product; however, the process of partial disassembly sequence ends when the disassembly process be uneconomic. Rickli and

Camelio [29, 37] in both of their papers addressed partial disassembly sequence. Rickli [37] used a Genetic Algorithm heuristic to determine the optimal partial disassembly sequence based on many factors. The costs of disassembly operation and the recovery processing, revenue, and environmental impacts are all factors the researchers used in method to optimize the partial disassembly sequence. The main goal in their proposed method is determining the set of disassembly arcs (disassembly operations) that minimizing the environmental impact and maximize the profitability from the partial disassembling of an EOL product. Also, Rickli and Camelio [29] considered the impact of the uncertainty in the quality of EOL product in determining the partial disassembly sequence. They used directed flow disassembly network as a base to find optimal or near optimal partial disassembly sequence. Many factors (i.e. sequence feasibility, expected profit per EOL product, profit standard deviation per EOL product and profit probability per EOL product) have been used as a base in their approach to converge to the optimal or near optimal partial disassembly sequence .

Smith et al. [36] proposed a partial disassembly sequence planning method to find an optimized disassembly plan by considering part order, part disassembly direction, number of reorientations, and numbers of tool changes to find a disassembly plan and an optimized disassembly stop. The results of the study showed that the new method of partial sequence dismantling could be used to decrease environmental costs and to improve economic benefits in contrast with conventional dismantling methods .

Yu-fei and Qiang [38] have proposed a multi-objective intelligent optimization algorithm for determining a feasible partial disassembly sequence. In their work, they considered the change in the direction of disassembly, the amount of disassembly pieces, and the disassembly's as optimization targets and then creates a multi-target optimization template for disassembly planning. Based on the solution of the multi-

target Pareto set and combined with the Ant Colony Algorithm, Yu-fei and Qiang [38] proposes an optimization algorithm for a multi-target ant colony to carry out partial disassembly sequence preparation based on Pareto set .

Selective disassembly is an optimal order of operations disassembling a particular component without taking into account the remaining parts [29]. Some of the works that have been done on selective disassembly like Luo et al. [39] introduced a method for integration of the multi-layer product representation and the optimal search in product selective disassembly planning. The multilayer representation is based on the product structure formed in product design. The method enables an efficient search for the disassembly sequence. They integrated a dynamic product data model with ant colony algorithm to find the near optimal disassembly sequence solution for a required selective disassembly .

Guo et al. [40] have addressed the resource constraints (e.g. disassembly operator and tools) to model and optimize disassembly sequence for selective disassembly operations to maximize profit. They used one scatter search algorithm with precedence preserved crossover combination operator (SS_PPX) and another scatter search algorithm with path-relink combination operator (SS_PR) to solve their proposed model. They have concluded that one of their proposed methods (SS_PPX) is better than their second proposed method (SS_PR) in computational efficiency .

Jin et al. [41] developed a systematic selective disassembly approach for handling Waste Electrical and Electronic Equipment with a maximum disassembly profit in accordance to the Waste Electrical and Electronic Equipment (WEEE) and Restriction of Hazardous Substances Directives. First, a space interference matrix at three-dimensional computer-aided design model is created based on the interference connection between individual components. A matrix analysis algorithm is then

implemented in a three-dimensional environment to obtain all the feasible disassembly sequences via the obtained space interference matrix. Secondly, an assessment and decision-making process is developed to evaluate an optimal selective disassembly sequence from the feasible disassembly sequences obtained. The assessment takes into account the disassembly benefit and the requirements of the Directives on Waste Electrical and Electronic Equipment and Restriction of Hazardous Substances, which govern recycling rates for different types of products and removal criteria for (1) hazardous, (2) heavy and (3) high-value items.

Song et al. [42] proposed a disassembly sequence planning (DSP) method to reduce additional efforts of removing extra parts in selectable disassembly. Their methodology has three parts, which includes a disassembly hybrid graphic model to describe the product disassembly information, an object inverse-directed method to optimize the disassembly design and a model reconstruction method to achieve a better DSP. According to the disassembly cost criteria and the parameters of disassembly tools, they found that the disassembly efficiency increases, and the disassembly cost decreases due to the use of partial destructive mode compared with non-destructive mode. They found that proposed partial destructive DSP is more efficient and economical. Wang et al. [43] addressed destructive operations to improve the efficiency of disassembly operations and recycling of a product. Their method considered destructive operations to determine the disassembly sequence for selective disassembly .

Sequential disassembly is a disassembly process that removes one component from its assembly by one disassembly operation. Sequential disassembly has two main categories, Complete Sequential Disassembly (CSD), or Incomplete Sequential Disassembly (ISD) (e.g. selective sequential disassembly, partial sequential

disassembly). In complete sequential disassembly, it is believed that one component will be disassembled at a time in full serial disassembly until the item is completely dismantled [43]. The main methods that have been used for Complete Sequential Disassembly (CSD) are AND/OR method, Petri-Net method [44], heuristic algorithm [45], hierarchical approach [46].

Moore et al. [44] proposed a Petri net (PN)-based method for the automatic generation of material recycling or recycling disassembly process plans (DPPs). They defined an algorithm for generating a disassembly precedence matrix (DPM) based on geometric disassembly from a product's CAD drawing. Then, they have defined an algorithm to produce a disassembly of Petri Net (DPN) automatically from the DPM. The resulting DPN can be analyzed using the method of reachability tree to produce feasible DPPs, and cost functions can be used to determine the optimum DPP because the generation of tree accessibility is NP-complete. To classify optimal or near-optimal DPPs, they developed a heuristic to explore the tree's most likely lowest cost branches dynamically. The cost function includes tool changes, movement direction changes, and individual (e.g., hazardous) part characteristics. Products containing complex AND/OR disassembly precedence relationships are compatible or can use their proposed method to determine to determine a complete disassembly sequence for an assembly .

Andres et al. [45] used a heuristic algorithm to determine a complete disassembly sequence for an assembly. They have proposed a two-phase approach when the disassembly system has a cellular configuration to determine the optimal disassembly sequence. Their proposed method starts with grouping operations into cells depending on the equipment they require in order to reduce the cost of acquiring machines. The aim is to band operations using similar equipment together in order to achieve good

levels of utilization of such equipment. It may be necessary to enforce full cell volume. Once the cells have been formed and the operations allocated to them, a metaheuristic algorithm (GRASP) is used to look for the sequence of disassembly for each component leading to the minimum number of intercellular movements. They have assumed that with a certain probability each disassembly function would be necessary. They impose that assumption to account for uncertainty about the condition in which the product may arrive irrespective of the other tasks. AND / OR precedence relationships are also listed in the disassembly activities. Their suggested solution is illustrated with a disassembly problem that is randomly generated .

Dong et al. [46] addressed a hierarchical approach to determine a complete disassembly sequence for an assembly. In their research, they proposed a novel approach to the automatic disassembly sequence generation from the hierarchically allocated liaison graph (HALG) representation of an assembly by recurrently decomposing the assembly into subassemblies. They have used engineering knowledge, design and demanufacturing domains, to build the HALG to increase the efficiency of their planning method. By eliminating the hidden surfaces to reduce the computational complexity of disassembly preparation, the boundary representation (B-Rep) models were simplified in their proposed method. The subassembly selection indices defined in terms of mobility, stability, and parallelism were proposed for each layer of HALG to evaluate the tentative subassemblies extracted and to select the preferred subassemblies. A number of assemblies, including some difficult items, are checked and the resulting findings are provided to check the reliability and efficacy of the method .

Typically, incomplete sequential disassembly sequence is accomplished by choosing an appropriate target element disassembly sequence from all available

disassembly sequences. However, AND/OR method, Petri net methods, also have used for determining an Incomplete Sequential Disassembly sequence planning. For example, Rai et al. [47] suggested a technique for a collection of selective disassembly sequences that are optimal or near-optimal. Their method includes actions to reach the maximum net income at the required disassembly depth while meeting economic constraints. A combination of Petri net modeling has been developed with heuristic search procedures. This combination provides an effective dismantling sequence generation process. The heuristic produces and searches for a partial accessibility graph to achieve an optimal or near-optimal disassembly sequence based on the Petri net model's firing sequence of transitions. The approach suggested reduces the search space in two areas: (1) pruning the tree of disassembly (DT) and (2) selective tracking of the map of accessibility. They have used two examples from the literature to show the effectiveness of the proposed methodology .

Chung et al. [48] presented an integrated approach to planning the sequence of selective disassembly. Their integrated approach developed in their selective disassembly sequence planning research is carried out on two matrices, precedence matrix (SD) subassembly division and route matrix (PD) subassembly division. As constructed by a matrix operation with a fastener-part connectivity matrix (FP) and fastener accessibility matrix (FA), the SD matrix represents the preceding division relationship between subassemblies in an assembly. The PD matrix built with part accessibility matrix (PA) provides the optimum disassembly chain (DC) for one part of the subassemblies (Ps sets) that involved in the removal of pieces selected for separation or replacement. They used two examples in their paper to demonstrate their approach's effectiveness and practicality for the selective disassembly process. Through the two examples presented, they claimed that the implemented approach could effectively

generate a feasible and near-optimal sequence plan for selective disassembly, ensuring both batch disassembly of components and accessibility of the tool to fasteners.

Parallel disassembly is a disassembly process that removes more than one component from its assembly at the same disassembly operation. Parallel disassembly has two main categories, Complete Parallel Disassembly (CPD), and Incomplete Parallel Disassembly (IPD) (e.g. Selective Parallel Disassembly, Partial Parallel Disassembly). In Complete Parallel Disassembly, it is presumed that more than one component will be disassembled at a time until the component is fully disassembled [49].

Parallel disassembly differentiates from sequential disassembly that the parallel disassembly employs more than one manipulator to perform disassembly tasks as well as multiple components disassembled at the same time [50]. However, parallel disassembly can be divided into two categories: asynchronous parallel disassembly (aPD) [50, 51, 52] and synchronous parallel disassembly (sPD) [53] .

Ren et al. [50] proposed asynchronous parallel disassembly planning (aPDP) in their work, eliminating the requirement for synchronization. Besides the constraints of precedence, they have appointed that the asynchronous parallel disassembly planning (aPDP) becomes highly operation time dependent. They have, however, designed an efficient disassembly encoding and decoding strategy. In their paper, a genetic algorithm has been used as a base for a metaheuristic approach to solve the asynchronous parallel disassembly planning (aPDP) problem. Their proposed algorithm applies to four products that require different complexity disassembly processes, and the results are compared with two literature-reported methods. They have suggested that when solving large-scale problems, the proposed approach can identify faster disassembly processes. Smith and Hung [56] have also addressed an

asynchronous parallel disassembly planning (aPDP) problem. The objective of their study is to create a novel method for green design for selective parallel disassembly planning. The method uses modular design theory to group components into modules, uses recursive rules to remove selected modules, thereby removing parts in parallel, thus reducing the number of movements and reorientations needed to remove components. In addition, they have shown that it is possible to use selective parallel disassembly to extract interlocked or occluded sections. As a consequence, many types of designs can use the process. Results of the study show that the system can be used to minimize disassembly measures, disassembly time and energy consumption, thereby increasing environmental impacts and improving the quality of the environment.

Parallel disassembly sequence planning (PDSP) can reduce costs and mitigate impacts on the environment [54]. Parallel methods of disassembly preparation will group parts into modules, and simultaneously remove grouped pieces. Consequently, they minimize motions and reorientations, reduce disassembly time, use of resources, and impacts on the environment, and can also eliminate occluded or interlocked pieces. However, the DPSP problem is not easily solved in a general form due to the PDSP of the complex products being restricted by various factors. Zhang et al. [52] have addressed that problem. In their paper, they introduced a PDSP approach based on fuzzy-rough sets to reduce time complexity. Five disassembly factors are specified and formulated, including assembly limit factor, disassembly precedence factor, the disassembly time factor, disassembly tool factor, and combination type factor. Considering the characteristics of PDSP, the parallel disassembly fuzzy-rough set mapping model is constructed. The components to be disassembled are taken as the universe of information and disassembly membership functions as the function of opposition is known as the relationship of indiscernibility. Instead, to produce the

optimal parallel disassembly sequence, the fuzzy-rough array mapping method of parallel disassembly is adopted .

Also, Pistolesi and Lazzerini [53] have addressed the synchronous parallel disassembly (sPD) problem for refurbished smartphone process as a disassembly is the first step in the refurbished process. Their paper provides a novel formulation of the question of simultaneous disassembly, optimizing the degree of parallelism, the rate of ergonomics, and how the workload of workers is managed while reducing the time of disassembly and the number of times the item has to be rotated. The problem is solved by using the Tensorial Memetic Algorithm (TeMA), a novel two-stage multi-objective (MaO) algorithm encoding parallel disassembly plans using tensors of the third order. TeMA first divides the goals into primary and secondary based on the priorities of a decision-maker and then seeks Pareto-optimal compromises (seeds) of the primary goals. TeMA conducts a fine-grained local search in the second stage, which explores the objective space regions around the seeds to improve the secondary goals. Two real-world renovation processes involving a smartphone and a washing machine have been reviewed for TeMA. The experiments showed that TeMA is statistically more accurate on average in the area of preference of the decision-maker than various efficient MaO algorithms.

1.1.3 Motivation and Significance

Consumer and industrial material end-of-life (EOL) treatment is a significant challenge, as well as an opportunity that communities around the globe face every day. The problem is to find the best way to dispose of a wide range of products properly, and the incentive is the potential benefits from responsible and sustainable reuse, recycling, and disposal, both economically and environmentally.

The importance of the proposed research can be summarized in three points:

First, it gives to the assembly's designers a prediction to know the change in the disassemble feasibility that will happen to their assembly in its lifetime after a specific amount of wear in some of the assembly's parts.

Second, all geometric feasible disassemble sequences of the assembly will be known while the assembly is still in design phase.

Third, this work can be used to minimize the research area for optimization methods (e.g. Genetic Algorithm, Practical Swarm Optimization method, Ant Colony optimization method) to give the optimal feasible disassembly sequence in less computing time. The Precedence Matrix at this work contains on just geometrical feasible disassemble steps because represents the summary of outcome for all collision tests done between the assembly parts.

1.1.4 Research Problems

1. No definitive method to automatically determine contact and non-contact disassembly interactions.
2. Precedence matrix currently must be generated by hand, limited ability to experiment or simulate disassembly at early design phases.
3. Typical disassembly analyses and research is static, meaning they evaluate one specific assembly or one design. Or optimize for modules based on recovery value but they do not incorporate wear mechanisms that may change disassembly sequence over the use phase.

1.1.5 Statement of Research Problem

Using geometrical data extracted from CAD design assembly files can be used to build an optimal or near optimal disassembly sequence automatically.

Hula et. Al [55] and Giudice and Fargione [56] are pointed out to the criticality of sequence feasibility aspect as an important issue to evaluate each step of disassembly

sequence to find out the possible sequence to disassemble a product. Lambert [57] referred to sequence feasibility as a critical issue for reducing the search area of getting the possible disassembly sequence. However, predicting the change in the geometrical disassemble feasibility due to corrosion that will happen during the lifetime of assembly in the early stage of assembly's life (i.e. design phase) has not studied before.

Considering the investigations presented in the introduction and studied in more detail in literature review section. I have found that there are several issues that are not covered by researchers. Some of these issues are listed below as research problems.

1. How to use component interaction data from CAD design models to automatically extract critical disassembly information.
2. Can we construct a precedence matrix from proven tests of contact, non-contact constraints?
3. Can we predict changes in the geometrical disassemble feasibility of an assembly during its lifetime in early design phase?

1.1.4 Contributions of the Research

1. The research methodology gives to the assembly's designers a method to predict the change in the disassemble feasibility that will happen to their assembly in its lifetime after a specific amount of wear in some of the assembly's parts after periods of active working life of the assembly. The designer can decide how much erosion, in other word, how much change in the assembly's parts after a periods of use life of the assembly depending on previous or similar products produced and used before the current design.
2. All geometric feasible disassemble sequences of the assembly will be known while the assembly is still in design phase. Hence, this will help in advance the automation of disassembly process.

1.1.5 Potential Impacts of the Research

1. Zhou et. al. [1] pointed out to "The actual disassembly process is full of uncertainties and randomness", however, at this work, checking the disassemble feasibility based on the actual geometric of the assembly's parts as a criterion to determine the feasible disassembly sequences will minimize the uncertainties and randomness for the actual disassembly process.
2. This work can be used to minimize the research area for optimization methods (e.g., Genetic Algorithm, Practical Swarm Optimization method, Ant Colony optimization method) to give the optimal feasible disassembly sequence in less computing time. The Precedence Matrix at this work contains on just geometrical feasible disassemble steps because represents the summary of outcome for all collision tests done between the assembly parts.

1.2 LITERATURE REVIEW

This review covers the relevant literature around the research of the subjects that are most related to the current work: 1) Methods of disassembly sequence planning such as graph methods, Matrix methods, and Geometric methods, 2) contact and non-contact constraint generation ,3) Inferring the geometric disassemble feasibility from collision test , 4) Disassembly Network to track disassemble feasibility

1.2.1 Methods of Disassembly Sequence Planning

Disassembly sequence planning tries to determine all feasible disassembly sequence, and therefore finding the optimal disassembly sequence [58]. Several new methods have been created in recent years to produce disassembly sequences and to decide the optimal one. Moore, Gungor & Gupta [44] referred to the criticality of this research area in the disassembly analysis by pointing out: "Disassembly process planning is critical in minimizing the amount of resources (e.g. time and money)

invested in disassembly and maximizing the level of automation of the disassembly process and the quality of the parts recovered".

The methods of disassembly process planning, and disassembly sequence generation can be classified as shown below:

1.2.1.1 Graph Methods

Graphs are a useful representation tool. Graphs can be viewed as an abstraction from fact, as shown by a number of researchers, there are several types of graphs that can be used to solve disassembly problems. At this section I mentioned the most related to the current work, the Disassembly network directed the flow. The Disassembly network directed the flow is a graph-based method begins at one node and finishes at a different node. Unlike a network disassembly graph, a directed flow disassembly network [32] begins from one node representing the assembled product. It stops at another node representing the full disassembly of all parts [35], as shown in figure 1.3. Liu et al. [59] have included a feasibility chart with directed disassembly network. The feasibility chart does not only define the restriction and adjacency relationships between various parts or sub-assemblies but also contains other disassembly details (disassembly method, time, etc.).

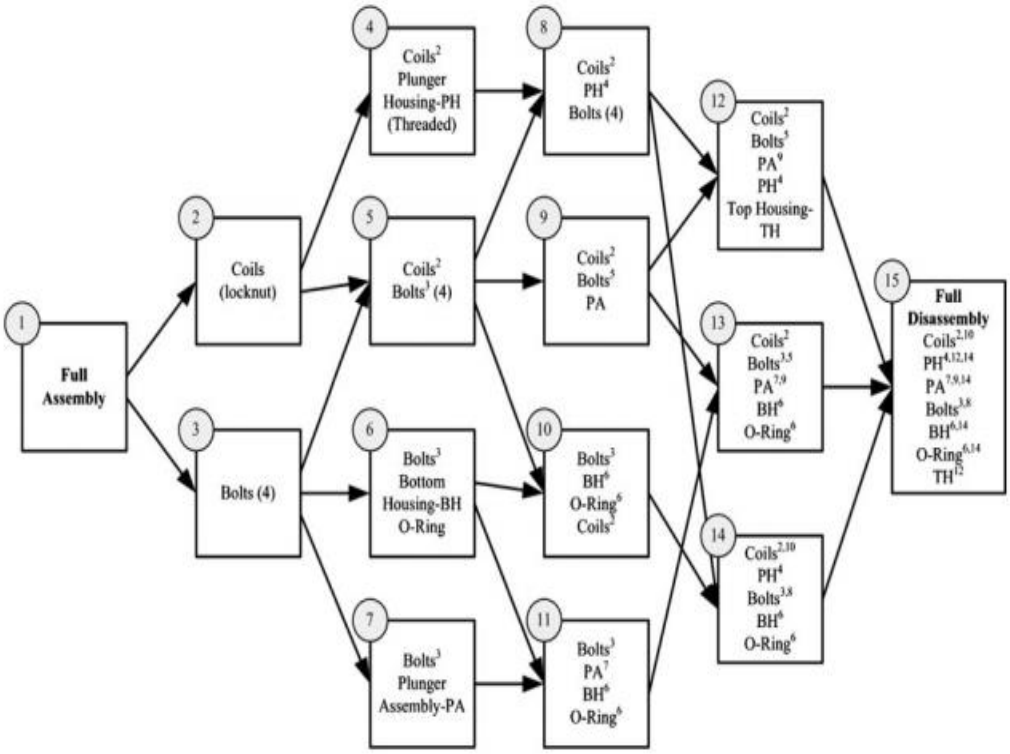

Figure 1.2: Directed disassembly of a solenoid valve [29].

1.2.1.2 Matrix Methods

Matrix-based approaches use multiple matrices to explain the disassembly precedence relationships between different components. The most common matrix-based method is the disassembly interference matrix method.

Chunming [60] described a simple way to build a matrix of disassembly interference. The main feature of Chunming [60] method is the disassembly interference matrix consists of ones and zeros only. However, the component r_{ij}[1] in the disassembly interference matrix equals to 1 if the component V_i has priority to disassemble before component V_j, otherwise, the r_{ij} equals to zero. Liu et al. [10] used interference matrix to show the disassemble feasibility of each component of a mechanical assembly. They referred to an important factor in the actual disassembly process (i.e., disassembly direction) where they built their disassembly interference

[1] The r_{ij} at the interference matrix represents the disassemble priority between component V_i and component V_j.

matrices. They did disassembly interference matrices based on the CAD product model, and they created disassembly interference matrices along with six directions (+ X, -X, + Y, -Y, + Z, -Z) according to the spatial interferences between different parts; however it is not clear if they did find disassembly interference metrices automatically or manually. The element d*ij*[2] indicates in the space interference matrix whether component *J* prevents the movement of component *I* along sd (sd = +X, -X, +Y, -Y, +Z, -Z) direction. If component *j* impedes the movement of component *I* along sd direction, d*ij* is 1; otherwise, d*ij* is 0. The feasible disassembly sequence can be produced after the disassembly interference matrices of all directions are obtained. However, components' disassembly directions of are not always at the six Cartesian directions (i.e., +X, -X, +Y, -Y, +Z, -Z) but could be the required disassembly directions are not orthogonal. The Gaussian sphere theory is used by [2, 61] to decide the disassembly direction of the parts of a product at the six Cartesian directions or at other directions. The extended interference matrix is another method proposed by [62] handle determination of non-orthogonal disassembly directions. A global coordinate system and a local coordinate system are simultaneously used with the extended interference matrix method to increase the diversity of disassembly directions. The global coordinate system described interference relationships between components viewed from a standard reference framework, while the local coordinating system described interference with disassembly from a component perspective. The extended method of interference matrix was established by translating and rotating relationships between the global coordinate system and the local coordinate system.

[2] The d_{ij} at the interference matrix represents the disassemble priority between component I and component J.

As with the techniques used in publications [63, 64, 65] various classification methods regarded the relations and components separately. Smith introduced a method of disassembling sequence-structure to represent spatial relations between components and connections [66, 67]. This approach concurrently built the disassembled element and interaction matrices (two matrices) and the disassembly motion matrices (2 matrices) for components and connections. The disassembly matrices were used to record the disassembly position of the individual parts and the disassembly motion matrices, to record contact parts that limit the disassembly of the target parts in certain directions. Compared to other matrix-based methods, this method helps reduce model complexity. In addition to the four-matrix method, [66, 67] the projection matrix for the components was used to record the number of blocking components for each component, which is the five-matrix disassembly sequence-structure method. This approach reduces the time to look for feasible sequence solutions compared with the four-matrix disassembly order-structure process. An apparent disadvantage of these methods is that the matrices should be manually generated, which can be a difficult task and time consuming due to the usual design complexity of assembly parts and the high number of parts that an assembly consists of them.

The disassembly interference matrix approach must document each part's relationship, even if there is no precedent between them, which naturally leads to information redundancy. The multi-layer representation approach was introduced to minimize processing time and file size [39, 68]. The Bill-of-Materials (BoM) represented by a list of elements from the material to basic components was used to produce the product's physical structure composed of different layers and nodes. A matrix was used for each subassembly of each layer to define the constraints between

various subassembly components. This method requires a smaller space to store the material template relative to the disassembly interference matrix. [39].

There are also matrix-based methods that are different from the above in terms of disassembly and support relationships. The disassembly transition matrix considers the disassembly operation to be the disassembly transition matrix of which column and row represent the disassembly operation and subsequent sub-assembly respectively [69]. The apparent drawback of this approach is that it should list all the potential subassemblies and disassembly operations. Since the actual disassembly operations are being affected by gravity, the enhanced support matrix was proposed to be closer to the real conditions [70]. The base component supporting other parts or attachments was first determined at the enhanced support matrix and then the supporting relationships of various components were regarded at the enhanced support matrix.

1.2.1.3 Geometry Base Methods

Srinivasan and Gadh [71] proposed the ‘ wave propagation ‘ approach, geometric development, to minimize complexity for optimal selective disassembly sequence production and pointed out that selective disassembly is often applied in applications for recovery processes, such as maintenance, only when a subset of parts from an assembly is disassembled. For the wave propagation method, two main types are given, i.e. Generation of’ disassembly waves’ to arrange parts in topological forms and analysis of intersection priorities for the disassembly waves in order to determine the optimal disassembly sequence automatically. This wave propagation method allows the exponential computational complexity to be reduced to polynomial time.

Srinivasan and Gadh [72] have further developed their’ wave propagation ‘approach by dividing the selective disassembly into three categories: selective one-part disassembly, selective multi-part disassembly, and selective large-

scale disassembly. They have studied and provided solutions for each of these three categories and presented selective 3D disassembly algorithms in a prototypical system. In addition, Srinivasan and Gadh [73] studied an effective disassembly technique using a mathematical model of a wave propagation assembly, focusing on multi-part disassembly, based on the multiple waves spreading algorithms and the algorithm of priority intersections.

Lee and Gadh [74], Shyamsundar & Gadh [75] applied both a non-destructive disassembly method and a destructive disassembly method to dismantle a product, based on the geometry of the assemblies. The non-destructive disassembly method utilizes a direction-based method to disassemble parts assuming only a single and linear transmission disassembly motion is being used. The key of this algorithm is to decide which of the interlocking parts of an assembly can be taken apart through linear transmission motion. As one part at a time is disassembled from the assembly the rest of the assembly is treated as one object. This disassembly routine is repeated until there are no more parts to disassemble, which means the non-destructive disassembly method is no longer available. After that, the destructive disassembly method is employed to continue the disassembly process. The destructive disassembly method cuts off along the interactive surface between two parts. The goal of the destructive disassembly algorithm is to eliminate parts by destruction and choosing the best locations to destruct parts. This cutting routine is repeated until the rest of the assembly can be disassembled using a non-destructive disassembly method.

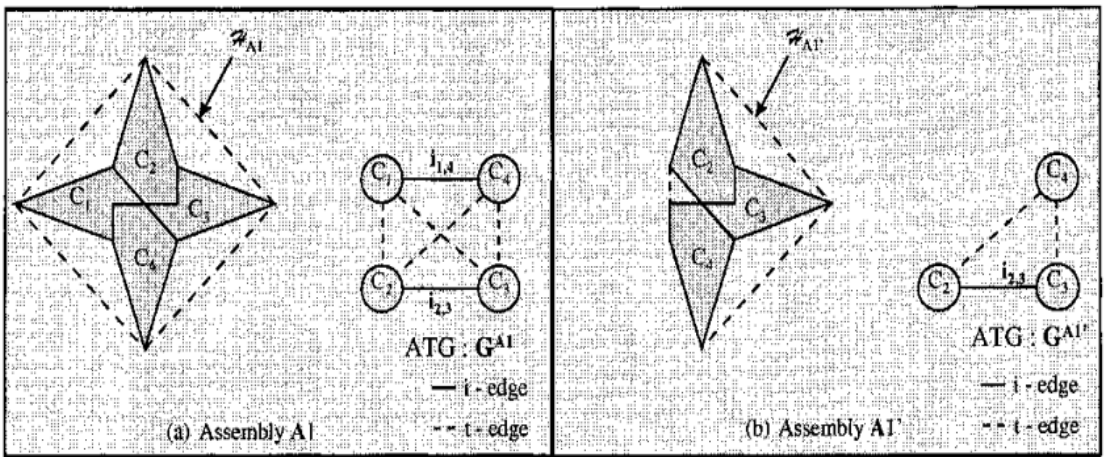

Figure 1.3: A valid assembly and an interlocking assembly [75].

Computer technology's advantage will enable geometry-based approaches to be used in process planning for disassembly. This will be widely used for simple software development due to its unique advantages.

1.2.2 Contact and Non-Contact Constraint Generation

Efficiently and rapidly accessing disassembly information in CAD can make end-of-use and disassembly considerations easier to integrate into design decisions. This information typically takes the form of precedence, interference, and disassembly direction. Both for assembly or disassembly operations, researchers have worked on finding feasible, no collision paths for assembling or disassembling parts of mechanical products [76, 77].

CAD model files were a source in previous works for generating assembly/disassembly sequences [78, 79-83]. Zha and Du [79] presented a STEP-based method to determine the assembly sequencing in the design stage by considering hierarchal structure, geometry, and feature of an assembly. Prior knowledge of the liaison relationship is required to implement this method. Gottipolu and Ghosh [80] present a methodology which extracts directly geometric and mobility assembly constraints from CAD assembly. They used the contact and translation functions (unidirectional matrices) to describe geometric and mobility constraints. Briceno and

Pochiraju [81] present a methodology for determining the disassembly feasibility for contact constraint and direction that is based on measuring the volume between two consecutive parts. Parts are meshed and ordered pairs of parts are evaluated to determine the volume between triangular meshes of the part plane with vertex point(s) from a target part. In their work, the STL file format of CAD assembly model was used to derive the parts geometry and mating information [81]. Bedeoui et. Al. [82] took the stability concept into account during assembly operations in developing assembly sequence planning for heavy machines. They developed interference and contact matrices from the extracted topological and geometrical assembly constraints from CAD design. Pintzos. Et al [83] in their proposed approach is on finding an assembly precedence diagram using assembly tiers. Their methodology is based on geometric characteristic extracted from CAD design identifies the parts or sub-assemblies that have assemble before or after other groups. The collision between parts or sub-assemblies of the examined assembly considered as a core in their method.

Vyas and Rickli [78] used the contact function to automatically extract part contact disassembly constraints from a STEP file and determine the disassembly operation feasibility, represented by a precedence matrix. They referred to the importance of the interference matrix (IM) for showing feasible disassembly of contact parts as it can contain basic disassembly information, and can be used in subsequent disassembly optimization and analysis methods. However, they did not show what direction is feasible for disassembly or determine non-contact interferences. Tao and Hu [84] proposed an approach to analyze the contact relations between assembly parts. Determining non-orthogonal assembly directions automatically was the main characteristic in their approach. Interferences. Su [85] proposed an approach called geometric constraint analysis (GCA) to analyze the geometrical constraints and

integrated their approach with CAD systems. Ou and Xu [86] developed a system able to retain assembly data from the CAD model and produce feasible assembly sequences automatically. Iacob et al. [87] proposed an approach that searches feasible disassembly sequences through exploiting the connection and the mobility of mechanical assembly. They used a virtual platform to simulate assembly/disassembly sequencing. Ben Hadj et. Al. [88] improved an algorithm checking the interferences between imaginary bounding boxes of all assembly parts, however, this algorithm does not consider the actual part faces shapes.

1.2.3 Inferring the Geometric Disassemble Feasibility from Collision Test

Geometric feasibility means it is possible to assemble or disassemble two sub-assemblies or parts without a collision [89]. Precedence relations of assembly must be fulfilled in the preparation of assembly sequences. Also, generating geometrically feasible disassembly sequences to get the components of the assembly into intact form (i.e. disassemble the assembly by non-destructive operation) requires collision free precedence relationships. Otherwise certain parts cannot be successfully assembled or disassembled. Therefore, the key point in geometric feasible assembly / disassembly sequence reasoning is to determine the precedence relationships in assembly / disassembly correctly and entirely.

In the generation process of disassembling parts of a component, considering the prior relationships between parts plays a critical role. Three methods of an assembly's representation have been stated by Lambert [90] in considering the precedence relations. The graphics represent nodes and hyperarchs, which symbolize the components or subassemblies of the product, and the relationship between the components of hyperarcs [91]. Also, the graph's construction is based on a product's hierarchical structure and then DSP can be generated by visualizing feasible

disassembly operations. Both geometrically feasible and unfeasible operations for the disassembly of a product [92] can therefore be generated by the use of AND/OR charts. The direct disassembly diagram has been used in this work to visualize the precedence relationships that ensure the collision-free disassembly steps. However, the number of disassembly sequences increases exponentially with increasing the number of assembly parts [93]. The proposed methodology at this work ensures solely geometrically feasible disassembly sequences are mentioned. The adjacent graph [94] is another form of representation system that requires the consideration of precedence relationships. This technique consists of showing along a direct or undirected line all relationships between parts, and the adjacent graph provides more detail than AND/OR graphs. Another alternate representation graph used in the DSP problem is the Net Petri (PN) graph. This approach offers a mathematical technique that is useful for producing DSPs [95].

Despite the effectiveness of these theoretical techniques to produce a product's DSP, a limitation has been discovered, especially with products having a higher number of components. Other types of investigations focused on the use of CAD data were developed with the advancement of tool design. In reality, a product's CAD data, such as topological or geometric data, is very useful for generating DSP. Also, in several investigations of the DSP problem, the transformation of CAD data into various matrix representations such as interference matrix and touch matrix were used [96, 97]. The advantages of these matrices were the product structure and the component limitations that could be given by automatic DSP search [98].

The approach based on the Interference Matrix (IM) was developed for the geometric feasibility analysis in ASP [99, 100, 101] but the IM is also commonly used in representation for disassembly sequencing tasks [100, 102]. An interference matrix

is an integer array where the matrix elements indicate whether the relative component is blocked in the same direction by another component (mainly coordinate direction of the axis) [99]. So, when a component is not blocked in the sequence by the other remaining parts during the DSP, the component can be assembled or disassembled in the corresponding direction without collisions. Yu, J., & Wang, C. [95] refers to the significant assembly relation model for Geometric Feasibility discrimination. An IM defines interference that occurs between parts when each part enters or leaves the assembly in the specified direction which implies the precedence of assembly or disassembly [103]. IM is easy to represent [102, 103]. Perrard and Bonjour [29] have considered IM a valuable tool for the creation of geometric assembly constraints for operations. While the IM has its advantages in reflecting the results of the collision tests, a description of the full results of the collision tests for each component is needed to provide specific disassembly details for methods of optimization [78]. In this paper, the precedence matrix used to secure the basic disassembly information and it secures the geometrical feasible disassembly sequences concluded from interference matrices resulted from performing the developed collision test.

An active research field that searches for successful methods of extracting assembly/Disassembly sequence information from CAD assembly models has been incorporated CAD assembly sequence solutions. In order to define assembly sequences rapidly and reliably during product creation, complex assemblies, the digital manufacturing thread, and model-based description patterns continue to inspire approaches. Assembly sequence analysis offers insights into the understanding of disassembly sequencing, but it is not assured that assembly and disassembly are one-to-one. A matrix method is proposed by Ou and Xu [99] to process knowledge retained from a CAD model. Their method conducts studies of stability and interference when

developing sequence plans for assembly. Hadj et al. [104] used collision analysis to define obstacles and generate feasible assembly sequences during part motion. Gottipolu and Ghosh [105] present a technique directly from the CAD model to derive geometric and mobility assembly constraints. Unidirectional matrices, called communication and translational functions, are used by Gottipolu and Ghosh [105]. Contact functions can be converted into disassembly sequencing and are essential to the determination of disassembly sequence contact constraints.

Disassembly details can be regarded as determining contact and translation functions similar to the contact and translation assembly sequence functions in [105]. Using and extending a similar contact mechanism, Briceno and Pochiraju [106] define a technique based on the CAD model to produce a disassembly series. As a tool for evaluation, they use a CAD model for data input and extraction and AND / OR graphs, concentrating mainly on disassembling one component from another component. Peng and Chung [107] discuss the accessibility and disassembly of components while illustrating the fasteners used to assemble components. To evaluate a full disassembly graph model, part-to-part disassembly assessment methods for the contact feature must be replicated for all contact constraints inside an assembly. Using Sim Mechanics, Emmanuel and Chinedu [108] produced a complete AND / OR graph for disassembly. Sim Mechanics creates physical relations with mass, principal moments of inertia, length, and surface area between parts of the assembly. Alternatively, Giri and Kanthababu approach disassembly sequence generation by using methods based on two-dimensional views [109].

The previous approaches, however, suffer from the unnecessary production of a vast number of results. Then, they also manipulate alternate ways to reduce the number of candidate solutions. Typically, they add other knowledge to the product model.

However, the assembly and disassembly issues are harmonious problems, therefore, it is feasible to use the same solution concepts like using the precedence graph in determining just feasible disassembly sequences. They have used a precedence graph in determining the assembly sequences in order to describe partial orders between assembly operations [110]. Another approach consists of using association matrices and interference matrices to take into account the geometry and the location of the sections of the product. This makes it possible to deduce certain geometric restrictions automatically and to minimize changes in the course of assembly [111]. In order to minimize the number of method modifications, some researchers add performing considerations, such as indicating a list of useful methods to accomplish an operation [112]. Other authors suggested incorporating a CAD deduction module to quantify any operating constraints (usually geometric constraints). However, this last approach would not decrease the testing space for the generation of the assembly proposal, but rather requires the number of questions posed to the user to be reduced [112]. In this work, to avoid excessive generation of a large number of results, a CAD file of an assembly and considering taking into account the geometry of parts to produce Interference Matrices through performing collision tests will be used to produce one Precedence Matrix provides just geometrical feasible disassembly sequences.

1.2.4 Applying Social Network Analysis into Disassembly Network to Predict Disassemble Feasibility

Social networks are networks that are used to understand people's interactions or transactions. Statistical context (graph theory) of the Social networks enables them to assess and define an individual's effect on the whole structure, while Social Network Analysis metrics help them to analyze and evaluate it. This work takes the advantage of the ability of social network metrics to reveal the disassemble feasibility of an assembly based on the geometrical data of the assembly's parts. Social networks are

networks that are used to understand people's interactions or transactions. Statistical context (graph theory) of the Social networks enables them to assess and define an individual's effect on the whole structure, while Social Network Analysis metrics help them to analyze and evaluate it. This work takes the advantage of the ability of social network metrics to reveal the disassemble feasibility of an assembly based on the geometrical data of the assembly's parts. Some centrality measures have been employed in scientometric evaluations [113, 114], communications networks [115], and power [116], and Water [117, 118] Networks to analyze the vulnerability due to crush and node failure at these networks. However, researchers have not yet exploited the potential for using group centrality metrics to examine disassemble feasibility changes due to changes in the design dimensions (due to wear along product life span). Therefore, this work proposes to examine how to employ the centrality metrics to indicate the change in the disassemble feasibility.

CHAPTER 2: AUTOMATED CONTACT AND NON-CONTACT CONSTRAINT GENERATION FOR DISASSEMBLY FEASIBILITY AND PLANNING

2.1 Abstract

Disassembly is an essential step for value recovery processes, but it is typically manually performed, which is time-consuming. Design for disassembly and automated disassembly methods can improve efficiency. However, critical disassembly information, such as disassembly precedence and direction must be easily and rapidly accessible. Previous research has evaluated contact constraints for product disassembly from a CAD assembly STEP file in order to determine if a disassembly operation is feasible, but efficient extraction of disassembly information and non-contact disassembly constraints is an ongoing area of study. Disassembly feasibility and direction for contact and non-contact interferences can be expressed as an interference matrix after disassembly information is extracted from CAD assembly designs. In this paper, a STEP file format is used as a source for part geometry to evaluate disassembly feasibility and direction for contact and non-contact disassembly interferences. The method proposed in this paper extracts geometrical data from STEP file to test collision relationships when removing assembled components. Non-contact and contact disassembly feasibility are presented as a weighted liaison graph. In future work, the approach will be implemented iteratively to determine disassembly precedence and direction at each stage of disassembly, and identify potential destructive disassembly opportunities.

2.2 Introduction

End-of-use products have potential advantages from reusing intact product parts. While the recycling process is convenient for retrieving raw material, it can have

negative side effect on the environment and eliminates remaining functional value. Disassembly plays a critical role in value recovery process scenarios (*i.e.* recycling, remanufacturing, rebuild, reuse, and maintenance processes) that address resource shortages and waste [119]. It is the first step in many value recovery processes like recycling, remanufacturing, reuse, and refurbish which offer can use parts of end-of-use products in new or remanufactured products. European and international standards and recommendations of environmental legislation (*e.g.* European Directive 2000/53/EC) indicate that the problem of dismantling and recycling of products is increasingly critical [2].

Disassembly can be defined as a systematic method for separating a product into its constituent parts, components, and subassemblies [2]. Complete product disassembly, selective disassembly of target components, and partial disassembly [2] are categories of disassembly [120]. In complete disassembly, all parts are dismantled while disassembling a product, while in selective disassembly specific target component(s) or subassembly(s) is dismantled. Partial disassembly aims to disassemble to the point where returns of dismantled components diminishes. Each category of disassembly types is more convenient for a certain value recovery processes. For example, complete disassembly is more convenient for rebuild processes where all assembly parts need to be examined to discover damage that needs to be replaced with new parts or remanufactured. Selective disassembly is convenient for reuse processes like the recovery of product components during remanufacturing operations [121], and partial/selective disassembly is suitable for maintenance because maintenance may not require the disassembly of all parts of an assembly.

In this paper, the objective is to automatically determine contact and non-contact disassembly interferences from CAD information. CAD files are used as a source for

extracting geometrical data to determine the interference matrix. In this work, the STEP (Standard for the Exchange of Product model data) file format is used as an input CAD file, which is supported by most CAD platforms. In addition, the STEP file uses fewer points and features to describe the geometry of CAD design parts compared with other CAD file formats (*i.e.* .stl files, .obj files). Since many CAD systems support STEP file format, the application of the proposed work can be broadly applied across CAD platforms. The developed approach reads the STEP file and extracts the needed geometrical data for determining disassembly contact and non-contact interferences automatically. Based on this disassembly information, a weighted liaison graph is used as to represent disassembly feasibility.

2.3 Methodology

To determining disassembly feasibility in the 6-principle cartesian axis for following procedure which is showed at Figure 2.1 has been followed to find an answer for checking disassembly feasibility in the principle cartesian axis.

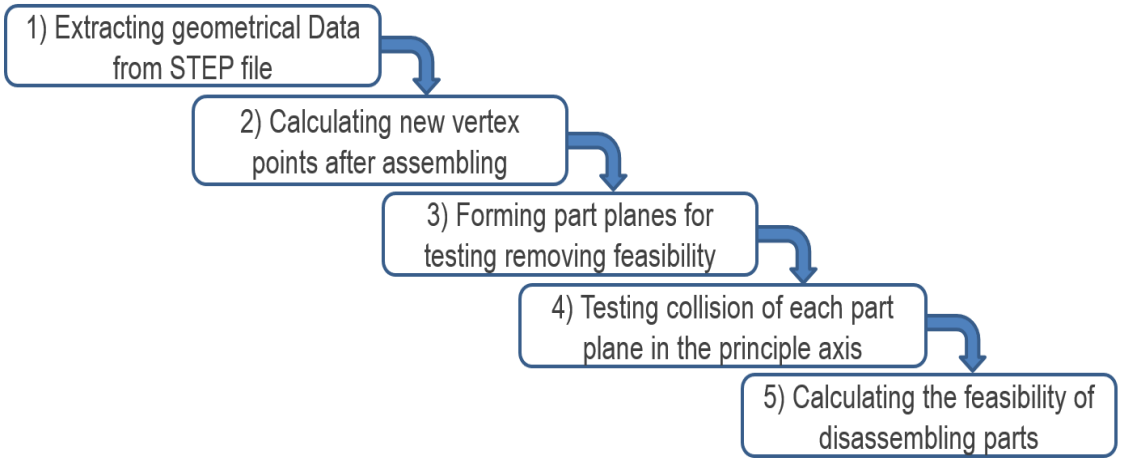

Figure 2.1: Flow chart of the contact and non-contact disassembly constraint generation approach.

The outputs of this method are 1) IM (interference matrix) for checking disassembly feasibility of contact and non-contact interferences, 2) determination of the feasible disassembly direction of each part, 3) evaluation of part disassembly feasibility.

A weighted liaison graph has been used to show the gradient of feasibility of disassembly of parts. This methodology is implemented on a six-part theoretical product assembly as a case study to show the results of the proposed method.

2.3.1 Extracting Geometry Data from STEP File

A standard CAD file format, STEP (Standard for The Exchange of Product model data) is the desired file format as a solution for interchangeability challenge between CAD platforms. The format of a STEP-File is defined in ISO 10303-21 as a clear text encoding of the exchange structure [122]. Ungerer and Buchanan [123] give a detailed explanation for each line presented by STEP files.

The STEP file is used as an assembly model input to my method in order to apply across different CAD platforms towards pursuit for make disassembly decisions at design. The STEP file describes the parts of an assembly by giving their vertex points and transforming points of each part according to an assembly coordinate system. These two groups of data are required in the proposed method to test the disassembly direction for each part.

2.3.2 Calculating New Vertex Points after Assembling

The STEP file is nearly the same in its structure, syntax, and semantics regardless of the originated CAD platform for that file [124]. In the STEP file, the description of every part of an assembly is given concerning its local part coordinate system. Since disassembly is started from a complete assembly, the values of all vertex points of its parts should be described relative to the Assembly Coordinate System. These values are not given in the assembly STEP file. STEP file includes the original vertex points of each part relative to each part coordinate system, and the transformation information required to transform each part into the Global Coordinate System (or Assembly Coordinate System).

Each part has its ITEM_DEFINED_ TRANSFORMATION string in STEP file. This string connects to two AXIS2_PLACEMENT_3D strings, where each one of these two strings gives two pieces of crucial information. First, the original and new Cartesian points and, second, the original and new reference direction vectors for these Cartesian points. This information is not given for the whole vertex points of parts just for the base point of each piece. Therefore, the difference between the values of the original and new base point has been used to calculate the new values of the remaining vertex points of that part. The difference value is de-scribed in Equation 2.1 as t_{ij} (transformation point for part *i*). The Cartesian points relate to the translation while the vectors relate to rotation of each part along to its coordinate axes. Equation 2.1 calculates the new value of the vertex points of the parts of an assembly after assembling all parts as a completed design product.

$$p'_{ij} = p_i + t_{ij} \qquad (2.1)$$

Where: p'_{ij} is the new vertex point of part *I* and transformed by the part *i* transformation point, t_{ij}. p_i is the old vertex point of part *i*. t_{ij} is the transformation point for part *i*. In the proposed method, new vertex points are needed to test the interferences or collisions in the path of removing parts.

2.3.3 Forming Part Planes for Testing Removing Feasibility

New values of vertex points are stored for each part as x, y, z coordinates. Then, the proposed method searches for the minimum and maximum values of x, y and z in the stored points to form planes that represent each part face. While most mechanical parts are assembled along six major axes: +x, -x, +y, -y, +z, -z [124], the disassembly of these parts are assumed to follow the same directions in this work. Therefore, to determine the disassemble feasibility, the proposed method checks the collision between parts planes for the principle axes +x, -x, +y, -y, +z, -z.

To check the disassemble feasibility at all the principle axis, the planes form at one of the principle axes at a time of testing interferences. The plane points should satisfy the constraints in the Equation 2.2.

$$Min.\overrightarrow{t_a} = ta$$
$$Min.\overrightarrow{R_a} < ta < max.\overrightarrow{R_a} \quad (2.2)$$

Where: t_a is the target axis, *i.e.* the planes are vertical and parallel with other principle axis, and R_a is the remainder of the principle axis. The formed part plane is parallel with them. For example, to form a plane of a face for part at x-axis, the below constraints functions need to be satisfied.

$$\text{Min. } x = x$$
$$\text{Min. } y < Y < \text{Max. } y \quad (2.3)$$
$$\text{Min. } z < Z < \text{Max. } z$$

The above equation (Eq. 2.3) forms a plane taking max and min values that are the edges of that surface. In this work, a six-part assembly has been included with basic entities like cylinder and regular blocks aligned to the principle axes +x, -x, +y, -y, +z, -z to simplify the description and the technique development.

2.3.4 Testing Collision of Each Part Plane in the Principle Axis

To dismantle a part from an assembly, determining the path that ensures no collision between the moved part and other parts is required. In this approach, the plane is formed by using the new vertex points stored. After formation of the plane, the vertex that forms other part planes is checked to determine if any point lies on that plane. If there is a point that lies on the plane, there is the presence of another part in its path. All stored points of other parts are examined. If any of these points satisfy the functions in Equation 2.3, the other part lies on the formed plane and the part has an interference

in that direction. If no vertex lies on that plane, the plane is moved forward and checked for the presence of other vertex.

2.3.5 Calculating the Feasibility of Disassembling Parts

From the resulting matrices of testing collision of each part plane in the principle axis section, it is possible to show the feasibility of disassembly operations by using a Weighted Liaison Graph (WLG) that was improved by Riggs and Hu [125]. The main idea behind WLG is that a larger size node has greater opportunity to be removed before other nodes that have smaller size. However, the nodes that have the same size can be disassembled without considering the precedence. The considered weight criterion in this paper is the part that has feasibility to disassemble in directions more than other parts, its node has size larger than other parts. The relationship matrix can identify the relations in the assembly model. The number of contact relations between two parts *i* and *j* can be described as follows:

$cre_{i,j} = 1;\ \ if\ there\ is\ contact\ between\ i\ and\ j;$

$cre_{i,j} = 0;\ if\ there\ is\ no\ contact\ between\ i\ and\ j;$

$cre_{i,j} =\ NA\ ;\ if\ i = j\ is\ Part\ i\ compared\ with\ itself$

This matrix is square and symmetrical. Its size N x N, where *N* is the total number of components. The aim of including the relationships matrix is to show the contact relation in matrix form as an initial step to draw the WLG.

$$cre = \begin{bmatrix} - & \cdots & cre_{ij} \\ \vdots & \ddots & \vdots \\ cre_{ij} & \cdots & - \end{bmatrix} \qquad (2.4)$$

Figure 2.2 shows three test cases for interference. (a) in-contact parts where parts in a position in the assembly touch each other physically. And (b) and (c) non-contact interferences cases where parts are not in a position in the assembly in which touch each other physically but may have disassembly interferences.

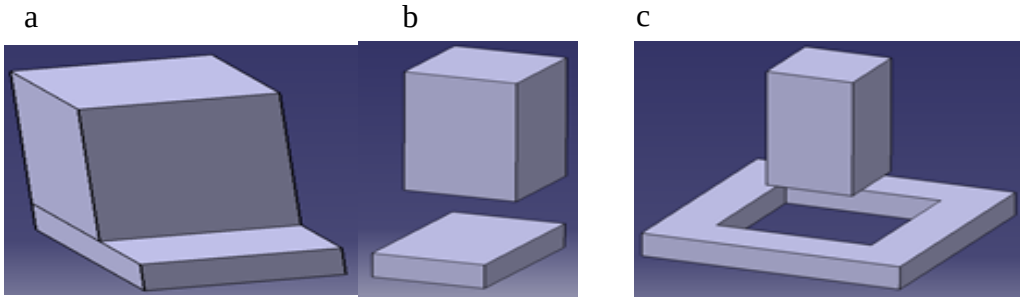

Figure 2.2: (a) In-contact part case; (b and c) non-contact part cases.

In Figure 2.2 (a), assembly consists of three parts all in contact with each other as shown in Equation 2.5. Figure 2.3 is the same assembly in Figure 2.2 (a) but exploded to show all three parts of the assembly.

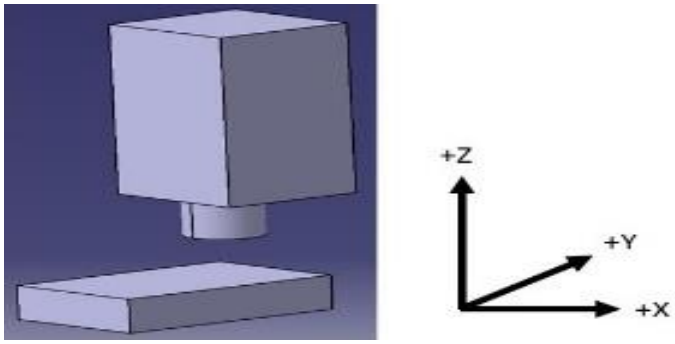

Figure 2.3: Exploded mode of the assembly in Figure 2.2 (a).

Equation 2.5 is the relationship matrix that shows the type of relationship among all the parts of the assembly in Figure 2.3 (a). All the parts of that assembly are in contact represented by a matrix of ones. The relationship of a part with itself is explained by (*NA*) sign.

$$cre = \begin{bmatrix} NA & 1 & 1 \\ 1 & NA & 1 \\ 1 & 1 & NA \end{bmatrix} \qquad (2.5)$$

The resulting interference matrix from the collision test explains the feasibility to or not to disassemble parts at one of the principle axial directions. Where 1 means that part *i* can be removed at direction *j*, 0 otherwise. Equation 6 is the resulted interference matrix of the assembly in Figure 2.3 (a).

$$\boldsymbol{D_{m,n}} = \begin{bmatrix} \mathbf{0} & \mathbf{0} & \mathbf{1} & \mathbf{0} & \mathbf{0} & \mathbf{0} \\ \mathbf{0} & \mathbf{0} & \mathbf{0} & \mathbf{0} & \mathbf{0} & \mathbf{0} \\ \mathbf{1} & \mathbf{1} & \mathbf{0} & \mathbf{1} & \mathbf{1} & \mathbf{1} \end{bmatrix} \quad (2.6)$$

$D_{m,n}$ in Equation 6 can be used to determine the parts that have the higher feasibility to disassemble first. In $D_{m,n}$, m (matrix rows) represent the part number from 1 to m and n (matrix columns) represent the six primary axes ($n_1 = +x$, $n_2 = +y$, $n_3 = +z$, $n_4 = -x$, $n_5 = -y$, and $n_6 = -z$). Table 1 shows the results of these calculations.

Table 2.1: Calculating disassembly precedency criterion for the assembly in Figure 2.2.

Part no.	+X	+Y	+Z	-X	-Y	-Z	Sum
Part 1	0	0	1	0	0	0	1
Part 2	0	0	0	0	0	0	0
Part 3	1	1	0	1	1	1	5

Then, based on the results of Table 2.1 and Equation 2.5, the Weighed Liaison graph depicts the relationships between parts and shows the suggested disassembility of each component (larger circle suggests easier disassembly).

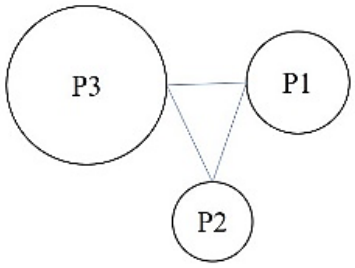

Figure 2.4: Weighted Liaison Graph showing feasible disassembly sequence for assembly in Figure 2.3 (a).

While all the parts of previous assembly are in contact, the parts of assemblies in Figures 2.2 (b) and (c) are not in contact. The relationship matrix for Figures 2.2 (b) and (c) are shown in Equation 2.7 and 2.8 respectively, where the zeros indicate that there is no contact between assembly parts.

$$\boldsymbol{cre} = \begin{bmatrix} \boldsymbol{NA} & \mathbf{0} \\ \mathbf{0} & \boldsymbol{NA} \end{bmatrix} \quad (2.7)$$

$$\boldsymbol{cre} = \begin{bmatrix} \boldsymbol{NA} & \mathbf{0} \\ \mathbf{0} & \boldsymbol{NA} \end{bmatrix} \quad (2.8)$$

The resulted interference matrix for assembly in Figure 2.3 (b) and Figure 2.3 (c) is shown in Equations 2.9 and 2.10, respectively.

$$\boldsymbol{D_{m,n}} = \begin{bmatrix} \mathbf{1} & \mathbf{1} & \mathbf{1} & \mathbf{1} & \mathbf{1} & \mathbf{0} \\ \mathbf{1} & \mathbf{1} & \mathbf{0} & \mathbf{1} & \mathbf{1} & \mathbf{1} \end{bmatrix} \qquad (2.9)$$

$$\boldsymbol{D_{m,n}} = \begin{bmatrix} \mathbf{1} & \mathbf{1} & \mathbf{1} & \mathbf{1} & \mathbf{1} & \mathbf{1} \\ \mathbf{1} & \mathbf{1} & \mathbf{1} & \mathbf{1} & \mathbf{1} & \mathbf{1} \end{bmatrix} \qquad (2.10)$$

Equations 2.8 and 2.9 can be used to determine the parts that have the higher feasibility to disassemble. Tables 2.2 and Table 2.3 show the results of these calculations. The zero for Part 1, -Z and Part 2, +Z indicate that a non-contact interference is present since Part 1 is above Part 2 in Figure 2.3 (b). Using the contact relationships matrix and the summation results of Table 2.2 and Table 2.3, Weighted Liaison Graph (WLG) are constructed in Figures 2.5 and 2.6. Nodes sizes in Figure 2.5 and 2.6 are the same because the summations values for Part 1 and 2 are equal in Tables 2.2 and 2.3, respectively.

Table 2.2: Calculating disassembly precedency criterion of the assembly in Figure 2.2 (b).

Part no.	+X	+Y	+Z	-X	-Y	-Z	Sum
Part 1	1	1	1	1	1	0	5
Part 2	1	1	0	1	1	1	5

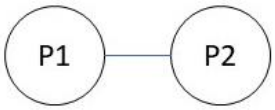

Figure 2.5: Weighted Liaison Graph showing feasible disassembly sequence for the assembly in Figure 2.3 (b).

Table 2.3: Calculating disassembly precedency criterion of the assembly in Figure 2.2 (c).

Part no.	+X	+Y	+Z	-X	-Y	-Z	Sum
Part 1	1	1	1	1	1	1	5
Part 2	1	1	1	1	1	1	5

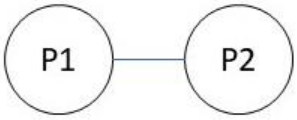

Figure 2.6: Weighted Liaison Graph showing feasible disassembly sequence for the assembly in Figure 2.2 (c).

2.4 Case Study

An example six-part assembly that has contact and non-contact interferences is used to demonstrate the proposed approach (Figure 2.7). The method was coded in Python with the input as STEP file, and the output as the interference matrix with six columns representing the principle Cartesian axes +x, -x, +y, -y, +z, -z and with rows equal to the number of parts of that assembly.

The case study example and all the previous examples mentioned is section 3.5 are done by using the CAD software (CATIA V5-6R2013) where they have been saved in. stp extension (as a STEP file) and then that STEP file saved as a text file with .txt extension to be ready to use by Python application. The time required to get the interference matrix from the Python application for six parts assembly case study is less than eleven seconds where the specification of the used system is as following: Windows 10, 64-bit operating system, Intel (R) i7-2600 CPU 3.4 GHz with RAM 8 GB.

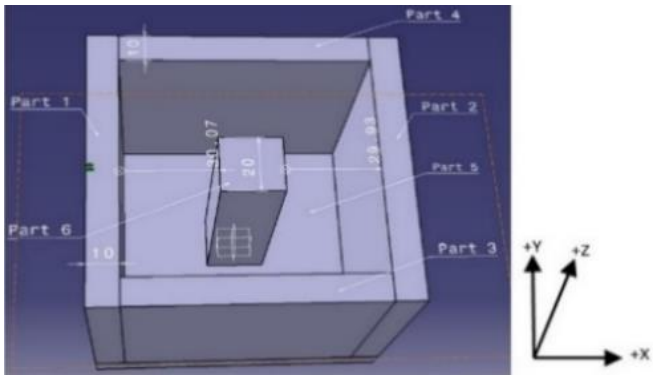

Figure 2.7: Six-Part case study assembly with contact and non-contact interferences.

The case study example is used for testing the proposed method, the lateral view shows all six parts. Parts 1 and 2 are the outer blocks parallel with Y-axis. Parts 3 and 4 are the inner blocks parallel with X-axis. Part 5 is the base block, and Part 6 is the

centre block. Executing the method resulted in the interference matrix in Equation 2.11 for feasible disassembly movements in one of the principal axes and contact relationship matrix (*cre*) in Equation 2.12.

$$\boldsymbol{D_{m,n}} = \begin{bmatrix} \mathbf{0} & - & - & - & - & \mathbf{0} \\ - & - & - & \mathbf{0} & - & \mathbf{0} \\ \mathbf{0} & \mathbf{1} & - & \mathbf{0} & - & \mathbf{0} \\ \mathbf{0} & - & - & \mathbf{0} & \mathbf{1} & \mathbf{0} \\ - & - & \mathbf{0} & - & - & \mathbf{1} \\ \mathbf{1} & \mathbf{1} & - & \mathbf{1} & \mathbf{1} & \mathbf{0} \end{bmatrix} \qquad (2.11)$$

$$cre = \begin{bmatrix} NA & 0 & 1 & 1 & 1 & 0 \\ 0 & NA & 1 & 1 & 1 & 0 \\ 1 & 1 & NA & 0 & 1 & 0 \\ 1 & 1 & 0 & NA & 1 & 0 \\ 1 & 1 & 1 & 1 & NA & 1 \\ 0 & 0 & 0 & 0 & 1 & NA \end{bmatrix} \qquad (2.12)$$

Where 1 means that there is enough space to move part *i* in direction *j* because either there is no contact interferences that prevent part *i* from moving in direction *j*, or there is a non-contact interference but there may be enough space to disassemble part *i* (*i.e.* the distance is enough that disassembly may be possible a movement too far in direction *j* with result in an interference). A 0 means part *i* cannot be disassembled at direction *j* because either there is contact interferences with part *i* or there is a non-contact interferences but with no space enough to remove part *i*, and (–) symbol means that part *i* is free to move in direction *j* for any amount of distance because neither contact nor non-contact interferences are present. The weight criterion of liaison graph can be calculated from Equation 11 and 12 shown in Table 4. The symbol (–) can be considered in Eq. (11) as a 1 in Table 4 to calculate the disassembly precedence criterion where 1 and the symbol (–) in Eq. (11) both refer to feasibility to disassemble part *i* at direction *j*.

Depending on the contact relationships matrix and the summation results of Table 4, it is possible to depict the weighted liaison graph as it is shown in Figure 8. As the liaison graph

shows in Figure 8, Parts 5 and 6 (base and center blocks) may be the best candidates to be disassembled first because they would not collide with any part if they are disassembled in direction of all principle axis except in the +Z direction for Part 5 or in the direction -Z for Part 6. Then Parts 1 and 2 (outer blocks) have the higher feasibility to disassemble before Parts 3 and 4 (inner blocks).

Table 2.4: Calculating disassembly precedency criterion

Part no.	+X	+Y	+Z	-X	-Y	-Z	Sum
Part 1 (outer block)	0	1	1	1	1	0	4
Part 2 (outer block)	1	1	1	0	1	0	4
Part 3 (inner block)	0	1	1	0	1	0	3
Part 4 (inner block)	0	1	1	0	1	0	3
Part 5 (base block)	1	1	0	1	1	1	5
Part 6 (centre block)	1	1	1	1	1	0	5

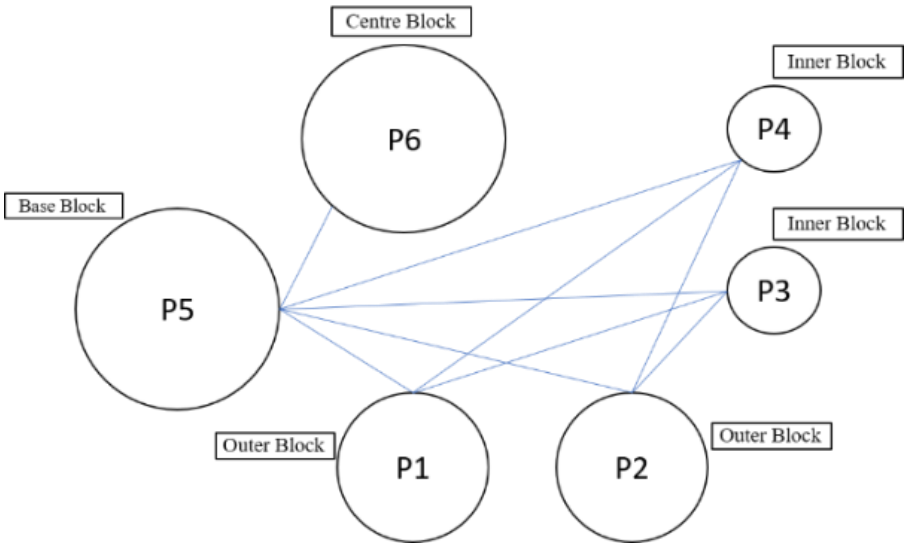

Figure 2.8: Weighted Liaison Graph showing feasible disassembly sequence for Six-part case study assembly.

In addition, the weighted liaison graph shows type of contacts between parts Part 5 is in contact with all parts, while Part 6 is not in contact with the any of the parts except with Part 5. Parts 1 and 2 are in contact with Parts 3 and 4. Parts 1 and 2 are in no contact with each other, and Parts 3 and 4 are in no contact with each other.

2.5 Conclusions

In this paper, a method is presented for determining disassembly contact and non-contact interferences and the direction of disassembly using a STEP file. The input is a STEP

assembly file, the output is a matrix that provides insight into the possible disassembly of a component along the principal axes. In addition, by considering the resulting matrix from the approach and the contact relationships matrix, a weighted liaison graph has been created to show disassembly opportunities. Repeating the approach iteratively after eliminating (disassembling) a component until only one component remains is expected to result in the disassembly precedence matrix that can then be used with disassembly optimization methods, though this is a direction of future work.

The method is limited to check disassembly non-contact interferences in the six principle axials. In future work, the proposed method will be used iteratively to obtain the disassembly precedence matrix, will be tested on more complex assemblies, and will be used to attempt to identify destructive disassembly opportunities to obtain selective components or materials. In addition, to address more complex assemblies, rotational matrices can be considered to evaluate more directions for non-contact inference identification. In the case of spiral-mate disassembly, two directions may be needed to represent the translational movement that results from part rotation. This will be addressed in future work that seeks to identify more types of joining actions that require disassembly and apply to a complex, real-world scenario.

CHAPTER 3: DEVELOPING ASSEMBLY'S PRECEDENCE MATRIX BASED ON COLLISION TEST RESULTS

3.1 Abstract

Disassembly sequence planning (DSP) is the foundation for disassembly process planning and design for disassembly (DFD). Integrating checking geometrical disassembly feasibility of non-destructive operations during product design is an important issue today, and it has received attention in the past decades due to environmental and economic pressures. Non-destructive operations require disassembly activities in order to recover components in intact form and require collision-free trajectories between components when disassembled. The number of disassembly sequences increases exponentially with an increasing number of assembly components. Thus, generating geometric feasible disassembly sequences is critical for determining the optimal disassembly sequencing. In this work, geometric collision data has been used to develop the disassembly precedence matrix that provides fundamental information for disassembly planning methods. Current methods often require enormous computational resources while, at the same time, often failing to locate geometrically feasible sequences of disassembly of products. This paper describes the results of utilizing disassembly collision methods to automatically extract geometrical data from STEP CAD assembly files to determine feasible disassembly operations. A method to determine a Precedence Matrix that describes all geometrically feasible disassembly operations for disassembly of a selected part or disassembly of a whole assembly to its components has been developed and tested. The extracted data from the STEP file characterizes the spatial properties of a component in an assembly and uses this collision test to determine the geometrically feasible disassembly sequences of the assembly. At this work, the Precedence Matrix has been updated by stating the feasible

disassembly direction for each assembly’s component base on the outcomes of the collision test.

3.2 Introduction

Disassembly sequence planning (DSP) is an NP-hard task [126], whereby a physically viable sequence respecting precedents between components is primarily defined. DSP offers a broad range of industrial applications, from the initial prototype to production, maintenance, and recycling, which encompasses each stage of the product life cycle. In order to minimize issues related to the exploitation and maintenance of assemblies, considering the disassembly constraints is important not only in the sense of the life end of a product but also in its life cycle [127]. The main contribution of this paper is the development of a method for representing the disassembly knowledge stored in Interference Matrices resulted from implementing a developed collision test to build a Precedence Matrix that provides the basic knowledge to determine all geometrically feasible disassembly sequences.

Disassembly is a unique process that is the focus of many scholars' research [126]. Effective disassembly involves developing disassembly sequence plans (DSPs) [127]. DSP is viewed in the design phase as a fundamental task for determining the accessibility of components or subassemblies as well as the disassembly path that allows for quantitative measurement of the disassembly feasibility of the product [128]. DSP consists of three types, full disassembly, partial disassembly, and selective disassembly. Complete disassembly completely disassembles all components of a product [129, 130], whereas selective disassembly target one or a portion of valuable components that can be recovered, reused, or recycled [131, 48]. Partial disassembly, which is the best order for disassembly operations to an optimum degree of disassembly, which decreases returns if surpassed [29]. The main distinction between

partial disassembly and selective disassembly is that the first focuses on the profitability effects of disassembly levels, while selective disassembly seeks to reclaim a certain component [1]. Disassembly may use an operation that is mainly focus on material of the parts rather than part recovery (destructive operation) or operation focus on getting on the assembly's parts in intact shape rather than material recovery (non-destructive operation). In this work, complete disassembly where the components are retrieved with non-destructive operations is considered.

Determining disassembly sequence based on the product's CAD file helps in generating the base knowledge for DSP, improving the efficiency of the recovery processes (i.e., re-manufacturing, maintenance, rebuilt, etc.), and enabling mechanical product designers to design their product in a way that ensures recovery of the highest value. Although the methods of disassembly optimization and analysis are well known, many of these methods rely on basic knowledge about disassembly which can be sorted as a Precedence Matrix (PM) [78]. Many feasible disassembly sequences can be concluded from basic information sorted in a PM [44]. The key to EOL product management could be a product design that enables product recovery at the End-Of-Life (EOL) of the product. It can increase the efficacy of the recovery process, thereby reducing the cost of recovery [133]. For example, it is possible to reap enormous benefits with the implementation of design for remanufacturing by including product simplification for disassembly [134].

Because of the need to produce complex, short life cycle goods, and global competition, life cycle design is, therefore, becoming increasingly relevant. Therefore, industrial product design needs to take into account aspects of the product life cycle such as assembly in manufacturing, servicing during consumer usage, and end-of-life recycling. Given that these aspects require disassembly operations, it is useful to

incorporate disassembly process from the early stages of its development phase into product design. There are many CAD platforms (i.e. CATIA, Solid Works, Auto CAD, etc.) used to design mechanical products. However, developing a method able to determine feasible disassembly sequences for a mechanical assembly based on geometrical data from a neutral file (e.g. STEP file) will ensure the flexibility of determining the disassembly sequences of an assembly constructed by whatever CAD platform.

The disassembly planning diagram models are feasible and can take many forms, including guided disassembly networks, AND / OR diagrams, liaison graphs, etc. [135]. Graph models are also transformed to a matrix of precedence. All the disassembly data must be precisely described by graph models and precedence matrices as they are the key source of input data for optimization of the disassembling sequence. This knowledge is often gathered manually, based on user feedback which is time-consuming and not conducive to product creation [37, 136]. By specifically, efficiently and rapidly producing graphs or prior art matrices from CAD assemblies, disassembly schedule methods can be incorporated into the initial stage for product design.

In this work, disassembly precedence relations have determined based on geometric feasibility, geometric feasibility analysis determined by using geometrical data stored at an assembly STEP CAD file. Geometric Disassembly Feasibility (GDF) is the precondition of the geometrical feasible disassembly sequence planning (DSP). Geometrical Feasible Disassembly Sequence requires having a collision-free direction and path while making two assembly units separated from geometric constraints. In this paper, the input is a neutral CAD file (i.e. STEP) file and the objective is to translate assembly information into a precedence matrix.

3.3 Methodology

3.3.1 Set Interference Matrices

The methodology approach is encapsulated in two main sections. The first section of the methodology starts with the reading of the STEP file to recognize and localize all the geometric parts (solids). The outcome of the first section is Interference Matrices (IMs) resulted from the developed collision test at this work. Each resulted Interference Matrix consists of six columns represent the six Cartesian directions, and number of rows equals to the number of assembly's parts at its disassembly level. Each row in the resulted Interference Matrix (IM) from the collision test represents a collision array for a tested part of an assembly. However, the number of rows in Interference Matrices changes at each level of disassembly, with the number of rows in each interference matrix at each disassembly level less in one row than the number of rows in each interference matrix compared to the previous disassembly level. Figure 3.1 shows the process of using collision test to determine feasible disassemble parts at each disassembly level. Each resulted interference matrix at each disassembly level sorts a number of feasible disassemble parts by considering disassembling one feasible disassemble part resulted from the previous disassembly level. The number of disassembly levels equals the number of original parts. From the STEP protocol, the assembly is broken down into parts composing it as well as its coordinates and directions. The parts are manipulated to move into six directions and the relationships of all part pairs are checked.

To detect the parts that can be disassembled by using the resulted Interference Matrix from collision test Each row and column in the resulted interference matrix the data collected from the relationship of the parts to decide whether or not a part can be disassembled and determining the feasible disassembly directions for these parts.

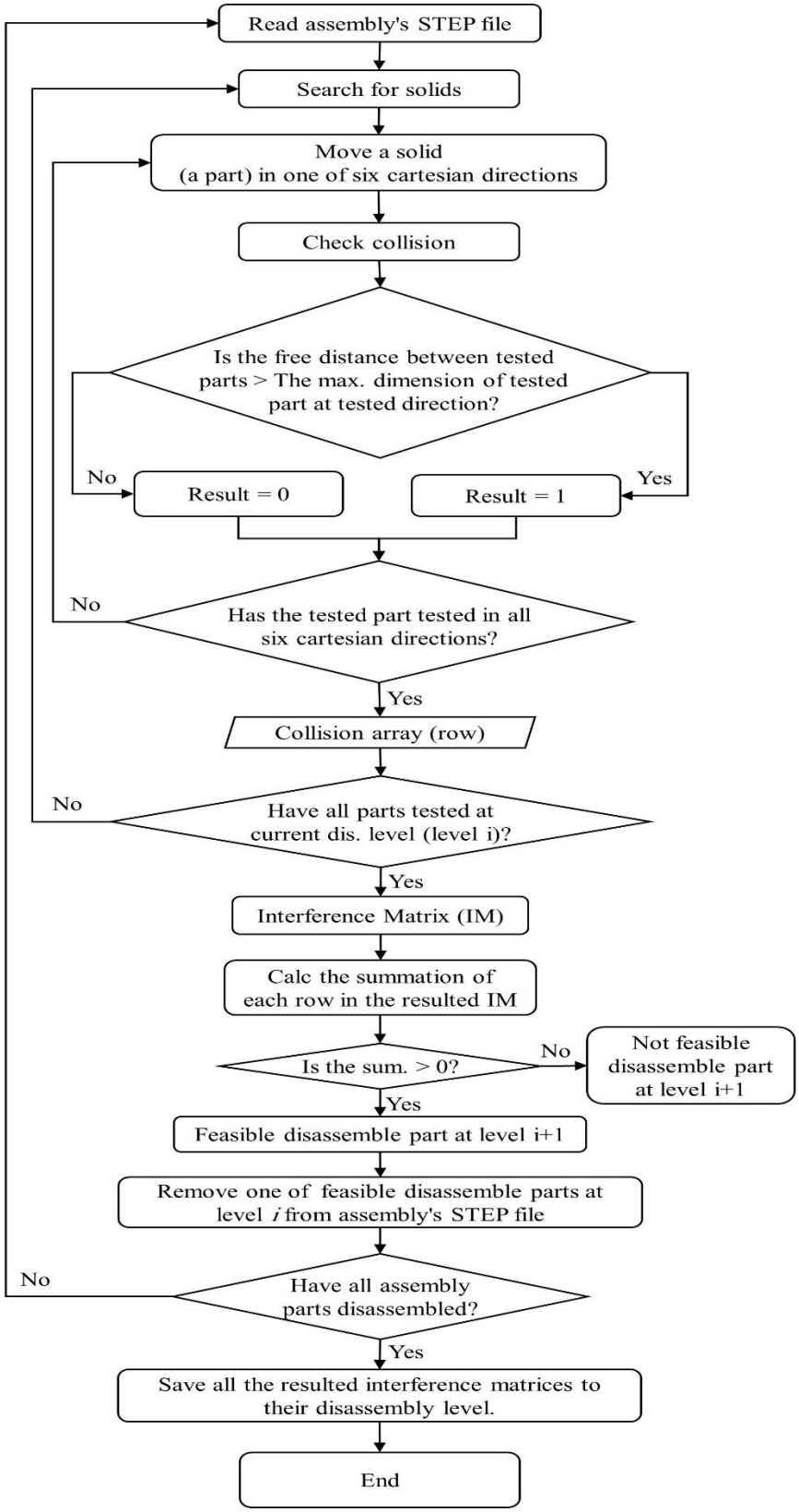

Figure 3.1: Collision test approach flowchart and forming Interference Matrices.

3.3.1.1 Collision Test

Collision assumption on the test is made based on the minimum distance between two parts. If an object has superficial contact with another, it has minimal distance equals to zero. The same value is assigned when an object interpolates another. Furthermore, contact between the two parts constrains the disassembly feasibility. The part is considered disassembled when it has no collision against all the others, in other words, it has minimum distance greater than zero against all the other parts.

The test results are performed by moving one part to the six directions. To do so, the approach has to read the STEP file and reconstruct all the solids independently from the assembly file. Then, one solid is chosen and moved to one direction assigned until it reaches the maximum perimeter in that direction. A contact check against all the other parts is made after each movement unit and saved in a collision array. At the end of the movement, the part is returned to the original position. The test is looped until all the parts are checked in the six directions.

Collision Test (Pseudo Code)

```
Solids = read Step File
Solid_check = 0
For number_of_solids
        Solids = read Step File
        Move = 0
        Current_solid = 0
        While (Move < maxDistance):
                For number_of_solids
                        If (Current_solid = Solid_check): Move(Solid_check)
                        Current_solid = +1
                Collision_array = Collision_check(Solid_check)
                Move = +1
        Solid_check = +1
```

3.3.1.2 Disassembly Feasibility

There are three possible situations while moving a part that has contact with another. The first occurs when it trespasses the other location, which will still be in contact at the end of the movement if the movement is less or equal to the diameter of the piece in that direction. The second situation happens when the part moves along the other surface, and it will not be free until it reaches the edge. The last occurs when it moves away from the contact, having a non-contact flag in the first movement unit. However, a non-contact flag during the movement doesn't mean that it is feasible to disassemble. The part can still hit another part that wasn't originally in contact, which would block the disassembly passage.

The disassembly feasibility test accounts for the original contact state to identify the possible scenarios. If the contact array starts 1 and the next movement unit continues with the same status between the same parts, they can be interpolated or just moving along the surface. The movement is continued until switch status to 0 or reaches the maximum perimeter in the current direction. If it doesn't change status along with the movement, it is assumed that it trespasses another part meaning that it is not possible to disassemble in the current direction, case 1. If status changed to 0, the test continues to check contact against all static parts, and it will switch again to 1 if there is a part blocking the movement, cases 2, 3 and 4. It will only be possible to disassemble if the array change from 1 to 0 once until it reaches the maximum perimeter, cases 5 and 6.

Contact_array = {1,...,1} (1) interpolation

Contact_array = {1,0,...,0,1} (2) surface or interpolation

Contact_array = {1,…,1,0,...,0,1,…,1,0} (3) interpolation

Contact_array = {1,...,1,0,...,0,1} (4) interpolation or surface

Contact_array = {1,0,...,0} (5) disassembled

Contact_array = {1,...,1,0,...,0} (6) surface contact – disassembled

The contact array is transformed into the disassembly feasibility matrix, F, or called Interference Matrix based on parts and direction. The matrix has a size of the number of parts *N* by 6. Each part is represented by a line and each direction is assigned a column, where $a_{n,1}, a_{n,2}, a_{n,3}, a_{n,4}, a_{n,5}, a_{n,6}$ represents potential disassembly of part *n* at X positive, X negative, Y positive, Y negative, Z positive, Z negative direction respectively. Thereby, $a_{i,j}$ will have value equals to 1 if it fits in the *Contact_array* case 5 or case 6, otherwise, it has value 0.

$$F = \begin{bmatrix} a_{1,1} & \dots & a_{1,6} \\ \vdots & \ddots & \vdots \\ a_{n,1} & \dots & a_{n,6} \end{bmatrix}$$

3.3.2 Constructing Precedence Matrix

The second section of the methodology collects the outcome Interference Matrices or disassembly feasibility matrices from the first section and develops a Precedence Matrix (PM). The PM consists of an equal number of rows and columns corresponding to the number of unique components of an assembly. The Interference Matrices composed of zeroes and ones. The resulting Interference Matrices from the first section of this work show the geometrically feasible parts to disassemble the tested assembly at a stage of the disassembly path.

Direct Disassembly Diagram (DDD) [6] has been used during determining the Interference Matrices. Direct Disassembly Diagram (DDD) is used to avoid the redundant resulting Interference Matrices that may appear after determining IMs for each disassembly level. Each IM resulted in disassembly level (*i*) guides to one or more feasible disassemble parts to be consider in determining the IMs for the next level (*i*+1). At disassembly level *i*, the resulted IMs from collision test may point out to the same feasible disassemble part. These identical results guide to determine redundant IMs at

disassembly level (i+1). Depicting DDD during the process of determining IMs shows the whole geometrical feasible disassembly parts at each disassembly level. Each node in the completed DDD represents one column and one row (M_i=N_i) in the Precedence Matrix. The used methodology at this work delivers the geometrical feasible disassembly sequences (GFDS). The GFDS are depicted in the DDD and shown in zero and one form in the PM.

3.3.3 Disassembly Sequence and Disassembly Directions

The disassembly sequence starts by assigning a score to directions and parts. The direction d_j and part p_i scores are results of equations 3.1 and 3.2 using $a_{i,j}$ values from the Interference matrix. Direction w is assigned to initial disassembly direction, set D, based on maximum score among the directions, equation 3.3, and it is chosen randomly among the set, equation 3.4. Within D_1, the part(s) that can be disassembled at this disassembly stage allocates to the direction(s) that has the highest score that is assigned to set P, equation 3.5. The part with the highest score is assigned to set P, equation 3.5. The disassembly sequence starts with the part on the set P. If there are n elements in set P, n different disassembly sequences are evaluated.

$$d_j = \sum_{i=1}^{n} a_{i,j} \quad (3.1)$$

$$p_i = \sum_{j=1}^{6} a_{i,j} \quad (3.2)$$

$$D = \{w | F(d_j) = \max(d_j)\} \quad (3.3)$$

$$D_1 = R\{\begin{matrix} w_1 \\ \vdots \\ w_n \end{matrix} \quad (3.4)$$

$$P = \{q | G(p_j) = \max(p_j) \wedge D_1 \rightarrow p_j\} \quad (3.5)$$

3.4 Case Study

With a view to providing a better explanation of the proposed method, one typical example has used at this work: Ballpoint pen, figure 3.2.

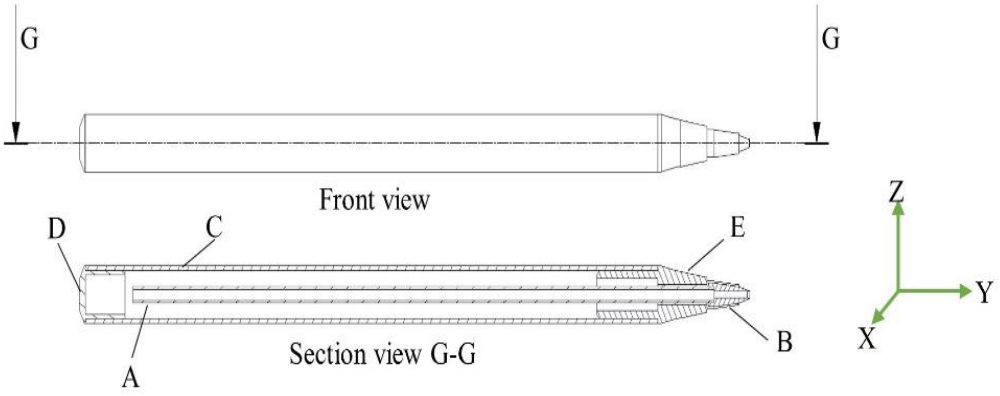

Figure 3.2: Ballpoint Pen example.

Neutral CAD design (i.e. STEP file) of the above example has been used to perform a collision test of disassembling the Ball point pen example. One Interference Matrix (IM) at disassembly level zero resulted from performing Collision test at the example's STEP file.

Table 3.1: Collision Test results (Interference Matrix) for the full assembly State (Ballpoint pen example) at disassemble level zero.

Node #0

		Part Name	X+	X-	Y+	Y-	Z+	Z-	Row Summation	Resulted new nods to the next level.	Feasible disassemble parts at level 0
1	Full Assembled	A	0	0	0	0	0	0	0		
		B	0	0	1	0	0	0	1	N1	B
		C	0	0	0	0	0	0	0		
		D	0	0	0	1	0	0	1	N2	D
		E	0	0	0	0	0	0	0		
		Column Summation	0	0	1	1	0	0			

At disassemble level zero, two parts can be disassembled (part B and part D), while the row summation of these parts are greater than zero. It is feasible to disassemble part B at Y+ direction and part D at Y- direction while the result of the summation of the table columns are greater than zero at Y+ direction for the B part and at Y- direction for the D part. The column summation at the Y+ column is greater than

zero and there is a common cell has one value in common between part B row and Y+ column .However, table 3.1 will lead to new two tables at the next disassembly level, level 1. To find the next geometrical feasible disassemble parts, collision test has been used by considering removing related data of Part B at the example's STEP file one run and the another run of collision test after removing related data of Part D at the example's STEP file.

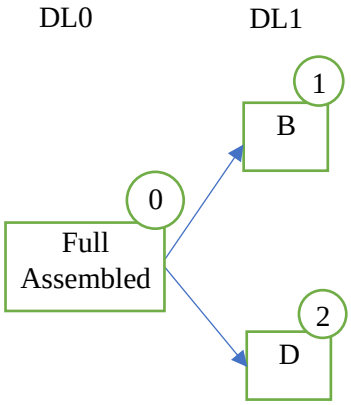

Figure 3.3: The DDD represents Disassembly Levels zero and 1.

Table 3.2: Collision Test results at level 1 (Interference Matrix) By removing part B.

									Resulted new nods to the next level.	Feasible disassemble parts at level 1
		Node #1								
1	B	Part Name	X+	X-	Y+	Y-	Z+	Z-	Row Summation	
		A	0	0	1	0	0	0	1	N3 BA
		C	0	0	0	0	0	0	0	
		D	0	0	0	1	0	0	1	N4 BD
		E	0	0	1	0	0	0	1	N5 BE
		Column Summation	0	0	2	1	0	0		

Table 3.3: Collision Test results at level 1 (Interference Matrix) By removing part D.

Node #2

2 D

Part Name	X+	X-	Y+	Y-	Z+	Z-	Row Summation
A	0	0	0	1	0	0	1
B	0	0	1	0	0	0	1
C	0	0	0	0	0	0	0
E	0	0	0	0	0	0	0
Column Summation	0	0	1	1	0	0	

Resulted new nods to the next level.	Feasible disassemble parts at level 1
N6	DA
N4	DB

At disassembly level 1, table 3.2 points to three geometrically feasible disassemble (i.e. part A, part D, and part E) after disassembling part B. Table 3.3 points to two geometrically feasible disassemble (i.e. part A, and part B) after disassembling part D. However, both tables (table 3.2 and table 3.3) point out to the feasibility to get parts B and D disassemble at this disassembly level (DL) (disassembly level 1), therefore, table 3.2 and table 3.3 will lead to four new tables at the next disassembly level, level 2. The disassembly direction at this level will be Y+ direction for parts A and E, and Y- for part D if disassembling part B before disassembling these three parts. Part A can be disassembled at Y- direction if disassembling part D before disassembling part A.

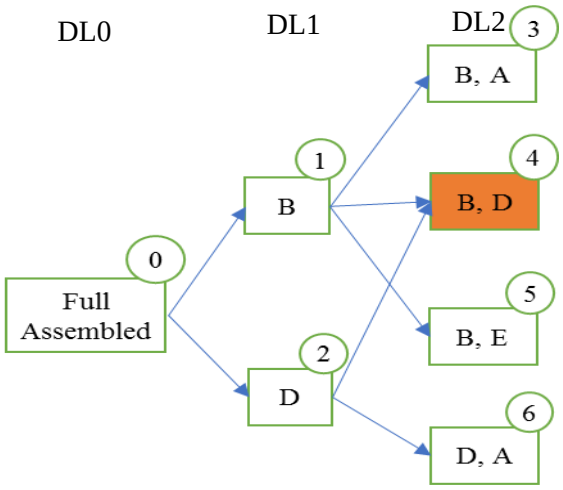

Figure 3.4: The DDD nodes represent Disassembly Level zero, level 1 and level 2.

The DDD shows it is geometrically feasible to have part B and part D disassembled at node number 3.4 whether if the disassembly sequence starts with disassembling part B (node 1) then part D (node 4) or disassembling part D (node 2) then part B (node 4).

Table 3.4: Collision Test results at level 2 (Interference Matrix) By disassembling parts B, and A.

Node #3

		Part Name	X+	X-	Y+	Y-	Z+	Z-	Row Summation	Resulted new nods to the next level.	Feasible disassemble parts at level 2
1	BA	C	0	0	0	0	0	0	0		
		D	0	0	0	1	0	0	1	N7	BAD
		E	0	0	1	0	0	0	1	N8	BAE
		Column Summation	0	0	1	1	0	0			

Table 3.5: Collision Test results at level 2 (Interference Matrix) By disassembling parts B, and D.

Node #4

		Part Name	X+	X-	Y+	Y-	Z+	Z-	Row Summation	Resulted new nods to the next level.	Feasible disassemble parts at level 2
2	BD	A	0	0	1	1	0	0	2	N7	BDA
		C	0	0	0	1	0	0	1	N9	BDC
		E	0	0	1	0	0	0	1	N10	BDE
		Column Summation	0	0	2	2	0	0			

Table 3.6: Collision Test results at level 2 (Interference Matrix) By disassembling parts B, and E.

Node #5

3 BE

Part Name	X+	X-	Y+	Y-	Z+	Z-	Row Summation	Resulted new nods to the next level.	Feasible disassemble parts at level 2
A	0	0	1	0	0	0	1	N8	BEA
C	0	0	1	0	0	0	1	N11	BEC
D	0	0	0	1	0	0	1	N10	BED
Column Summation	0	0	2	1	0	0			

Table 3.7: Collision Test results at level 2 (Interference Matrix) By disassembling parts D, and A.

Node #6

4 DA

Part Name	X+	X-	Y+	Y-	Z+	Z-	Row Summation	Resulted new nods to the next level.	Feasible disassemble parts at level 2
B	0	0	1	0	0	0	1	N7	DAB
C	0	0	0	1	0	0	1	N12	DAC
E	0	0	0	0	0	0	0		
Column Summation	0	0	1	1	0	0			

Tables 3.4, 3.5, 3.6, and 3.7 state the feasible disassemble parts at disassembly level 2. Table 3.4 states that it is geometrically feasible to disassemble part D at Y- direction after disassembling parts B, and A. The same disassembly state (i.e. get parts B, A, and D disassembled at disassembly level 2) is stated by table 3.5, however with a different disassembly sequence. It starts with disassembling parts b, and D then part A, and that means there is a redundant node highlighted in gray color (BAD, or BDA disassembly sequence) that needs to be not stated in the DDD and Precedence Matrix (PM) to avoid redundancy. Also, table 3.4 states that part E can be disassembled at Y+

direction after disassembling parts B, and A. Table 6 refers to the same disassembly state, however with different disassembly sequence starts with disassembling parts B, E and then disassembling part A at Y+ direction, therefore, one redundant node or disassembly sequence which they are highlighted in blue color will not be stated in the DDD and in the PM because they are state the feasibility to disassemble the same parts (parts B, E, and A) at this disassembly level (i.e. level 2). Parts B, D, and E can be disassembled at this level (level 2) in different disassembly sequences, either starting with disassembling parts B, D, then E as resulted from table 3.5 or starting with parts B, E and the part D disassembly sequence as resulted from table 3.6, and as usual one disassembly sequence needs to be stated at the DDD and in PM while both disassembly sequences states the geometrical feasibility to disassemble parts B, D, and E at this disassembly level (level 2). Tables 3.5 and 3.6 state the geometrical disassemble feasibility to have parts b, E, and D, however with different disassembly sequences.

At this disassembly level (level 2), tables 3.5, 3.6, and 3.7 refer to the geometrically feasible to disassemble part C at this level in different disassembly sequencing. Part C can be disassembled after disassembling parts B, and D, after disassembling parts B, and E, or after disassembling parts D and A. Figure 3.5 shows the DDD for the first four disassembly levels (DLs).

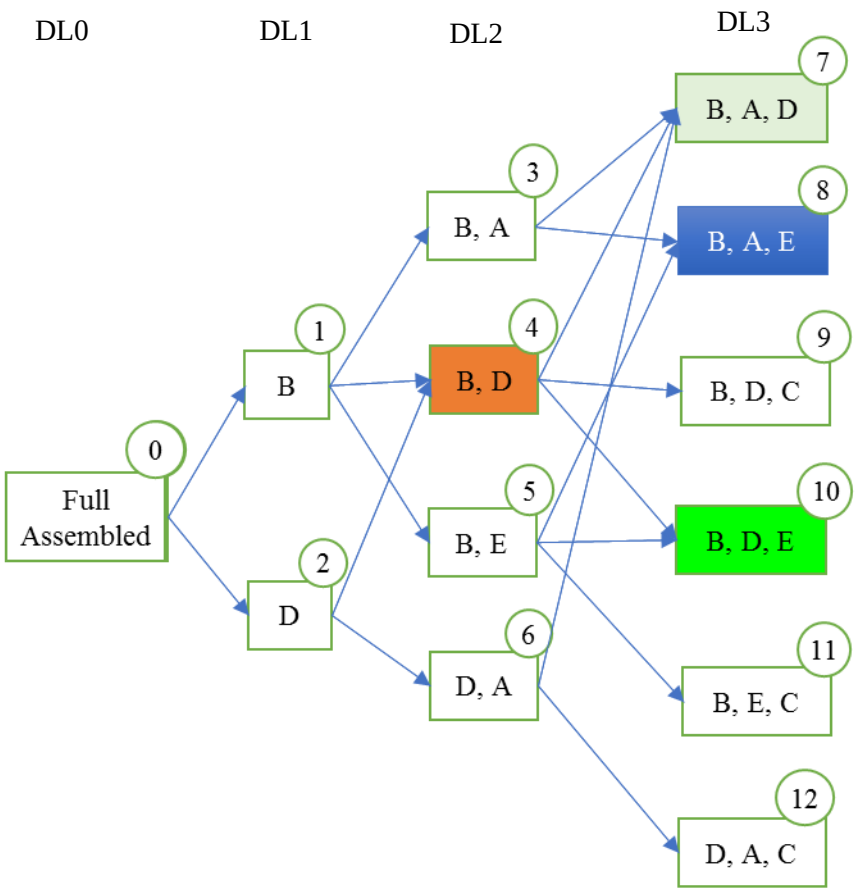

Figure 3.5: The DDD nodes represent Disassembly Levels zero, 1, 2 and 3.

As it is showing in figure 3.5, six new collision tests need to perform to determine the next geometrically feasible disassemble at the disassembly level 3. Performing methodology at this work ends when disassembling the whole parts of an assembly (Ballpoint Pen example at this work). The below six tables (Tables 3.8, 3.9, 3.10, 3.11, 3.12, 3.13) represent the collision test results (Interference Matrices) and feasible disassembly direction for the feasible disassembly parts. Even though it has been resulted twelve new nodes to be consider for the next disassembly level (level 4) from interference matrices at this disassembly level (level 3), there are three feasible disassemble sequences to disassemble one feasible disassemble part at this level. That means there are three nodes are redundant to show at the DDD or the PM. Therefore, four feasible disassemble node to consider in performing collision test to determine next feasible disassembly parts at the next level.

Table 3.8: Collision Test results at level 3 (Interference Matrix) By disassembling parts B, A and D.

Node #7

		Part Name	X+	X-	Y+	Y-	Z+	Z-	Row Summation	Resulted new nods to the next level.	Feasible disassemble parts at level 3
1	BAD	C	0	0	1	0	0	0	1	N13	BADC
		E	0	0	0	1	0	0	1	N14	BADE
		Column Summation	0	0	1	1	0	0			

Table 3.9: Collision Test results at level 3 (Interference Matrix) By disassembling parts B, A and E.

Node #8

		Part Name	X+	X-	Y+	Y-	Z+	Z-	Row Summation	Resulted new nods to the next level.	Feasible disassemble parts at level 3
2	BAE	C	0	0	1	0	0	0	1	N15	BAEC
		D	0	0	0	1	0	0	1	N14	BAED
		Column Summation	0	0	1	1	0	0			

Table 3.10: Collision Test results at level 3 (Interference Matrix) By disassembling parts B, D and C.

Node #9

		Part Name	X+	X-	Y+	Y-	Z+	Z-	Row Summation	Resulted new nods to the next level.	Feasible disassemble parts at level 3
3	BDC	A	0	0	1	1	0	0	2	N13	BDCA
		E	0	0	1	0	0	0	1	N16	BDCE
		Column Summation	0	0	2	1	0	0			

Table 3.11: Collision Test results at level 3 (Interference Matrix) By disassembling parts B, D and E.

Node #10

		Part Name	X+	X-	Y+	Y-	Z+	Z-	Row Summation	Resulted new nods to the next level.	Feasible disassemble parts at level 3
4	BDE	A	0	0	1	1	0	0	2	N14	BDEA
		C	0	0	1	1	0	0	2	N16	BDEC
		Column Summation	0	0	0	0	1	1			

Table 3.12: Collision Test results at level 3 (Interference Matrix) By disassembling parts B, E and C.

Node #11

		Part Name	X+	X-	Y+	Y-	Z+	Z-	Row Summation	Resulted new nods to the next level.	Feasible disassemble parts at level 3
5	BEC	A	1	1	1	0	1	1	5	N15	BECA
		D	1	1	0	1	1	1	5	N16	BECD
		Column Summation	2	2	1	1	2	2			

Table 3.13: Collision Test results at level 3 (Interference Matrix) By disassembling parts D, A and C.

Node #12

		Part Name	X+	X-	Y+	Y-	Z+	Z-	Row Summation	Resulted new nods to the next level.	Feasible disassemble parts at level 3
6	DAC	B	1	1	0	1	1	1	5	N13	DACB
		E	1	1	1	0	1	1	5	N15	DACE
		Column Summation	2	2	1	1	2	2			

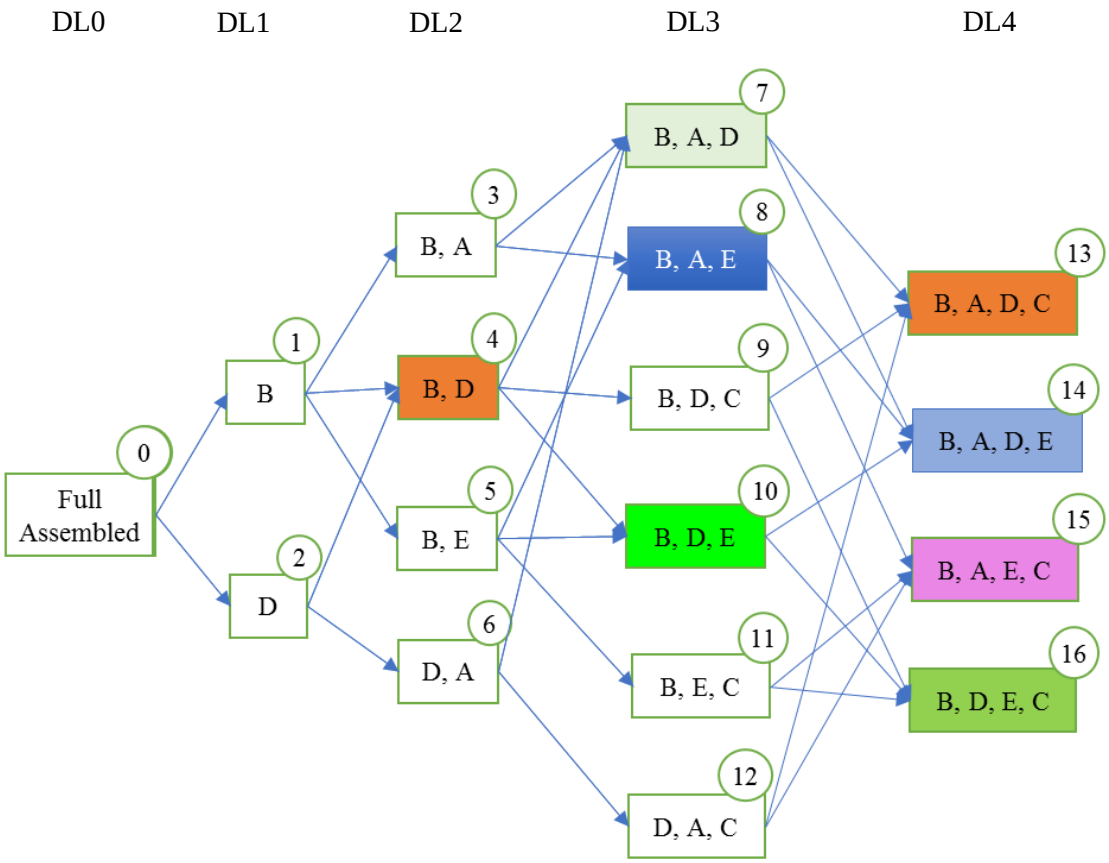

Figure 3.6: The DDD nodes represent Disassembly Levels zero, 1, 3, and 4.

The DDD shows the geometrical feasibility to get a group of parts disassembled stated at the same node. For example, the group of parts (B, A, D, C) can be disassembled by following the stated disassembly sequences at disassembly level 3 plus the resulted feasible disassemble part at this level (level 4). Figure 3.5 show all geometrical feasible disassembly sequences to get the stated group parts at level 4 nodes disassembled.

Table 3.14: Collision Test results at level 4 (Interference Matrix) By disassembling parts B, A, D and C.

Node #13

		Part Name	X+	X-	Y+	Y-	Z+	Z-	Row Summation	Resulted new nods to the next level.	Feasible disassemble parts at level 5 (Full Disassembled)
1	BADC	E	1	1	1	1	1	1	6	N17	BADCE
		Column Summation	1	1	1	1	1	1			

Table 3.15: Collision Test results at level 4 (Interference Matrix) By disassembling parts B, A, D and E.

Node #14

		Part Name	X+	X-	Y+	Y-	Z+	Z-	Row Summation	Resulted new nods to the next level.	Feasible disassemble parts at level 5 (Full Disassembled)
2	BADE	C	1	1	1	1	1	1	6	N17	BADEC
		Column Summation	1	1	1	1	1	1			

Table 3.16: Collision Test results at level 4 (Interference Matrix) By disassembling parts B, A, E and C.

Node #15

		Part Name	X+	X-	Y+	Y-	Z+	Z-	Row Summation	Resulted new nods to the next level.	Feasible disassemble parts at level 5 (Full Disassembled)
3	BAEC	D	1	1	1	1	1	1	6	N17	BAECD
		Column Summation	1	1	1	1	1	1			

Table 3.17: Collision Test results at level 4 (Interference Matrix) By disassembling parts B, D, E and C.

			Resulted new nods to the next level.	Feasible disassemble parts at level 5 (Full Disassembled)
4	BDEC	Node #16	N18	BDECA

Part Name	X+	X-	Y+	Y-	Z+	Z-	Row Summation
A	1	1	1	1	1	1	6
Column Summation	0	0	0	0	1	1	

All the four IMs at tables (3.13, 3.14, 3.15, and 3.16) refers to the case study assembly (Ball point Pen) has been fully disassemble while one part left as a final part to be considered as disassembled. Level 5 is considered as final disassembly level for this case example while at this work one part to be considered in disassembling at each level and this case example consists of five parts.

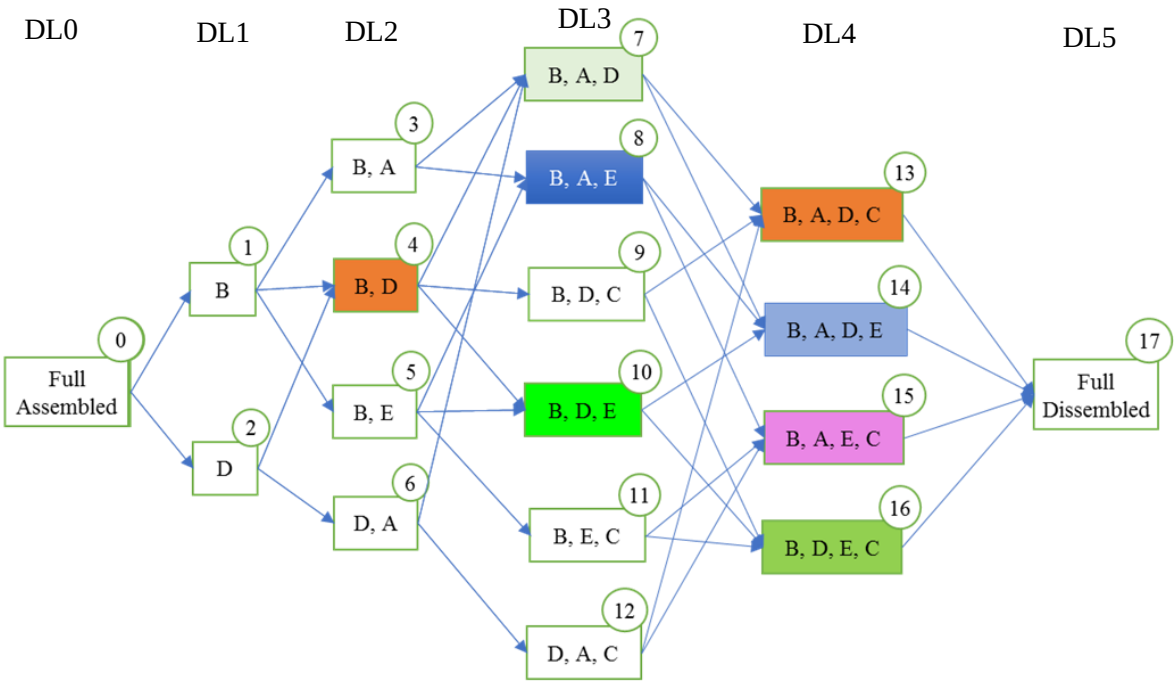

Figure 3.7: The DDD nodes represent Disassembly Levels zero, 1, 3, 4, and 5 (the full DDD explains all disassembly levels and disassembly states).

Table 3.18 gives all geometrical feasible disassembly sequences in matrix form. However, the DDD required to define the disassembly node.

Table 3.18: Precedence Disassembly Matrix (PM) of the Ballpoint Pen Example.

	N0	N1	N2	N3	N4	N5	N6	N7	N8	N9	N10	N11	N12	N13	N14	N15	N16	N17
N0	0	1	1	0	0	0	0	0	0	0	0	0	0	0	0	0	0	0
N1	0	0	0	1	1	1	0	0	0	0	0	0	0	0	0	0	0	0
N2	0	0	0	0	1	0	1	0	0	0	0	0	0	0	0	0	0	0
N3	0	0	0	0	0	0	0	1	1	0	0	0	0	0	0	0	0	0
N4	0	0	0	0	0	0	0	1	0	1	1	0	0	0	0	0	0	0
N5	0	0	0	0	0	0	0	0	1	0	1	1	0	0	0	0	0	0
N6	0	0	0	0	0	0	0	1	0	0	0	0	1	0	0	0	0	0
N7	0	0	0	0	0	0	0	0	0	0	0	0	0	1	1	0	0	0
N8	0	0	0	0	0	0	0	0	0	0	0	0	0	0	1	1	0	0
N9	0	0	0	0	0	0	0	0	0	0	0	0	0	1	0	0	1	0
N10	0	0	0	0	0	0	0	0	0	0	0	0	0	0	1	0	1	0
N11	0	0	0	0	0	0	0	0	0	0	0	0	0	0	0	1	1	0
N12	0	0	0	0	0	0	0	0	0	0	0	0	0	1	0	1	0	0
N13	0	0	0	0	0	0	0	0	0	0	0	0	0	0	0	0	0	1
N14	0	0	0	0	0	0	0	0	0	0	0	0	0	0	0	0	0	1
N15	0	0	0	0	0	0	0	0	0	0	0	0	0	0	0	0	0	1
N16	0	0	0	0	0	0	0	0	0	0	0	0	0	0	0	0	0	1
N17	0	0	0	0	0	0	0	0	0	0	0	0	0	0	0	0	0	0

3.5 Conclusion

The disassembly planning automation requires to put the structure of an assembly in a way that meets machine understanding. Representing the interferences that may appear through disassembly assembly's parts in a matrix form represents a convenient form to be readable by machines. At this work, Precedence Matrix has been built based on Interference matrices resulted from the collision test to ensure mentioning just the geometrical feasible disassembly sequences in the final Precedence Matrix. The Direct Disassembly Diagram (DDD) is constructed on the investigated geometric feasibility which integrates collision detection for each given component in an assembly. By using the Direct Disassembly Diagram (DDD), the redundant disassembly states or nodes can be easily discovered, therefore, there is no need to perform the collision tests at the

disassembly level i +1 for redundant disassembly states. A traditional case study was used to demonstrate the proposed methodology in building the final Precedence Matrix. Also, the mentioned methodology at this work for constructing the Precedence Matrix of the assembly using the Interference matrices was the result of the collision tests developed. At this stage, however, the work does not consider applying visual and tangible technologies to verify the work in the aspects of holistic perception.

CHAPTER 4: PREDICTING THE CHANGE IN THE GEOMETRICAL DISASSEMBLE FEASIBILITY OF MECHANICAL ASSYMBLIESDUE TO WEAR: A STUDY OF ASSISTING THE DESIGN FOR DISASSEMBLY BY UTILIZING THE CENTRALITY METRICS

4.1 Abstract

Mechanical devices (assemblies) are made up of many parts and structures that are assembled to meet the users' mechanical, practical, and comfort requirements. In general, assemblies in their life span needs to maintain, repair, update or dismantle separately at their End-of-Use, leading to waste of some of their parts. Design for Disassembly (DFD) methods seek to minimize waste by developing assemblies that allow components, elements, and materials to be reused. One important feature is the interface between the elements of the assemblies. Indeed, the ease of dismantling assemblies varies greatly based on the form of interaction (contact, non-contact), usability, and assembly sequence. Today, methods such as the hierarchical pattern framework advocate mapping component relationships using nodes and edges, which describe components and relations, respectively. While a network is described within the context of this system, it appears that the networks are mostly used as a visual aid for the assessor to qualify component interactions. The ability of graph theory in general and social network research, in particular, to classify assemblies' disassemble networks is explored in this article. To do so, comparisons between graph theory metrics will be studied to reveal the key parallels, disparities, and opportunities for using centrality metrics in determining the disassemble viability of assemblies during the design process. In addition, a discussion of social networks' particular interest in DFD will be created. Finally, this study suggests that designers use state-of-the-art expertise from

other fields such as data processing and network analytics to characterize and analyze disassembly, allowing them to minimize waste and improve product reuse in buildings.

4.2 Introduction

In recent years of environmental awareness, the steadily increasing consumption of industrial products is facing environmental issues for both consumers and manufacturers. These products sooner or later have to be dumped in landfills after their life cycle are over. Product life cycle becomes short not only because they fail but also because they go out of style or become technologically obsolete. As a commodity approaches the end of its usable life, however, it does the most environmental harm. The disposal of this product by conventional means, such as landfill or incineration, represents an unsustainable loss of raw material resources and poses another problem because the product does not simply disappear after disposal. Since the value of preserving the environment and natural resources may soon predominate the cost of recycling, then it is expected to face a growing demand to dispose of old products constructively by removing hazardous materials, retrieving reusable components, and recycling.

Although it is rarely possible to recycle a product completely, it would be noteworthy to maximize the recycled resources and to minimize the rubbish of the remaining product. Product recovery is usually performed in two ways: recycling and remanufacturing [137]. The retrieval of parts and materials has proven to be effective using disassembly. However, the process of disposing and recycling old products which includes the cost of handling, sorting, and disassembly will play an important role. Some manufacturers have incorporated take-back regulations into their goods, requiring them to be responsible for the environmentally sustainable recycling or disposal of their end-of-life products. The law is meant to provide suppliers with a

financial incentive to design more environmentally sustainable goods and to reduce waste's environmental effects by increasing the amount recovered and recycled. Product disassembly aims to acquire pure secondary materials and distinguish environmentally sensitive materials from other materials [138]. One of the potential end-of-use disposal solutions for discontinued products is the disassembly of the assembly into its components. Even though disassembly may seem to provide a way to minimizing the environmental problems, it should be mentioned that the cost of disassembly and the market process for recycled materials is less than the environmental benefits. Good maintenance and servicing can prolong the product life cycle; these tasks typically necessitate partial disassembly to replace or restore components that are incorporated with other parts in the product framework. The main issue is how to predict changes in the disassemblability of an assembly during its lifetime in early design phases. Despite the fact that graph theory, the mathematical basis of network structures, is well defined and commonly used today, it seems that the disassembling industry, or at least assembly designers, are not yet using it to analyze, grasp, or refine assembly designs. Assemblies consist of components linked and attached physically and their connections affect the disassembling priority and then disassembling feasibility. Fortunately, graph theory offers metrics and theories that enable such structures to be quantified and qualified. However, this work exercising Is it feasible to use centrality metrics in measuring disassembly ability? or could network analysis help to assess disassembly ability for mechanical assemblies? If yes, which centrality metric is the fittest? Finally, this work provides an approach to use the centrality metrics in disassembly study.

4.2.1 Design for Disassembly

The production of products with a low environmental impact is becoming increasingly relevant. Many designers are recognizing this and, as a result, are requiring tools and techniques that will enable them to design responsibly. One technique that can be used is design for disassembly (DFD). The product can be disassembled to allow for repairs, increase serviceability, and affect product end-of-life priorities such as reuse, remanufacture, and recycling. There are 2 basic methods of disassembly which are usually used: (1) non-destructive disassembly and (2) destructive disassembly. In this work, only non-destructive disassembly has been considered in the disassembly process. It is important to consider in the designing for disassembly of an assembly that the designed assembly should be easy to disassemble to get the most value of the assembly's parts at its End-of-Use phase. therefore, the assembly needs to disassemble by non-destructive operations to get the most of its parts intact for reuse or remanufacturing purposes and can easily be recycled.

4.2.2 The Importance of Centrality

Centrality is a key principle in graph analytics for defining critical nodes in a graph. It's used to determine the value (or "centrality," as in how "central" a node is in a graph) of different nodes in a graph. Based on how "importance" is described, each node can now be significant from a different perspective. Each metric of centrality determines the value of a node from a particular viewpoint and provides important theoretical knowledge about the graph and its nodes. Some of centrality metrics that have been used in this work.

4.2.2.1 Degree Centrality

Degree centrality assigns a ranking to each node based solely on the number of ties it holds. degree centrality measures the number of simple, "one hop" connections

each node has to other nodes in the network. Degree Centrality is defined mathematically as D (i) for node i as below:

$$D(i) = \sum_j m(i,j) \qquad (4.1)$$

Where m (i,j) = 1 if there is a link from node i to node j. [139]

4.2.2.2 Betweenness Centrality

Betweenness centrality measures the number of times a node is found on the shortest path between other nodes. This metric identifies growing nodes in a network act as ‘bridges' between other nodes. This is accomplished by first finding all of the shortest paths and then calculating how many times each node lands on one of them [140]. Mathematically, Betweenness centrality is defined as [140]:

$$B(i) = \sum_{a,b} \frac{g\ aib}{g\ ab} \qquad (4.2)$$

Where a, b is any pair of nodes in the graph

$g\ aib$ is the number of shortest paths from node a to b passing through i.

$g\ ab$ is the number of shortest paths from node a to b.

4.2.2.3 Closeness Centrality

Closeness centrality assigns a score to each node depending on how connected they are to the rest of the network's nodes. Closeness centrality assigns a score to each node depending on how connected they are to the rest of the network's nodes [140]. Closeness centrality defined as C(i) as below [139]:

$$C(i) = \sum_j d(i,j) \qquad (4.3)$$

Where :

d (a,b) = Number of edges between two nodes (a, b) on the shortest path from a to b, if there is a path from a to b.

d(a , b) = 0, if a = b

d(a , b) = ∞ (Infinity) , if no path exists from a to b

4.3 Methodology

The proposed methodology at this work is consisting of two parts to track the change in the geometrical disassemble feasibility of a mechanical assembly over its lifetime. The first part of the methodology is performing the collision test developed in the previous work presented in the previous chapter to determine Direct Disassembly Diagram (DDD). The used Direct Disassembly Diagram shows all the geometrical feasible disassembly sequences for the tested mechanical assembly because it has been depicted based on the results of the collision tests between the assembly's parts. While the DDD is a diagram shows the direct relations between the disassembly nodes, number of available social network metrics (i.e. Centrality Metrics) is used to evaluate the geometrical disassemble feasibility of a mechanical assembly. Centrality metrics have been used to analyze the DDD. Analyzing the DDD is the second part of the proposed methodology at the present work. To predict the change in the disassemble feasibility when the tested assembly is still in the design phase, it is needed to do changing in the dimensions of the assembly's parts that may expose to wear into its lifetime due the corrosion that happens due to the friction between the assembly's parts, like the wear that happens in bushing due to the friction between the shaft spindles inside the busing. After processing the analyzing of the DDD of original design of the tested assembly by using centrality metrics, the same process of analyzing should be repeated after manipulating in parts dimensions. The change in dimensions in the parts

that may expose to wear during the parts using lifetime. The amount of change in parts dimensions should simulate the amount of changing in the parts dimensions that may happen due to corrosion after a period of real working time.

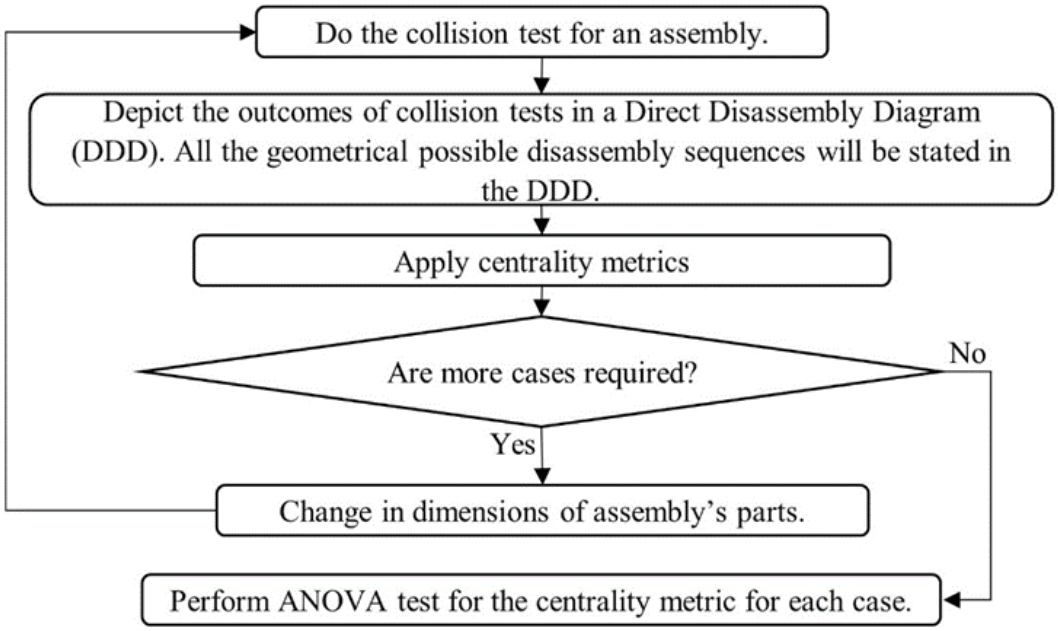

Figure 4.1: Proposed Methodology for Predicting disassemble feasibility.

4.4 Case Study

The selected product category is a simple mechanical assembly (figure 3). The case example consists of seven parts. While the intended disassembly operations at this work are non-destructive and disassembling one part at on disassembly step, this case example requires seven disassembly levels to get the assembly full disassembled. The most expositing parts in this assembly to wear due to friction with other assembly's parts are the Bushings. The friction that happens between the bushings and shaft during operation mode causes mainly wear for the bushings. The shaft in its role holds the roller. Therefore, the effect of bushings wears on the disassemble feasibility has been considered in this work.

Case 1 represents the original design with no wear on bushings. Case 2 considers one of the bushings has been completely corroded and Case 3 considers both shaft support bushings to be have been completely corroded. Figure 4.4, 4.5, 4.6 represents the Direct Disassembly Diagram (DDD) represents the geometrical disassembly feasibility sequences for Case 1, Case 2, Case 3 respectively. The proposed method in this work has been applied to the Roller Guide (figure 4.2) with assuming all the Roller Guide parts are rigid. Table 1 states the addressed cases for the Roller Guide example in this work.

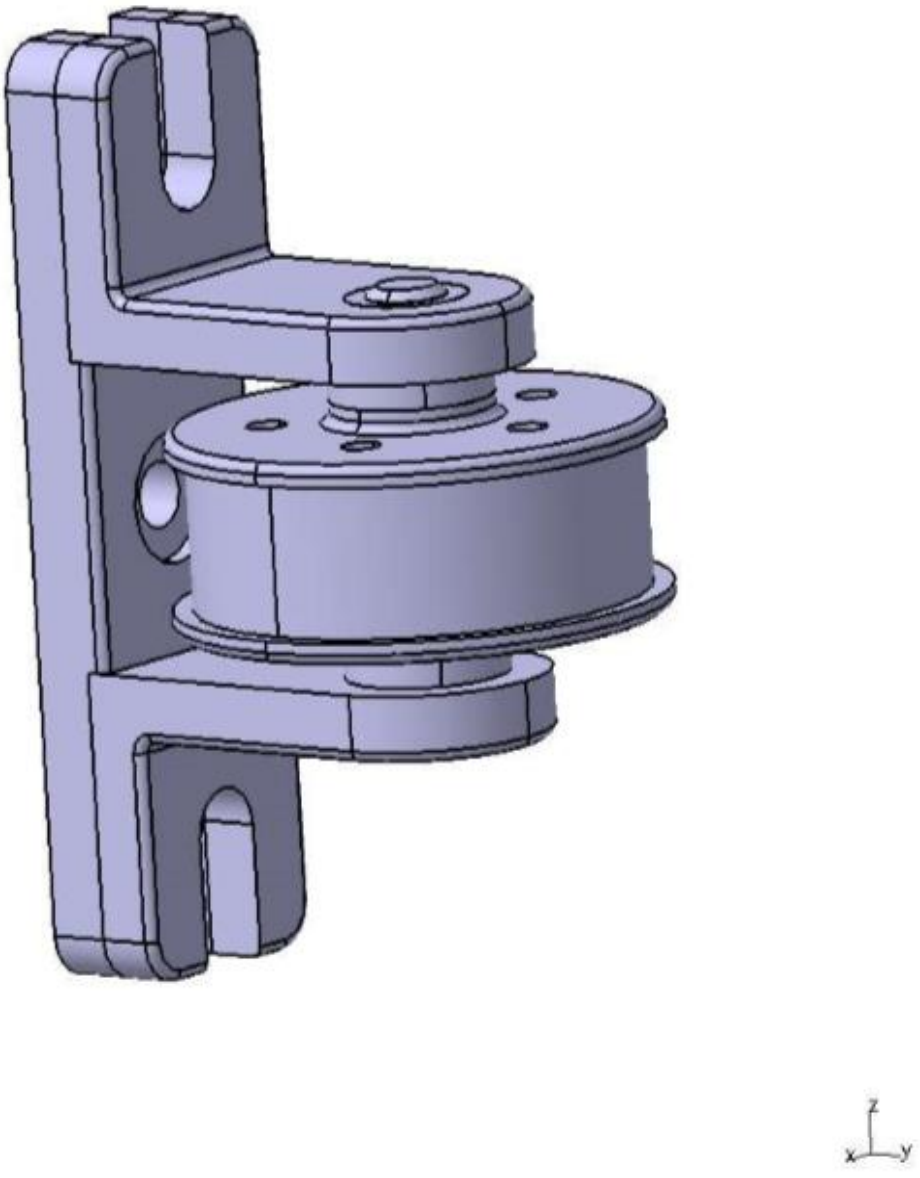

Figure 4.2: Roller Guide case study

Table 4.1: Stating the addressed case studies.

	Shaft r = 9.52 mm 0% Corrosion
One Bushing t = 3.18 mm 0 %Corrosion	Case 1
One Bushing t = 0.0 mm 100 %Corrosion	Case 2
Two Bushings t = 0.0 mm 100 %Corrosion	Case 3

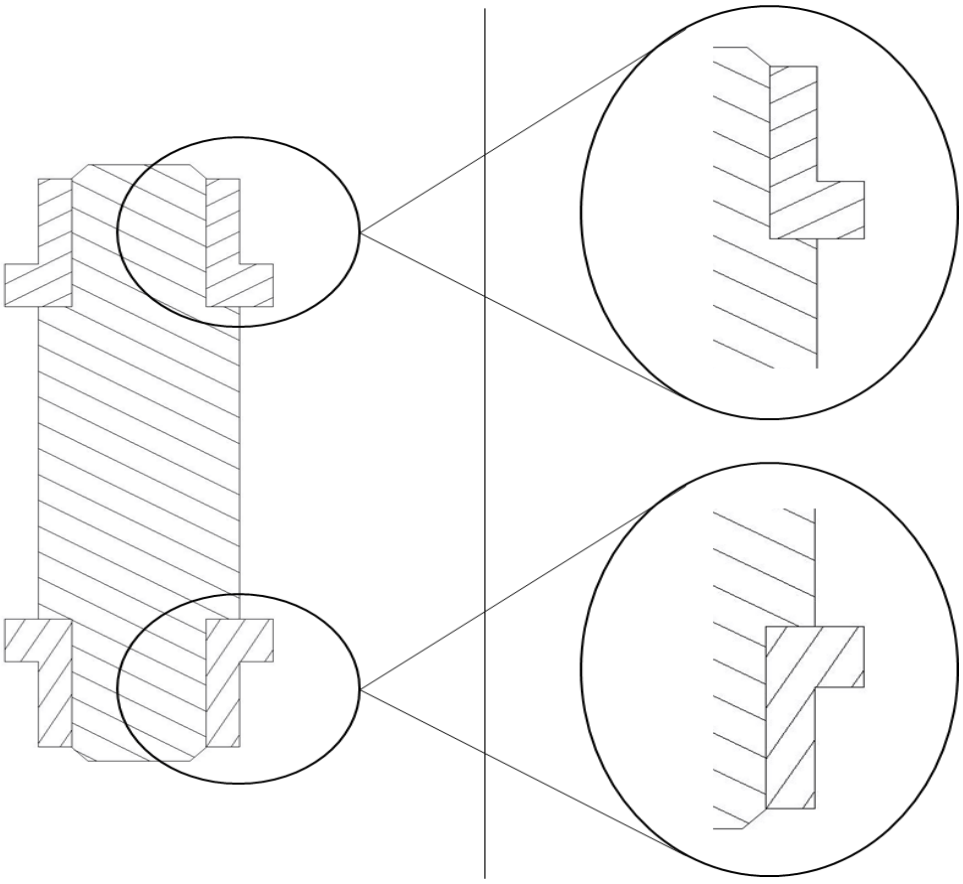

Figure 4.3: Sectional view for the parts in action at Case 1.

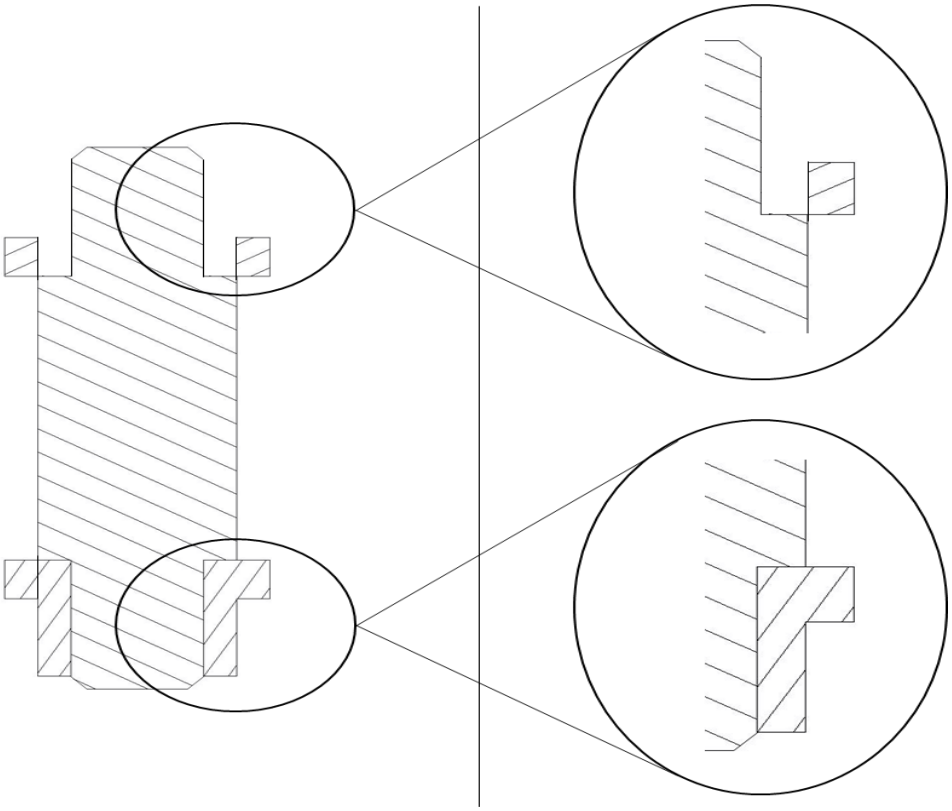

Figure 4.4: Sectional view for the parts in action at Case 2.

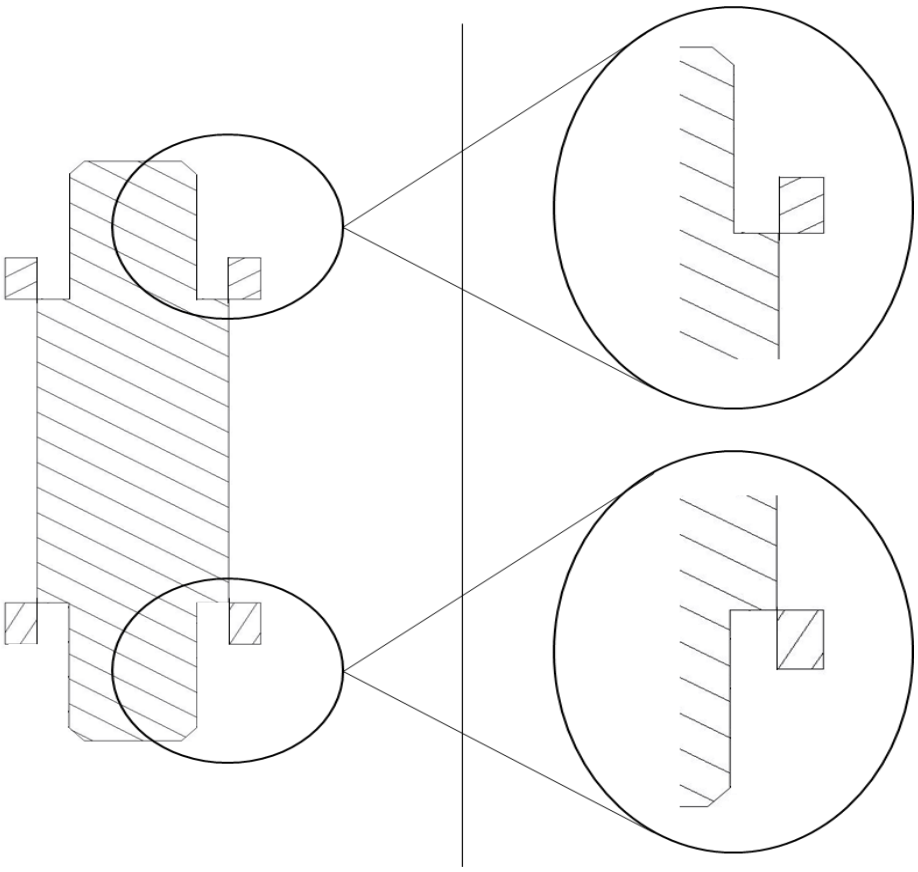

Figure 4.5: Sectional view for the parts in action at Case 3.

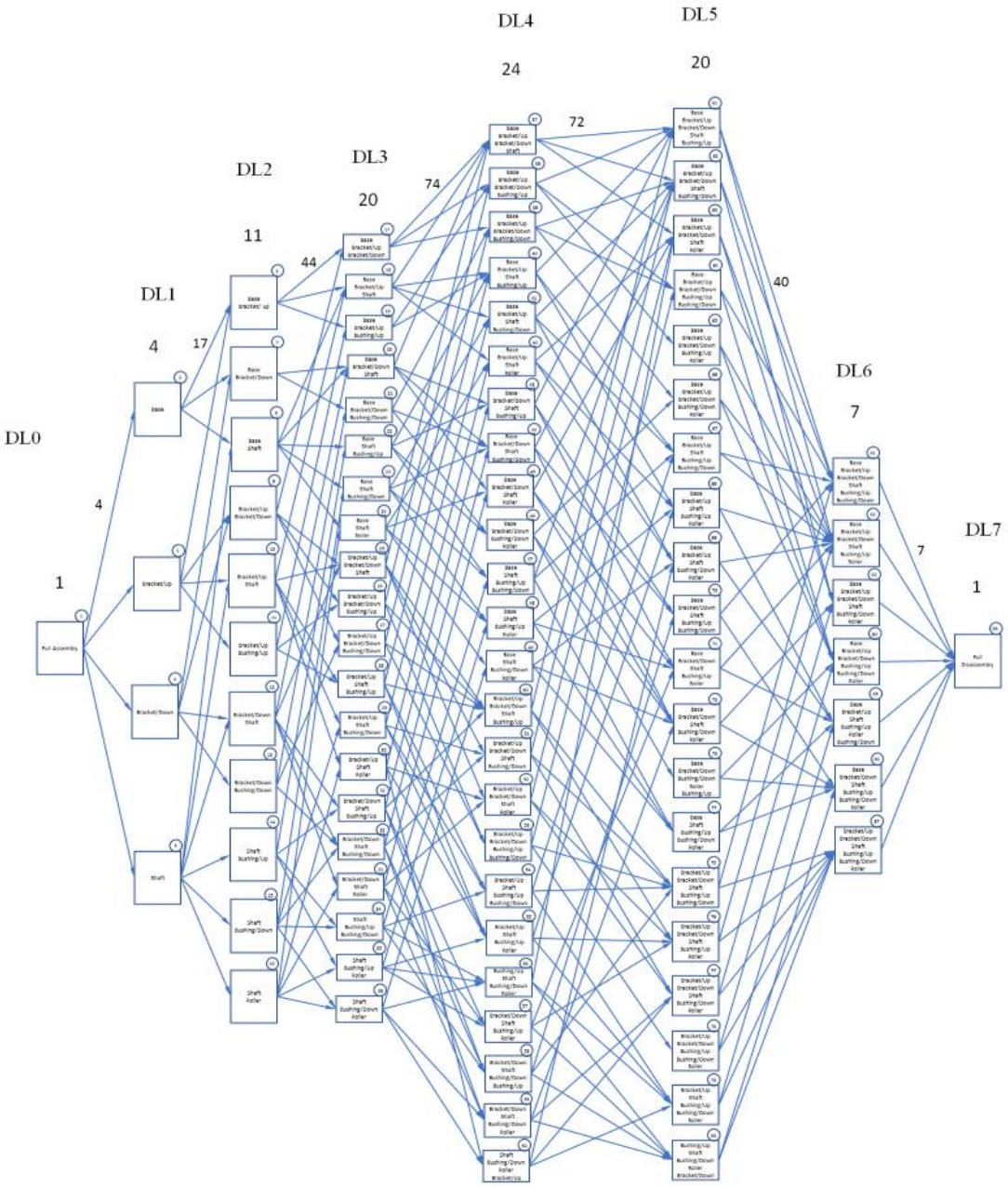

Figure 4.6: The DDD for Case 1.

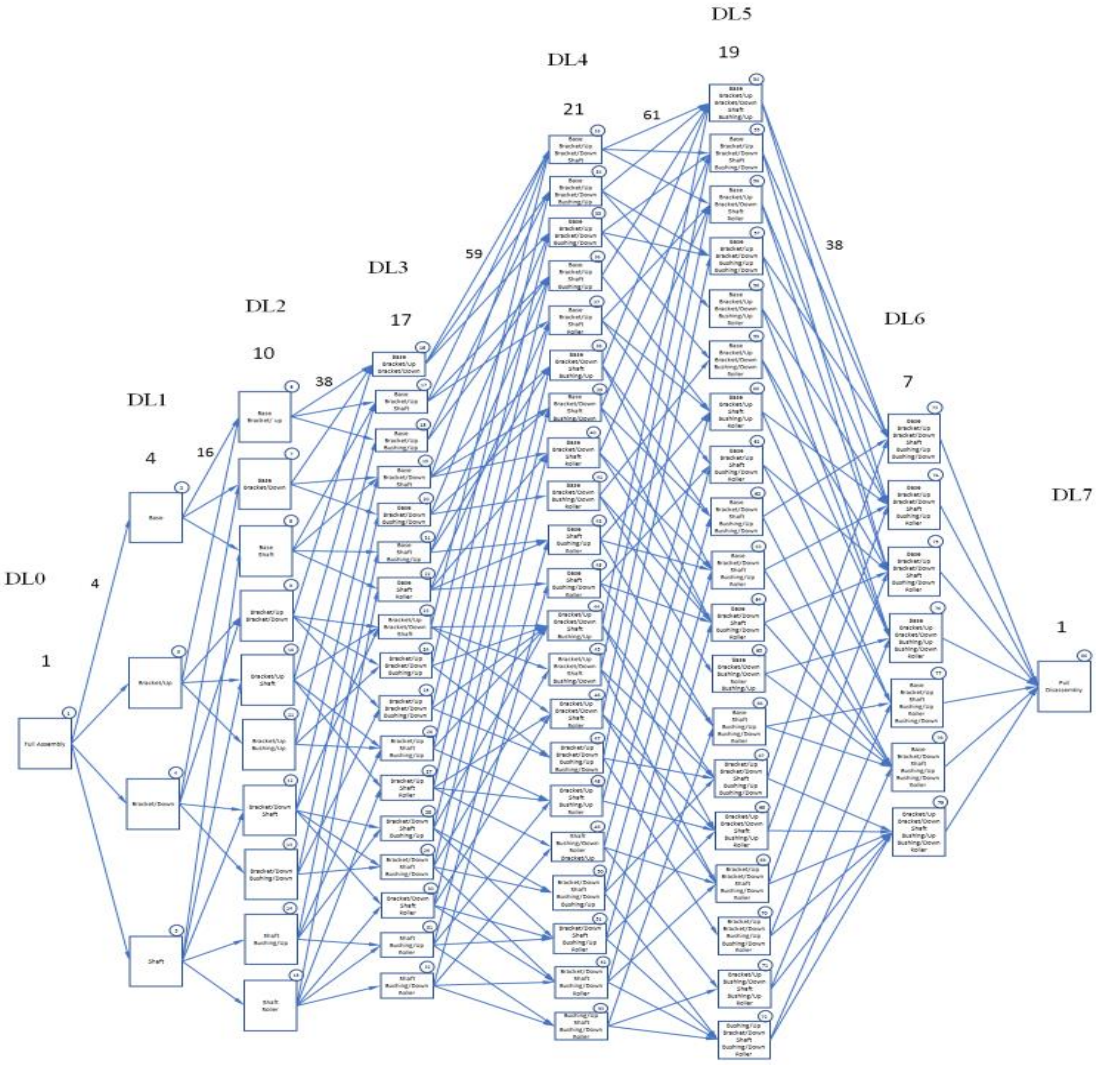

Figure 4.7: The DDD for Case 2

4.5 Discussion

4.5.1 Disassemble Feasibility Analysis for the Whole Assembly's DDDs

The tracking precision of changing in the disassemble feasibility of a mechanical disassembly increases by increasing the number of corrosion simulation runs. The analysis of the disassemble feasibility should run after every change in the dimensions of the part after a period of the assembly's working time. In all the resulted DDD for each case, the number of disassembly levels are the same, however the number of nodes for each disassembly level is different for each case. The number of disassembly nodes

is increasing after considering one of the bushings at the Roller Guide has been 100% wear and this rising continue for case 3 when considering both bushings are 100% wear.

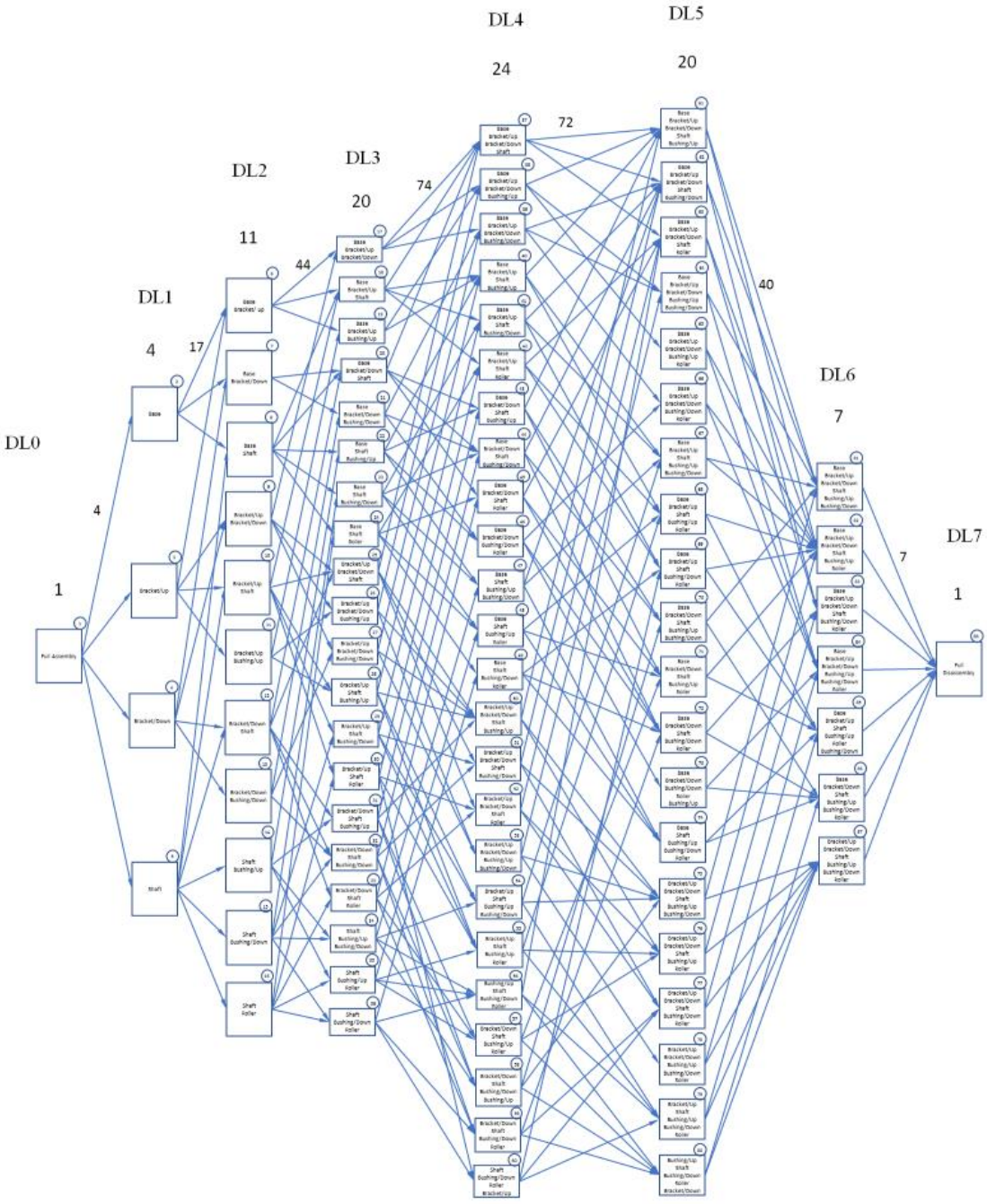

Figure 4.8: The DDD for Case 3.

Table 4.2 shows the change in the disassembly nodes for each disassembly level for each case.

Table 4.2: Disassembly level nodes for each case

		Level 0	Level 1	Level 2	Level 3	Level 4	Level 5	Level 6	Level 7
Case 1	Roller Guide BEFORE manipulation in Bushing parts dimension	1	3	5	9	13	13	7	1
Case 2	Roller Guide AFTER manipulation in ONE Bushing part dimension	1	4	10	17	21	19	7	1
Case 3	Roller Guide AFTER manipulation in TWO Bushing parts dimensions	1	4	11	20	24	20	7	1

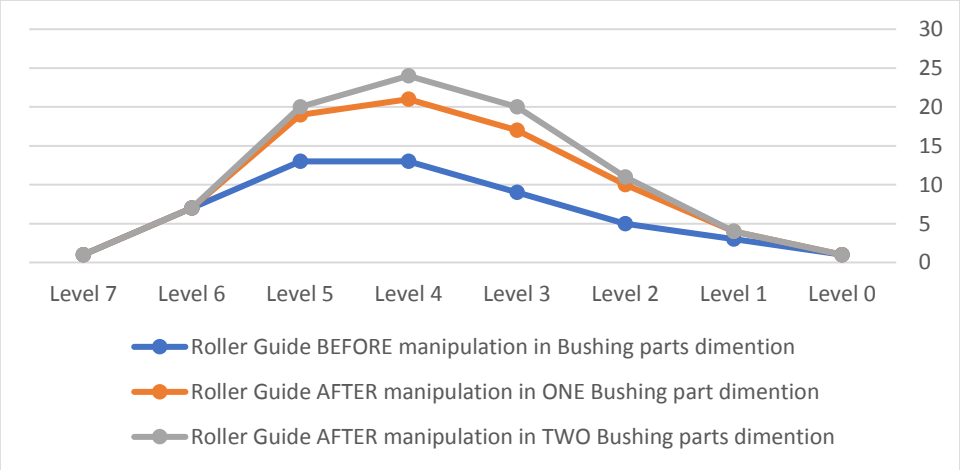

Figure 4.9: Disassemble feasibility level Chart

By noticing the increasing in the number of nodes and the number of connections between the disassembly level's nodes in the DDDs for each case in Figures 4.4, 4.5, 4.6, it is easy to conclude that the number of feasible geometrical disassembly sequences rises with rising the corrosion in the mechanical assembly. However, to measure how much change in disassemble feasibility is happening due to the wear or change in the parts of assembly dimensions, this work proposed using the relations between the nodes in the developed DDD for each case study to study the change in the disassemble feasibility. Centrality metrics which are developed for analyzing the social

network has been used to measure the weight of each node in the DDDs in point view of each metric. Gephi ® software [141] is used to perform the measuring of some of centrality metric. Appendix B has the weight values for each node at the DDD for each case in point view of three centrality metrics (i.e. Closeness Centrality, Betweenness Centrality, and Degree). Tables 4.3, 4.4, and 4.5 represent respectively the calculation results of Closeness Centrality, Betweenness Centrality, and Degree for each node in each case.

Table 4.3: The calculation results of Closeness Centrality, Betweenness Centrality, and Degree for each node in Case 1.

Case 1			
ID	Closeness Centrality	Betweenness Centrality	Degree
1	0.24757282	0	3
2	0.296	20.97857143	4
3	0.296	20.97857143	4
4	0.27777778	6.042857143	3
5	0.36231884	38.6025641	5
6	0.37313433	26.15586081	5
7	0.33962264	21.54285714	4
8	0.37313433	26.15586081	5
9	0.33962264	21.54285714	4
10	0.42857143	36.97106227	5
11	0.46875	35.83113553	6
12	0.46875	35.83113553	6
13	0.44827586	10.56895604	4
14	0.44827586	10.56895604	4
15	0.44444444	27.54542125	5
16	0.44827586	10.56895604	4
17	0.44827586	10.56895604	4
18	0.44444444	27.54542125	5
19	0.58333333	37.38717949	6
20	0.58333333	37.38717949	6
21	0.58333333	14.96108059	5
22	0.58333333	14.96108059	5
23	0.58333333	16.25531136	5
24	0.58333333	14.96108059	5
25	0.58333333	14.96108059	5
26	0.58333333	14.68113553	5

Case 1			
ID	Closeness Centrality	Betweenness Centrality	Degree
27	0.54545455	11.94093407	4
28	0.54545455	11.94093407	4
29	0.58333333	14.68113553	5
30	0.54545455	11.94093407	4
31	0.54545455	11.94093407	4
32	0.75	16.56245421	5
33	0.75	15.17358059	5
34	0.75	15.17358059	5
35	0.75	15.17358059	5
36	0.75	15.17358059	5
37	0.75	9.66007326	5
38	0.75	10.53076923	5
39	0.75	10.53076923	5
40	0.75	9.66007326	5
41	0.75	3.718681319	3
42	0.75	15.46208791	5
43	0.75	15.46208791	5
44	0.75	3.718681319	3
45	1	7.900274725	5
46	1	7.900274725	5
47	1	7.467032967	5
48	1	7.467032967	5
49	1	7.90952381	7
50	1	2.677930403	3
51	1	2.677930403	3
52	0	0	7

Table 4.4: The calculation results of Closeness Centrality, Betweenness Centrality, and Degree for each node in Case 2.

Case 2			
ID	Closeness Centrality	Betweenness Centrality	Degree
1	0.26072607	0	4
2	0.29710145	10.50903393	4
3	0.30496454	15.04686537	5
4	0.30625	19.59038792	5
5	0.31976744	29.85371277	6
6	0.35483871	20.25152642	5
7	0.36111111	28.29916274	5
8	0.375	29.8865223	6
9	0.36986301	31.50518514	6
10	0.375	29.55932687	6
11	0.3559322	8.873636467	4
12	0.3875	41.56490269	7
13	0.35714286	12.65078756	4
14	0.375	11.63371544	5
15	0.3875	22.77523438	6
16	0.4516129	38.07316848	6
17	0.44827586	31.3702573	6
18	0.42307692	12.9976362	4
19	0.46875	43.71203863	7
20	0.4516129	27.53898997	5
21	0	0	2
22	0.46875	28.33231303	6
23	0.46875	38.43456099	7
24	0.4516129	22.13750145	5
25	0.44444444	24.07464442	5
26	0.44444444	22.41614343	6
27	0.46875	24.7960168	6
28	0.46875	23.94878621	6
29	0.46875	25.90799878	6
30	0.46875	19.90269097	6
31	0.46875	21.26043999	6
32	0.46875	10.09681336	5
33	0.58333333	37.35609341	7
34	0.58333333	33.88475555	6
35	0.58333333	32.01598125	6
36	0.54545455	20.18501837	5
37	0.58333333	26.23191927	6
38	0.58333333	16.73468212	5
39	0.58333333	24.06297231	6
40	0.58333333	21.26139401	6

Case 2			
ID	Closeness Centrality	Betweenness Centrality	Degree
41	0.58333333	13.07648856	4
42	0.58333333	13.76520001	5
43	0.58333333	11.93298097	5
44	0.58333333	42.0434779	8
45	0.58333333	15.68373799	5
46	0.58333333	20.49010828	6
47	0.58333333	20.48913035	5
48	0.54545455	14.13872123	5
49	0.58333333	14.12513222	5
50	0.58333333	13.65173102	5
51	0.58333333	17.40453951	6
52	0.58333333	16.76834032	6
53	0.58333333	12.69759535	5
54	0.75	28.58130365	7
55	0.75	19.58578449	6
56	0.75	18.97385588	6
57	0.75	15.57143403	5
58	0.75	6.385649371	3
59	0.75	8.712532145	4
60	0.75	22.63584348	6
61	0.75	11.18883185	5
62	0.75	11.44213872	5
63	0.75	14.4132313	6
64	0.75	17.68783394	7
65	0.75	2.79171791	3
66	0.75	9.101545509	5
67	0.75	17.19503359	6
68	0.75	20.57370265	6
69	0.75	13.92279161	6
70	0.75	4.095515348	3
71	0.75	5.835493549	4
72	0.75	13.30576097	6
73	1	11.76645369	6
74	1	14.09208068	7
75	1	12.02932637	7
76	1	5.950138093	6
77	1	6.617864387	5
78	1	10.00922825	7
79	1	10.53490853	7
80	0	0	7

Table 4.5: The calculation results of Closeness Centrality, Betweenness Centrality, and Degree for each node in Case 3.

Case 3			
ID	Closeness Centrality	Betweenness Centrality	Degree
1	0.26283988	0	4
2	0.28494624	11.2339686	4
3	0.30718954	16.36369729	5
4	0.29577465	16.65961294	5
5	0.32211538	38.74272117	7
6	0.35820896	23.53826561	5
7	0.31818182	24.40345701	4
8	0.35833333	49.30297509	7
9	0.36470588	33.09487189	6
10	0.3875	35.93999791	7
11	0.35820896	9.839009768	4
12	0.37606838	44.69759143	7
13	0.35353535	14.0795678	4
14	0.36538462	16.59415122	5
15	0.38	16.38598146	6
16	0.3875	17.12413082	6
17	0.4516129	28.06436406	5
18	0.46875	36.19638659	7
19	0.42857143	13.91795384	4
20	0.421875	71.27329147	7
21	0.43589744	33.60180277	5
22	0.45652174	37.66528042	6
23	0.45714286	20.8093434	6
24	0.46875	22.25043235	6
25	0.46875	34.74287477	7
26	0.4516129	21.97295937	5
27	0.44444444	27.45385835	5
28	0.46875	22.33272226	6
29	0.46153846	19.65719093	6
30	0.46875	35.01575025	7
31	0.45714286	29.13340774	6
32	0.45238095	37.42150683	7
33	0.45238095	62.5492475	7
34	0.45945946	18.24015545	6
35	0.45945946	17.58243341	6
36	0.44117647	6.119038241	4
37	0.58333333	33.59852158	7
38	0.58333333	30.14328897	6
39	0.57142857	23.21842722	5
40	0.58333333	41.55198316	8
41	0.57142857	19.423027	6
42	0.58333333	21.51382464	6
43	0.57142857	35.41614276	7
44	0.57142857	25.91835495	6

Case 3			
ID	Closeness Centrality	Betweenness Centrality	Degree
45	0.57142857	35.25626465	5
46	0.57142857	17.14808298	5
47	0.5625	25.526086	6
48	0.58333333	20.65134589	6
49	0.57142857	12.81094859	5
50	0.58333333	34.11218793	8
51	0.58333333	22.60114101	6
52	0.58333333	15.64503218	5
53	0.58333333	21.90478537	5
54	0.57142857	23.00013786	6
55	0.58333333	27.65042937	7
56	0.57142857	22.93461361	6
57	0.57142857	17.6694574	6
58	0.58333333	22.4135808	5
59	0.58333333	23.0247647	6
60	0.5625	25.86757139	6
61	0.75	23.31516947	7
62	0.75	32.44118013	8
63	0.75	24.35161756	7
64	0.75	14.07440694	5
65	0.75	5.6997779	3
66	0.75	10.79377805	4
67	0.75	23.05888071	7
68	0.75	21.59780083	6
69	0.75	25.20356007	7
70	0.75	7.144806264	4
71	0.75	16.83361442	6
72	0.75	20.67367021	6
73	0.75	6.614900095	3
74	0.75	13.75131106	5
75	0.75	21.35648588	7
76	0.75	16.94594295	6
77	0.75	16.71109854	6
78	0.75	4.395627777	3
79	0.75	19.68212731	6
80	0.75	18.35424384	6
81	1	14.64720659	7
82	1	20.10176545	10
83	1	9.856285457	5
84	1	5.706385262	6
85	1	10.58165611	6
86	1	7.371377436	6
87	1	11.7353237	7
88	0	0	7

ANOVA test has been used to analyze the centrality metrics values for each case and to show if there is a happening change in the disassemble feasibility along with the change in some of the assembly's parts due to wear. Betweenness Centrality and Degree metrics have revealed that change in the disassemble feasibility at confidence level 95% as it is shown in the tables 4.6, 4.7, and 4.8.

Table 4.6: ANOVA Values for Betweenness Centrality metric.

Betweenness Centrality metric

Analysis of Variance

Source	DF	Adj SS	Adj MS	F-Value	P-Value
Factor	2	1655	827.3	7.03	0.001
Error	220	25894	117.7		
Total	222	27548			

Means

Factor	N	Mean	StDev	95% CI
BC Case 1	53	15.69	9.98	(12.76; 18.63)
BC Case 2	81	18.72	9.98	(16.35; 21.10)
BC Case 3	89	22.57	12.04	(20.30; 24.83)

Pooled StDev = 10.8489

Table 4.7: ANOVA Values for Degree Centrality metric

Degree Centrality metric

Analysis of Variance

Source	DF	Adj SS	Adj MS	F-Value	P-Value
Factor	2	43.50	21.748	17.82	0.000
Error	217	264.85	1.221		
Total	219	308.35			

Means

Factor	N	Mean	StDev	95% CI
D Case1	52	4.692	0.919	(4.390; 4.994)
D Case2	80	5.500	1.091	(5.257; 5.743)
D Case3	88	5.841	1.212	(5.609; 6.073)

Pooled StDev = 1.10476

Table 4.8: ANOVA Values for Closeness Centrality metric

Closeness Centrality metric

Analysis of Variance

Source	DF	Adj SS	Adj MS	F-Value	P-Value
Factor	2	0.02597	0.01298	0.30	0.744
Error	220	9.63148	0.04378		
Total	222	9.65745			

Means

Factor	N	Mean	StDev	95% CI
Closeness Centrality Case 1	53	0.5988	0.2278	(0.5421; 0.6554)
Closeness Centrality Case 2	81	0.5743	0.2103	(0.5285; 0.6201)
Closeness Centrality Case 3	89	0.5727	0.1964	(0.5290; 0.6164)

Pooled StDev = 0.209235

The Means of Variance resulted from ANOVA test of the centrality metrics that points to the change in disassemble feasibility between the cases is used to show the percentage amount of change between cases. Equation 4.4 is used to measure the change.

$$FC = \frac{Case_{i+1} - Case_i}{Case_i} \times 100\% \qquad (4.4)$$

Table 4.6 states the percentage change in the means of variance resulted from ANOVA test which are considered as a metric disassemble feasibility change. In the viewpoint of Betweenness centrality metric, the disassemble feasibility will increase in 52.8% if one bushing completely worn, and 62.67% if both bushings completely worn. However, Degree metric shows that the disassemble feasibility will increase in 17.0% if one bushing completely worn, and 23.20% if both bushings completely worn.

Table 4.9: The percentage change in the Means of variance resulted from ANOVA test.

Centrality metrics	Case 1 to Case 2	Case 2 to Case 3
Betweenness	52.8%	9.87%
Degree	17.0%	6.20%

Figure 4.8 depicts the percentage change in the geometrical disassemble. feasibility in terms of the Betweenness and Degree Centrality metrics.

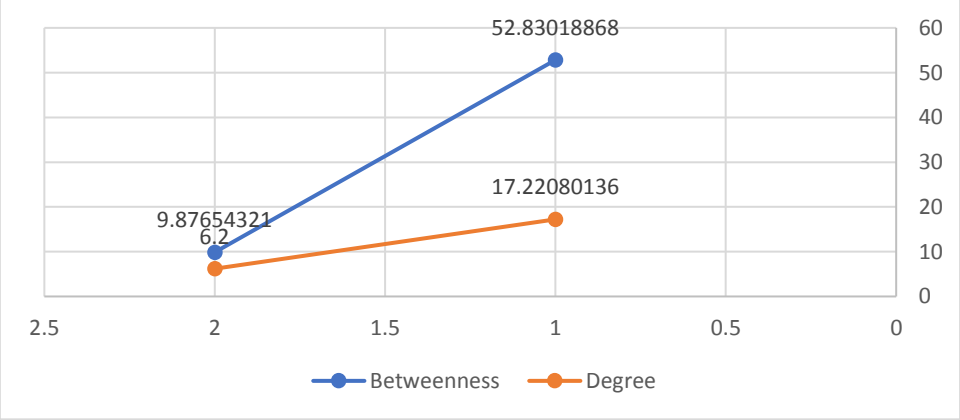

Figure 4.10: The percentage change in the geometrical disassemble feasibility.

4.5.2 Disassemble Feasibility Analysis for the Disassembly Levels of the Assembly's DDDs

To give more explanation for the gradual change of the disassembly feasibility that happens along the multiple disassembly levels of the disassembly sequences, the same analysis method that followed for disassemble feasibility analysis for the whole assembly's DDDs has been used at this section. The following are the analysis level by level of disassembly for the three case studies.

4.5.2.1 Disassembly Level Zero to Disassembly Level One

The calculation results of Closeness, Betweenness, and Degree Centrality metrics for each node in Case 1, Case 2, and Case 3 at disassembly level 1 are presented in tables 4.10, 4.11, and 4.12 respectively.

Table 4.10: The calculation results of Closeness Centrality, Betweenness Centrality, and Degree for each node in Case 1 at disassembly level 1.

ID	Closeness	Betweenness	Degree
1	1	0	3
2	0	0	1
3	0	0	1
4	0	0	1

Table 4.11: The calculation results of Closeness Centrality, Betweenness Centrality, and Degree for each node in Case 2 at disassembly level 1.

ID	Closeness	Betweenness	Degree
1	1	0	4
2	0	0	1
3	0	0	1
4	0	0	1
5	0	0	1

Table 4.12: The calculation results of Closeness Centrality, Betweenness Centrality, and Degree for each node in Case 3 at disassembly level 1.

ID	Closeness	Betweenness	Degree
1	1	0	4
2	0	0	1
3	0	0	1
4	0	0	1
5	0	0	1

The ANOVA test for the Closeness centrality metric values of disassemble level zero to one is shown in table 4.13. The Closeness metric at this level did not show there is a difference in means of the Closeness centrality metric values, therefore tracking the change in disassemble feasibility is not feasible at this disassembly level with this metric.

Table 4.13: The ANOVA test for the Closeness centrality metric values of disassemble level zero to one.

Analysis of Variance

Source	DF	Adj SS	Adj MS	F-Value	P-Value
Factor	2	0.00714	0.003571	0.02	0.983
Error	11	2.35000	0.213636		
Total	13	2.35714			

There was no observable difference in means in Betweenness centrality metric values of disassemble level zero to one. The degree centrality metric values of disassemble level zero to one is shown at table 4.14. At this level, Degree centrality metrics also did not show a change in disassemble feasibility

Table 4.14: The ANOVA test for the Degree centrality metric values of disassemble level zero to one.

Analysis of Variance

Source	DF	Adj SS	Adj MS	F-Value	P-Value
Factor	2	0.0286	0.01429	0.01	0.991
Error	11	17.4000	1.58182		
Total	13	17.4286			

4.5.2.2 Disassembly Level Zero to Disassembly Level Two

The calculation results of Closeness, Betweenness, and Degree Centrality metrics for each node in Case 1, Case 2, and Case 3 at disassembly level 2 are presented in tables 4.15, 4.16, and 4.17 respectively.

Table 4.15: The calculation results of Closeness Centrality, Betweenness Centrality, and Degree for each node in Case 1 at disassembly level 2.

ID	Closeness	Betweenness	Degree
1	0.61538462	0	3
2	1	2	4
3	1	2	4
4	1	1	3
5	0	0	2
6	0	0	1
7	0	0	2
8	0	0	1
9	0	0	2

Table 4.16: The calculation results of Closeness Centrality, Betweenness Centrality, and Degree for each node in Case 2 at disassembly level 2.

ID	Closeness	Betweenness	Degree
1	0.58333333	0	4
2	1	1.5	4
3	1	2.5	5
4	1	2.5	5
5	1	3.5	6
6	0	0	2
7	0	0	2
8	0	0	2
9	0	0	2
10	0	0	2
11	0	0	1
12	0	0	2
13	0	0	1
14	0	0	1
15	0	0	1

Table 4.16: The calculation results of Closeness Centrality, Betweenness Centrality, and Degree for each node in Case 2 at disassembly level 2.

ID	Closeness	Betweenness	Degree
1	0.58333333	0	4
2	1	1.5	4
3	1	2.5	5
4	1	2.5	5
5	1	3.5	6
6	0	0	2
7	0	0	2
8	0	0	2
9	0	0	2
10	0	0	2
11	0	0	1
12	0	0	2
13	0	0	1
14	0	0	1
15	0	0	1

The ANOVA test for the Closeness centrality metric values of disassemble level zero to one is shown at the table 4.17. The Closeness metric at this level also did not show there is a difference in means of the Closeness centrality metric values, therefore tracking the change in disassemble feasibility is not feasible at this disassembly level with this metric.

Table 4.17: The ANOVA test for the Closeness centrality metric values of disassemble level zero to two.

Analysis of Variance

Source	DF	Adj SS	Adj MS	F-Value	P-Value
Factor	2	0.08164	0.04082	0.19	0.827
Error	37	7.88976	0.21324		
Total	39	7.97139			

No difference in means in Betweenness centrality metric values and Degree centrality values at disassemble level zero to two. At this level, Betweenness and Degree centrality metrics also did not show a change in disassemble feasibility. Tables 4.18 and 4.19 are the ANOVA test for Betweenness and Degree metrics respectively.

Table 4.18: The ANOVA test for the Betweenness centrality metric values of disassemble level zero to two.

Analysis of Variance

Source	DF	Adj SS	Adj MS	F-Value	P-Value
Factor	2	0.1069	0.05347	0.04	0.964
Error	37	53.9931	1.45927		
Total	39	54.1000			

Table 4.19: The ANOVA test for the Degree centrality metric values of disassemble level zero to two.

Analysis of Variance

Source	DF	Adj SS	Adj MS	F-Value	P-Value
Factor	2	0.2944	0.1472	0.05	0.947
Error	37	99.3056	2.6839		
Total	39	99.6000			

4.5.2.3 Disassembly Level Zero to Disassembly Level Three

The calculation results of Closeness, Betweenness, and Degree Centrality metrics for each node in Case 1, Case 2, and Case 3 at disassembly level 3 are presented in tables 4.20, 4.21, and 4.22 respectively.

Table 4.20: The calculation results of Closeness Centrality, Betweenness Centrality, and Degree for each node in Case 1 at disassembly level 3.

ID	Closeness	Betweenness	Degree
1	0.425	0	3
2	0.6	6	4
3	0.6	6	4
4	0.625	2	3
5	1	5.66666667	5
6	1	5.66666667	5
7	1	3.5	4
8	1	5.66666667	5
9	1	3.5	4
10	0	0	3
11	0	0	2
12	0	0	2
13	0	0	1
14	0	0	1
15	0	0	2
16	0	0	1
17	0	0	1
18	0	0	2

Table 4.21: The calculation results of Closeness Centrality, Betweenness Centrality, and Degree for each node in Case 2 at disassembly level 3.

ID	Closeness	Betweenness	Degree
1	0.41333333	0	4
2	0.58823529	3.833333333	4
3	0.6	6	5
4	0.59090909	6.5	5
5	0.5862069	10.66666667	6
6	1	4.833333333	5
7	1	4.833333333	5
8	1	7	6
9	1	7	6
10	1	6.333333333	6
11	1	2.416666667	4
12	1	9.166666667	7
13	1	2.5	4
14	1	3.416666667	5
15	1	5.5	6
16	0	0	3
17	0	0	3
18	0	0	2
19	0	0	3
20	0	0	2
21	0	0	2
22	0	0	2
23	0	0	3
24	0	0	2
25	0	0	2
26	0	0	3
27	0	0	2
28	0	0	2
29	0	0	2
30	0	0	2
31	0	0	2
32	0	0	1

Table 4.22: The calculation results of Closeness Centrality, Betweenness Centrality, and Degree for each node in Case 3 at disassembly level 3.

ID	Closeness	Betweenness	Degree
1	0.40697674	0	4
2	0.57894737	4.083333333	4
3	0.59090909	6.533333333	5
4	0.59090909	6.116666667	5
5	0.58333333	14.26666667	7
6	1	5.5	5
7	1	3.5	4
8	1	9.166666667	7
9	1	7.666666667	6
10	1	8.733333333	7
11	1	2.5	4
12	1	8.066666667	7
13	1	2.416666667	4
14	1	3.666666667	5
15	1	4.416666667	6
16	1	5.366666667	6
17	0	0	2
18	0	0	3
19	0	0	2
20	0	0	3
21	0	0	2
22	0	0	2
23	0	0	2
24	0	0	2
25	0	0	3
26	0	0	2
27	0	0	2
28	0	0	2
29	0	0	2
30	0	0	3
31	0	0	2
32	0	0	3
33	0	0	1
34	0	0	2
35	0	0	2
36	0	0	2

The ANOVA test for the Closeness, Betweenness, and Degree centrality metric values of disassemble level zero to three are shown at the tables 4.23, 4.24, and 4.25 respectively. The Closeness, Betweenness, and Degree centrality metrics at this level also did not show there is a difference in means of their values, therefore tracking the change in disassemble feasibility is not feasible at this disassembly level with these metrics.

Table 4.23: The ANOVA test for the Closeness centrality metric values of disassemble level zero to three.

Analysis of Variance

Source	DF	Adj SS	Adj MS	F-Value	P-Value
Factor	2	0.0074	0.003689	0.02	0.982
Error	83	17.1247	0.206322		
Total	85	17.1321			

Table 4.24: The ANOVA test for the Betweenness centrality metric values of disassemble level zero to three.

Analysis of Variance

Source	DF	Adj SS	Adj MS	F-Value	P-Value
Factor	2	2.543	1.271	0.12	0.891
Error	83	911.897	10.987		
Total	85	914.440			

Table 4.25: The ANOVA test for the Degree centrality metric values of disassemble level zero to three.

Analysis of Variance

Source	DF	Adj SS	Adj MS	F-Value	P-Value
Factor	2	7.562	3.781	1.31	0.276
Error	83	239.833	2.890		
Total	85	247.395			

4.5.2.4 Disassembly Level Zero to Disassembly Level Four

The calculation results of Closeness, Betweenness, and Degree Centrality metrics for each node in Case 1, Case 2, and Case 3 at disassembly level 4 are presented in tables 4.26, 4.27, and 4.28 respectively.

Table 4.26: The calculation results of Closeness Centrality, Betweenness Centrality, and Degree for each node in Case 1 at disassembly level 4.

ID	Closeness	Betweenness	Degree
1	0.32608696	0	3
2	0.42222222	11.75	4
3	0.42222222	11.75	4
4	0.42307692	3.5	3
5	0.58823529	17.66666667	5
6	0.61111111	13.33333333	5
7	0.6	9.333333333	4
8	0.61111111	13.33333333	5
9	0.6	9.333333333	4
10	1	8.333333333	5
11	1	12.75	6
12	1	12.75	6
13	1	3.666666667	4
14	1	3.666666667	4
15	1	9.75	5
16	1	3.666666667	4
17	1	3.666666667	4
18	1	9.75	5
19	0	0	3
20	0	0	3
21	0	0	2
22	0	0	2
23	0	0	2
24	0	0	2
25	0	0	2
26	0	0	2
27	0	0	2
28	0	0	2
29	0	0	2
30	0	0	2
31	0	0	2
32	0	0	2

Table 4.27: The calculation results of Closeness Centrality, Betweenness Centrality, and Degree for each node in Case 2 at disassembly level 4.

ID	Closeness	Betweenness	Degree
1	0.32704403	0	4
2	0.42	6.56965812	4
3	0.43396226	9.63551507	5
4	0.421875	11.93880535	5
5	0.425	19.85602146	6
6	0.61538462	9.974358974	5
7	0.58823529	13.22222222	5
8	0.6	16.52606838	6
9	0.61111111	15.54991646	6
10	0.6	16.13726624	6
11	0.61538462	4.739268042	4
12	0.6	23.67084378	7
13	0.57894737	6.389933166	4
14	0.6	7.298852901	5
15	0.6	13.49126984	6
16	1	11.08333333	6
17	1	10.87820513	6
18	1	3.814102564	4
19	1	16.41666667	7
20	1	8.833333333	5
21	0	0	2
22	1	11.35	6
23	1	14.85150376	7
24	1	6.360275689	5
25	1	6.884085213	5
26	1	8.91504402	6
27	1	9.75	6
28	1	9.532894737	6
29	1	10.42857143	6
30	1	8.303571429	6
31	1	8.372222222	6
32	1	4.226190476	5
33	0	0	4
34	0	0	3
35	0	0	3
36	0	0	3

ID	Closeness	Betweenness	Degree
37	0	0	3
38	0	0	2
39	0	0	3
40	0	0	3
41	0	0	1
42	0	0	2
43	0	0	2
44	0	0	5
45	0	0	2
46	0	0	3
47	0	0	2
48	0	0	3
49	0	0	2
50	0	0	2
51	0	0	3
52	0	0	3
53	0	0	2

Table 4.28: The calculation results of Closeness Centrality, Betweenness, Centrality, and Degree for each node in Case 3 at disassembly level 4.

ID	Closeness	Betweenness	Degree
1	0.3258427	0	4
2	0.40983607	7.566161616	4
3	0.42622951	10.91208236	5
4	0.40506329	11.25693473	5
5	0.42708333	24.26482129	7
6	0.6	12.08499278	5
7	0.57142857	9.582178932	4
8	0.5862069	26.38658009	7
9	0.6	17.03573649	6
10	0.6	21.92479187	7
11	0.6	5.167893218	4
12	0.57575758	26.45956821	7
13	0.57142857	6.817002442	4
14	0.61111111	7.761111111	5
15	0.60869565	8.514199689	6
16	0.63157895	8.265945166	6
17	1	9.053246753	5
18	1	14.07272727	7
19	1	3.835714286	4
20	1	16.78106061	7
21	1	9.366071429	5
22	1	12.81666667	6
23	1	9.6875	6
24	1	12.5	6
25	1	13.76543457	7
26	1	6.585714286	5
27	1	8.285714286	5
28	1	8.577489177	6
29	1	9.003496503	6
30	1	17.36702742	7
31	1	15.73333333	6
32	1	15.56880342	7
33	0	0	1
34	0	0	3
35	0	0	2
36	0	0	2

ID	Closeness	Betweenness	Degree
37	0	0	4
38	0	0	3
39	0	0	2
40	0	0	5
41	0	0	3
42	0	0	3
43	0	0	2
44	0	0	4
45	0	0	2
46	0	0	2
47	0	0	2
48	0	0	2
49	0	0	1
50	0	0	5
51	0	0	3
52	0	0	2
53	0	0	2
54	0	0	2
55	0	0	3
57	0	0	1
58	0	0	1
59	0	0	1
60	0	0	2

The ANOVA test for the Closeness, betweenness, and Degree centrality metric values of disassemble level zero to three are shown at the tables 4.29, 4.30, and 4.31 respectively. The Closeness, Betweenness, and Degree centrality metrics at this level also did not show there is a difference in means of their values, therefore tracking the change in disassemble feasibility is not feasible at this disassembly level with these metrics.

Table 4.29: The ANOVA test for the Closeness centrality metric values of disassemble level zero to four.

Analysis of Variance

Source	DF	Adj SS	Adj MS	F-Value	P-Value
Factor	2	0.0410	0.02049	0.11	0.894
Error	141	25.7101	0.18234		
Total	143	25.7511			

Table 4.30: The ANOVA test for the Betweenness centrality metric values of disassemble level zero to four.

Analysis of Variance

Source	DF	Adj SS	Adj MS	F-Value	P-Value
Factor	2	55.26	27.63	0.60	0.551
Error	141	6507.41	46.15		
Total	143	6562.66			

Table 4.31: The ANOVA test for the Degree centrality metric values of disassemble level zero to four.

Analysis of Variance

Source	DF	Adj SS	Adj MS	F-Value	P-Value
Factor	2	16.21	8.103	2.70	0.071
Error	141	423.35	3.002		
Total	143	439.56			

4.5.2.5 Disassembly Level Zero to Disassembly Level Five

The calculation results of Closeness, Betweenness, and Degree Centrality metrics for each node in Case 1, Case 2, and Case 3 at disassembly level 5 are presented in tables 4.32, 4.33, and 4.34 respectively.

Table 4.32: The calculation results of Closeness Centrality, Betweenness Centrality, and Degree for each node in Case 1 at disassembly level 5.

ID	Closeness	Betweenness	Degree
1	0.27388535	0	3
2	0.33707865	17.65	4
3	0.33707865	17.675	4
4	0.34	4.675	3
5	0.43181818	31.31190476	5
6	0.45238095	21.26904762	5
7	0.42857143	15.95	4
8	0.45238095	21.70793651	5
9	0.44	13.76111111	4
10	0.58333333	25.19444444	5
11	0.625	27.0547619	6
12	0.625	27.76031746	6
13	0.61538462	7.880952381	4
14	0.61538462	7.880952381	4
15	0.63636364	18.55	5
16	0.61538462	8.421230159	4
17	0.61538462	8.421230159	4
18	0.66666667	13.83611111	5
19	1	20.18333333	6
20	1	23.31666667	6
21	1	8.748809524	5
22	1	8.748809524	5
23	1	9.604761905	5
24	1	9.548809524	5
25	1	9.548809524	5
26	1	8.566666667	5
27	1	5.475	4
28	1	5.475	4
29	1	11.78333333	5
30	0	0	2
31	0	0	2
32	0	0	3
33	0	0	3
34	0	0	3
35	0	0	2
36	0	0	2

ID	Closeness	Betweenness	Degree
37	0	0	3
38	0	0	3
39	0	0	3
40	0	0	3
41	0	0	1
42	0	0	3
43	0	0	1
44	0	0	1

Table 4.32: The calculation results of Closeness Centrality, Betweenness Centrality, and Degree for each node in Case 2 at disassembly level 5.

ID	Closeness	Betweenness	Degree
1	0.27952756	0	4
2	0.33333333	9.330338553	4
3	0.34285714	13.36205563	5
4	0.33870968	17.43169611	5
5	0.35294118	26.87590971	6
6	0.43243243	16.45918257	5
7	0.42553191	23.66175164	5
8	0.44680851	25.29146728	6
9	0.4375	26.44587564	6
10	0.44680851	25.04937922	6
11	0.44117647	7.352382428	4
12	0.45454545	35.65547592	7
13	0.41818182	10.84146541	4
14	0.44680851	10.23794333	5
15	0.45454545	20.00507656	6
16	0.6	28.33214248	6
17	0.61538462	22.87929912	6
18	0.6	8.931328671	4
19	0.625	33.58834788	7
20	0.6	21.69180147	5
21	0	0	2
22	0.625	22.32392576	6
23	0.625	29.72759396	7
24	0.6	16.44394508	5
25	0.58823529	18.13937219	5
26	0.63636364	16.19176064	6
27	0.625	19.89876374	6
28	0.625	18.66910558	6
29	0.625	20.42731735	6
30	0.625	15.77511208	6
31	0.625	16.761481	6
32	0.625	8.218703008	5
33	1	21.35520848	7
34	1	20.12917749	6
35	1	19.25598086	6
36	1	9.451688312	5

ID	Closeness	Betweenness	Degree
37	1	15.3363	6
38	1	10.2661	5
39	1	14.2846	6
40	1	12.6747	6
41	1	9.21347	4
42	1	8.30145	5
43	1	7.33443	5
44	1	23.7517	8
45	1	9.59861	5
46	1	12.2535	6
47	1	13.2042	5
48	1	7.28237	5
49	1	9.5006	5
50	1	8.33889	5
51	1	10.1754	6
52	1	10.0839	6
53	1	8.20774	5
54	0	0	5
55	0	0	4
56	0	0	4
57	0	0	3
58	0	0	1
59	0	0	2
60	0	0	4
61	0	0	3
62	0	0	3
63	0	0	4
64	0	0	5
65	0	0	1
66	0	0	3
67	0	0	4
68	0	0	4
69	0	0	4
70	0	0	1
71	0	0	2
72	0	0	4

Table 4.32: The calculation results of Closeness Centrality, Betweenness Centrality, and Degree for each node in Case 3 at disassembly level 5.

ID	Closeness	Betweenness	Degree
1	0.2801418	0	4
2	0.3125	10.146482	4
3	0.3418803	14.83032	5
4	0.3197674	14.919268	5
5	0.3532934	35.103929	7
6	0.4285714	19.974341	5
7	0.3552632	21.051572	4
8	0.4069767	42.24856	7
9	0.4285714	28.527141	6
10	0.4545455	31.004824	7
11	0.4285714	8.3772061	4
12	0.4204545	39.156611	7
13	0.4126984	11.562376	4
14	0.4225352	14.604521	5
15	0.4366197	14.36652	6
16	0.4545455	15.126329	6
17	0.6	21.912389	5
18	0.625	28.096847	7
19	0.5833333	10.18929	4
20	0.4878049	60.33023	7
21	0.5882353	24.938429	5
22	0.5833333	29.723655	6
23	0.625	16.680058	6
24	0.625	18.067416	6
25	0.625	27.718169	7
26	0.6	16.829271	5
27	0.5882353	21.548199	5
28	0.625	17.193545	6
29	0.6	16.464041	6
30	0.625	27.785944	7
31	0.625	24.178457	6
32	0.6111111	25.865203	7
34	0.6	54.599457	7
35	0.6111111	14.779558	6
36	0.6111111	13.158274	6
33	0.6	4.9415683	4
37	1	19.739994	7
38	1	18.537808	6
39	1	14.557228	5
40	1	24.822944	8
41	1	11.516301	6
42	1	14.283186	6
44	1	21.359626	7
45	1	15.057713	6
46	1	22.117491	5
43	1	11.622369	5
47	1	16.314014	6
48	1	13.576554	6
49	1	8.3640623	5
50	1	20.545439	8
51	1	14.525188	6
52	1	10.749225	5
53	1	14.080383	5
54	1	14.573899	6
55	1	20.115078	7
60	0	0	3
57	1	10.016634	6
58	1	15.750974	5
59	1	15.131362	6
56	1	16.642527	6
61	0	0	5
62	0	0	6
63	0	0	5
64	0	0	3
65	0	0	1
66	0	0	2
67	0	0	5
68	0	0	4
69	0	0	4
70	0	0	2
71	0	0	4
72	0	0	4
73	0	0	1
74	0	0	3
75	0	0	5
76	0	0	4
77	0	0	3
78	0	0	1
79	0	0	3
80	0	0	4

The ANOVA test for the Closeness, betweenness, and Degree centrality metric values of disassemble level zero to three are shown at the tables 4.33, 4.34, and 4.35 respectively. The Closeness centrality metric at this level also did not show there is a difference in means of their values, however, Betweenness, and Degree show the change in disassemble feasibility is feasible at this disassembly level with these metrics.

Table 4.33: The ANOVA test for the Closeness centrality metric values of disassemble level zero to five.

Analysis of Variance

Source	DF	Adj SS	Adj MS	F-Value	P-Value
Factor	2	0.1150	0.05751	0.39	0.681
Error	193	28.7874	0.14916		
Total	195	28.9024			

Table 4.34: The ANOVA test for the Betweenness centrality metric values of disassemble level zero to five.

Analysis of Variance

Source	DF	Adj SS	Adj MS	F-Value	P-Value
Factor	2	800.1	400.0	3.34	0.037
Error	193	23085.4	119.6		
Total	195	23885.5			

Means

Factor	N	Mean	StDev	95% CI
Betweenness Case 1 DL5	44	9.32	9.35	(6.07; 12.57)
Betweenness Case 2 DL5	72	11.75	9.79	(9.21; 14.29)
Betweenness Case 3 DL5	80	14.50	12.59	(12.09; 16.91)

Pooled StDev = 10.9368

Table 4.35: The ANOVA test for the Degree centrality metric values of disassemble level zero to five.

Analysis of Variance

Source	DF	Adj SS	Adj MS	F-Value	P-Value
Factor	2	49.86	24.931	11.42	0.000
Error	193	421.34	2.183		
Total	195	471.20			

Means

Factor	N	Mean	StDev	95% CI
Degree Case 1 DL5	44	3.864	1.374	(3.424; 4.303)
Degree Case 2 DL5	72	4.861	1.456	(4.518; 5.205)
Degree Case 3 DL5	80	5.175	1.549	(4.849; 5.501)

Pooled StDev = 1.47754

Betweenness centrality metric in table 4.34 and Degree centrality metrics in table 4.35 have shown there is a change is happening in the disassemble feasibility at this disassembly level (i.e., Disassembly level 5). While the P-Value of the ANOVA test of the disassembly nodes by term of Betweenness metric is less than 0.05, it means that there is a change is happening in the disassemble feasibility. The amount of change in disassemble feasibility can be found by using equation 4.4. Table 4.36 shows how much the raise in the geometrical disassemble feasibility at the disassembly level five in terms of Betweenness and Degree centrality metrics.

Table 4.36: The percentage change in the Means of variance resulted from ANOVA test.

Centrality metrics	**Case 1 to Case 2 at DL5**	**Case 2 to Case 3 at DL5**
Betweenness	26.00%	23.40%
Degree	25.80%	6.45%

4.5.2.6 Disassembly Level Zero to Disassembly Level Six

The calculation results of Closeness, Betweenness, and Degree Centrality metrics for each node in Case 1, Case 2, and Case 3 at disassembly level 6 are presented in tables 4.37, 4.38, and 4.39 respectively.

Table 4.37: The calculation results of Closeness Centrality, Betweenness Centrality, and Degree for each node in Case 1 at disassembly level 6.

ID	Closeness	Betweenness	Degree
1	0.251256	0	3
2	0.302521	20.55	4
3	0.302521	20.55	4
4	0.285714	5.9	3
5	0.375	37.503663	5
6	0.387097	25.514835	5
7	0.354167	20.733333	4
8	0.387097	25.514835	5
9	0.354167	20.733333	4
10	0.458333	34.880952	5
11	0.5	34.428938	6
12	0.5	34.428938	6
13	0.48	10.193864	4
14	0.48	10.193864	4
15	0.478261	26.242857	5
16	0.48	10.193864	4
17	0.48	10.193864	4
18	0.478261	26.242857	5
19	0.666667	34.254762	6
20	0.666667	34.254762	6
21	0.666667	13.844872	5
22	0.666667	13.844872	5
23	0.666667	15.054212	5
24	0.666667	13.844872	5
25	0.666667	13.844872	5
26	0.666667	13.649817	5
27	0.625	10.939286	4
28	0.625	10.939286	4
29	0.666667	13.649817	5
30	0.625	10.939286	4
31	0.625	10.939286	4
32	1	13.07381	5
33	1	12.089881	5
34	1	12.089881	5
35	1	12.089881	5
36	1	12.089881	5
37	1	7.5721612	5
38	1	8.3862637	5
39	1	8.3862637	5
40	1	7.5721612	5

ID	Closeness	Betweenness	Degree
41	1	3.04158	3
42	1	12.7833	5
43	1	12.7833	5
44	1	3.04158	3
45	0	0	4
46	0	0	4
47	0	0	4
48	0	0	4
49	0	0	6
50	0	0	2
51	0	0	2

Table 4.38: The calculation results of Closeness Centrality, Betweenness Centrality, and Degree for each node in Case 2 at disassembly level 6.

ID	Closeness	Betweenness	Degree
1	0.2635135	0	4
2	0.3030303	10.3644556	4
3	0.3111111	14.8403249	5
4	0.3116883	19.3167218	5
5	0.3253012	29.4784976	6
6	0.3684211	19.7305568	5
7	0.3731343	27.6500704	5
8	0.3880597	29.248626	6
9	0.3823529	30.8006508	6
10	0.3880597	28.9375393	6
11	0.3703704	8.66249189	4
12	0.4	40.7057744	7
13	0.3670886	12.4104732	4
14	0.3880597	11.4444656	5
15	0.4	22.4093515	6
16	0.4814815	36.5628719	6
17	0.48	30.0662744	6
18	0.4545455	12.3635935	4
19	0.5	42.0663649	7
20	0.4814815	26.672168	5
21	0	0	2
22	0.5	27.4355055	6
23	0.5	37.0261198	7
24	0.4814815	21.2250854	5
25	0.46875	23.309196	5
26	0.4782609	21.4361866	6
27	0.5	24.0675052	6
28	0.5	23.1012606	6
29	0.5	25.0400474	6
30	0.5	19.2482688	6
31	0.5	20.565335	6
32	0.5	9.81421689	5
33	0.6666667	34.3918056	7
34	0.6666667	31.4300924	6
35	0.6666667	29.9684589	6
36	0.625	18.3897036	5
37	0.6666667	24.4223116	6
38	0.6666667	15.6113823	5
39	0.6666667	22.312292	6
40	0.6666667	19.7121682	6

ID	Closeness	Betweenness	Degree
41	0.66667	12.4542	4
42	0.66667	12.8287	5
43	0.66667	11.1381	5
44	0.66667	38.905	8
45	0.66667	14.6146	5
46	0.66667	19.003	6
47	0.66667	19.2632	5
48	0.625	12.9505	5
49	0.66667	13.3331	5
50	0.66667	12.7229	5
51	0.66667	16.0668	6
52	0.66667	15.5671	6
53	0.66667	11.9146	5
54	1	22.6234	7
55	1	15.6419	6
56	1	15.0371	6
57	1	12.6621	5
58	1	5.23409	3
59	1	7.15593	4
60	1	18.5621	6
61	1	9.05666	5
62	1	9.17452	5
63	1	11.431	6
64	1	14.0484	7
65	1	2.25096	3
66	1	7.26344	5
67	1	13.7409	6
68	1	16.4918	6
69	1	11.0729	6
70	1	3.35353	3
71	1	4.64382	4
72	1	10.5555	6
73	0	0	5
74	0	0	6
75	0	0	6
76	0	0	5
77	0	0	4
78	0	0	6
79	0	0	6

Table 4.39: The calculation results of Closeness Centrality, Betweenness Centrality, and Degree for each node in Case 3 at disassembly level 6.

ID	Closeness	Betweenness	Degree
1	0.26543	0	4
2	0.28889	11.095757	4
3	0.31293	16.15638	5
4	0.29952	16.464491	5
5	0.32673	38.283372	7
6	0.37097	23.023918	5
7	0.32381	24.053206	4
8	0.36522	48.421538	7
9	0.375	32.463446	6
10	0.4	35.208248	7
11	0.37097	9.6259538	4
12	0.38393	43.979145	7
13	0.3617	13.830584	4
14	0.37374	16.387518	5
15	0.38947	16.127689	6
16	0.4	16.878753	6
17	0.48148	27.183099	5
18	0.5	34.780902	7
19	0.45833	13.311864	4
20	0.43333	70.029763	7
21	0.45714	32.551982	5
22	0.47619	36.96753	6
23	0.48387	20.161593	6
24	0.5	21.592156	6
25	0.5	33.532769	7
26	0.48148	21.192124	5
27	0.46875	26.70268	5
28	0.5	21.447236	6
29	0.48571	19.059183	6
30	0.5	34.045437	7
31	0.48387	28.469971	6
32	0.47368	36.308477	7
34	0.47368	61.995931	7
35	0.48485	17.676312	6
36	0.48485	17.06859	6
33	0.46667	5.9223997	4
37	0.66667	31.067193	7
38	0.66667	28.119544	6
39	0.63636	21.908065	5
40	0.66667	38.665532	8
41	0.63636	18.0077	6
42	0.66667	20.0028	6
44	0.63636	33.0448	7
45	0.63636	24.3571	6

ID	Closeness	Betweenness	Degree
46	0.63636	34.1486	5
43	0.63636	16.3078	5
47	0.61538	24.3014	6
48	0.66667	19.4339	6
49	0.63636	12.0179	5
50	0.66667	31.4951	8
51	0.66667	21.1209	6
52	0.66667	14.5999	5
53	0.66667	20.7274	5
54	0.63636	21.7409	6
55	0.66667	25.896	7
60	0.63636	21.5353	6
57	0.63636	16.4638	6
58	0.66667	21.6094	5
59	0.66667	21.7192	6
56	0.61538	24.7098	6
61	1	18.0155	7
62	1	26.9967	8
63	1	20.0828	7
64	1	11.5706	5
65	1	4.69186	3
66	1	9.32109	4
67	1	18.3399	7
68	1	17.808	6
69	1	21.0402	7
70	1	5.92998	4
71	1	13.892	6
72	1	17.7511	6
73	1	5.91233	3
74	1	11.6729	5
75	1	17.2438	7
76	1	13.4052	6
77	1	13.6343	6
78	1	3.66985	3
79	1	16.4919	6
80	1	15.5298	6
81	0	0	6
82	0	0	9
83	0	0	4
84	0	0	5
85	0	0	5
86	0	0	5
87	0	0	6

The ANOVA test for the Closeness, betweenness, and Degree centrality metric values of disassemble level zero to three are shown at the tables 4.40, 4.41, and 4.42 respectively. The Closeness centrality metric at this level (DL6) also did not show there is a difference in means of their values, however, Betweenness, and Degree show the change in disassemble feasibility is feasible at this disassembly level with these metrics.

Table 4.40: The ANOVA test for the Closeness centrality metric values of disassemble level zero to six.

Analysis of Variance

Source	DF	Adj SS	Adj MS	F-Value	P-Value
Factor	2	0.0130	0.006490	0.07	0.931
Error	214	19.5509	0.091359		
Total	216	19.5639			

Table 4.41: The ANOVA test for the Betweenness centrality metric values of disassemble level zero to six.

Analysis of Variance

Source	DF	Adj SS	Adj MS	F-Value	P-Value
Factor	2	1513	756.5	5.66	0.004
Error	214	28616	133.7		
Total	216	30129			

Means

Factor	N	Mean	StDev	95% CI
Betweenness Case 1 DL6	51	13.90	10.51	(10.71; 17.09)
Betweenness Case 2 DL6	79	16.75	10.65	(14.18; 19.31)
Betweenness Case 3 DL6	87	20.55	12.87	(18.11; 23.00)

Pooled StDev = 11.563

Table 4.42: The ANOVA test for the Degree centrality metric values of disassemble level zero to six.

Analysis of Variance

Source	DF	Adj SS	Adj MS	F-Value	P-Value
Factor	2	49.75	24.876	21.46	0.000
Error	214	248.02	1.159		
Total	216	297.77			

Means

Factor	N	Mean	StDev	95% CI
Degree Case 1 DL6	51	4.510	0.925	(4.213; 4.807)
Degree Case 2 DL6	79	5.392	1.043	(5.154; 5.631)
Degree Case 3 DL6	87	5.747	1.183	(5.520; 5.975)

Pooled StDev = 1.07655

The amount of change in disassemble feasibility can be found by using equation 4.4. Table 4.43 shows how much the raise in the geometrical disassemble feasibility at the disassembly level five in terms of Betweenness and Degree centrality metrics.

Table 4.43: The percentage change in the Means of variance resulted from ANOVA test.

Centrality metrics	Case 1 to Case 2 at DL5	Case 2 to Case 3 at DL5
Betweenness	20.50%	22.68%
Degree	19.55%	6.58%

4.5.2.7 Disassembly Level Zero to Disassembly level Seven

The work that should be done here is the same work that has been done at the section 4.5.1 at this dissertation, while at this disassembly level (i.e., DL7) the whole assembly has been disassembled.

4.6 Discussion

This chapter of my study presents the preliminary explanation of a method to quantify the impact of change in the geometrical disassemble feasibility of mechanical assemblies. This method uses connects between the disassembly nodes to evaluate the change in the disassemble feasibility due to wear in assembly's parts. This work serves two aims, the aim of this work which is tracking the change in the geometrical disassemble feasibility of mechanical assemblies, and the secondary aim which is which centrality metrics that are able to reveal the change that is happing in the assembly dimension parts due to wear. Not all centrality metrics reflect the change in disassemble feasibility. At this work the Betweenness, and Degree centrality metrics successfully reveal that disassemble feasibility will increase in 52.8% if one bushing completely worn, and 62.67% if both bushings completely worn. Also, Degree metric shows that the disassemble feasibility will increase in 17.0% if one bushing completely worn, and 23.20% if both bushings completely worn.

The monitoring accuracy of changing in the disassemble feasibility of a mechanical assembly improves by increasing the number of corrosion simulation runs. Therefore, more runs are required to give a clearer picture of the increasing or decreasing in the disassemble feasibility that may happen over a fixed amount of operating times of mechanical assembly. Where the wear of mechanical assemblies takes a high curve of wear at the beginning of the assembly life, buts quickly that high wear takes slow wear curve in its normal operating life and the high wear curve come back at the end of the assembly life use.

The change in the geometrical disassemble feasibility is not happening from the first disassembly levels, however, the change in the disassemble feasibility is happening at the end disassembly levels. At least this change in the disassemble feasibility has been approved in the case study at this chapter of work. The change in the disassemble feasibility happened in the DL5 and continued at DL6, and DL7. Where five out of seven parts of the case study assembly at this work were disassembled at the disassembly level 5 (DL5), representing 70% of the assembly's parts and that may indicate it is not possible to detect the change in the disassemble feasibility at the disassembly level that represents less than 70% of disassembling the whole assembly.

The Closeness centrality metric did not track the change in the disassemble feasibility at all disassembly levels, however, the Betweenness and Degree centrality metrics both indicates the change in the disassemble feasibility starting from the first disassembly level that started change in the disassemble feasibility (i.e., Disassembly Level 5 (DL5)) reaching to the end of DLs (i.e., DL7). That is due to the nature of the used centrality metrics. Where the both of Betweenness and Degree centrality metrics weight the nodes of the DDDs based on the number of the relationships of a node with other nodes in the diagram and that may indicate to the criticality of each step in

disassembly sequences, however, the Closeness centrality metric takes into consideration how much a node is close to any other node in the diagram, in other words it measures the mean distance between any two nodes in the diagram and not the relationships of a node with other adjacent nodes.

CHAPTER 5: CONCLUSION AND FUTURE WORKS

5.1 Summary and Conclusion

This dissertation focuses on tracking the possible change in the geometrical disassemble feasibility of mechanical assemblies when the assembly is in design phase. Chapter 2 focused on using component interaction data from CAD design models to automatically extract critical disassembly information for contact and non-contact assembly's parts. Chapter 3 focused on construct a precedence matrix from proven collision tests of contact, non-contact constraints. Chapter 4 focused on predicting changes in the geometrical disassemble feasibility of an assembly during its lifetime in early design phase.

The dissertation chapters examine three adjacent levels down to predicting the change in geometrical disassemble feasibility of an assembly while the assembly is still in design phase. At the first level, the aim was developing a method able to read and extract geometrical data from CAD STEP file of the assembly and then developing a collision test uses these extracted data and able to show the assembly's parts that can be removed or disassembled from the assembly. The outcome of collision test has been in matrices called Interference Matrices. These interference matrices present two information, the feasible parts that can be disassemble at that disassembly level and the feasible directions for these parts to disassemble

At the second level, the outcomes of the developed collision test have been used to determine feasible geometrical disassembly sequences of the assembly and summarized all steps of these disassembly sequences in one graph called Direct Disassembly Diagram (DDD). One Precedence Matrix has been used to save all feasible disassemble sequence steps in a matrix form. However, by applying collision test to determine disassembly sequences, we can make sure that all the resulted disassembly

sequences are practically feasible. While the collision test showed no obstacles in front of these feasible parts to disassemble that denied them from moving at one of six principle directions subject study.

The third level at this study aims to predict the change in disassemble feasibility that may happen due to erosion or missing some parts of the assembly during the use life of the assembly. To do so, three cases have been considered at this level for one case study example (i.e., typical design of Roller Guide). The first case represents the original design of the case study example. The second case considers on of the parts of the Roller Guide has been 100% corroded or broke (i.e., bushing part at one of the Roller guide side). The third case considers that two parts of the Roller Guide have been corroded or broke (i.e. the bushings at the two sides of the Roller Guide). The relationships between all the steps of the feasible disassemble sequences have been evaluated by using some of Centrality Metrics (Degree Centrality, Betweenness Centrality, and Closeness Centrality). ANOVA test has been used to check the ability of the used Centrality Metrics in the evaluation in monitoring the change in the disassemble feasibility of the three studied cases. Degree, and Betweenness Centrality metrics has shown their ability to predict the change in the disassemble feasibility for the three case studies. 52.80% disassemble feasibility changed from the original design to 100% wear in one of case study assembly part and 9.87% disassemble feasibility changed from the original design to 100% wear in two of case study assembly part in terms of Betweenness metric. 17.00% disassemble feasibility changed from the original design to 100% wear in ONE of case study assembly part and 6.20% disassemble feasibility changed from the original design to 100% wear in two of case study assembly part in terms of Degree metric.

This dissertation's main accomplishments can be summarized as follows:

1. Determine disassembly contact and non-contact interferences and the direction of disassembly by Using a STEP file to as input, and the output is a matrix that provides insight into the possible disassembly of a component along the principal axes.
2. The Interference Matrices resulted from the collision test has been used to build a Precedence Matrix that ensures mentioning just the geometrical feasible disassembly sequences.
3. Track the change in the geometrical disassemble feasibility in a mechanical assembly over the used lifetime of the assembly in design phase of the assembly.

5.2 Future Works

1. Develop a method to check the disassemble feasibility for assemblies' parts at more than the six-principle directions.
2. Developing a method that eliminate interaction of human in developing Precedence Matrix.
3. Test the prediction model on different mechanical assemblies to examine the centrality metrices and conclude the most metric that can show the change in the disassemble feasibility.
4. Build an automated prediction model to predict the change in the geometrical disassemble feasibility based on the time interval of an assembly using life.

APPENDIX

Journal Publications to Be Submitted

R1. Alrufaifi, H., Prioli J., & Rickli, J. L. "Developing Assembly's Precedence Matrix Based on Collision Tests Results."

Conference Publications

C1. Alrufaifi, H., Kumar, B., & Rickli, J. L. (2019). Automated Contact and Non-Contact Constraint Generation for Disassembly Feasibility and Planning. *Procedia CIRP*, *80*, 548-553.

REFERENCES

[1] Zhou, Z., Liu, J., Pham, D. T., Xu, W., Ramirez, F. J., Ji, C., & Liu, Q. (2019). Disassembly sequence planning: recent developments and future trends. Proceedings of the Institution of Mechanical Engineers, Part B: Journal of Engineering Manufacture, 233(5), 1450-1471.

[2] Mitrouchev, P., Wang, C. G., Lu, L. X., & Li, G. Q. (2015). Selective disassembly sequence generation based on lowest level disassembly graph method. The International Journal of Advanced Manufacturing Technology, 80(1-4), 141-159.

[3] Soh, S. L., Ong, S. K., & Nee, A. Y. C. (2014). Design for disassembly for remanufacturing: methodology and technology. Procedia CIRP, 15, 407-412.

[4] Guide Jr, V. D. R. (2000). Production planning and control for remanufacturing: industry practice and research needs. Journal of operations Management, 18(4), 467-483.

[5] Duflou, J. R., Seliger, G., Kara, S., Umeda, Y., Ometto, A., & Willems, B. (2008). Efficiency and feasibility of product disassembly: A case-based study. CIRP Annals, 57(2), 583-600.

[6] Ryan, A., O'Donoghue, L., & Lewis, H. (2011). Characterising components of liquid crystal displays to facilitate disassembly. Journal of cleaner production, 19(9-10), 1066-1071.

[7] Ghazilla, R. A. R., Sakundarini, N., Taha, Z., Abdul-Rashid, S. H., & Yusoff, S. (2015). Design for environment and design for disassembly practices in Malaysia: ' practitioner's perspectives. Journal of Cleaner Production, 108, 331-342.

[8] Umeda, Y., Miyaji, N., Shiraishi, Y., & Fukushige, S. (2015). Proposal of a design method for semi-destructive disassembly with split lines. CIRP Annals, 64(1), 29-32.

[9] Hegarty, M. (2008). The Little Book of Living Green. Andrews McMeel Publishing.

[10] Liu, S., & Boyle, I. M. (2009). Engineering design: perspectives, challenges, and recent advances. Journal of Engineering Design, 20(1), 7-19.

[11] Wiendahl, H. P., Seliger, G., Perlewitz, H., & Bürkner, S. (1999). A general approach to disassembly planning and control. Production Planning & Control, 10(8), 718-726.

[12] Mok, S. M., Wu, C. H., & Lee, D. T. (1999, November). A hierarchical workcell model for intelligent assembly and disassembly. In Proceedings 1999 IEEE International Symposium on Computational Intelligence in Robotics and Au'omation. CIRA'99 (Cat. No. 99EX375) (pp. 125-130). IEEE.

[13] Salomonski, N., & Zussman, E. (1999). On-line predictive model for disassembly process planning adaptation. Robotics and Computer-Integrated Manufacturing, 15(3), 211-220.

[14] Gupta, S. M., & Gungor, A. (2001, May). Product recovery using a disassembly line: challenges and solution. In Proceedings of the 2001 IEEE International Symposium on Electronics and the Environment. 2001 IEEE ISEE (Cat. No. 01CH37190) (pp. 36-40). IEEE

[15] García, M. A., Larré, A., López, B., & Oller, A. (2000, October). Reducing the complexity of geometric selective disassembly. In Proceedings. 2000 IEEE/RSJ International Conference on Intelligent Robots and Systems (IROS 2000) (Cat. No. 00CH37113) (Vol. 2, pp. 1474-1479). IEEE

[16] Brennan, L., Gupta, S. M., & Taleb, K. N. (1994). Operations planning issues in an assembly/disassembly environment. International Journal of Operations & Production Management, 14(9), 57-67.

[17] Agrawal, S., & Tiwari, M. K. (2008). A collaborative ant colony algorithm to stochastic mixed-model U-shaped disassembly line balancing and sequencing problem. International journal of production research, 46(6), 1405-1429.

[18] Martinez, M., Pham, V. H., & Favrel, J. (1997, September). Dynamic generation of disassembly sequences. In 1997 IEEE 6th International Conference on Emerging Technologies and Factory Automation Pro'eedings, EFTA'97 (pp. 177-182). IEEE.

[19] Zussman, E., & Zhou, M. C. (2000). Design and implementation of an adaptive process planner for disassembly processes. IEEE Transactions on Robotics and Automation, 16(2), 171-179.

[20] Salomonski, N., & Zussman, E. (1999). On-line predictive model for disassembly process planning adaptation. Robotics and Computer-Integrated Manufacturing, 15(3), 211-220.

[21] Ilgin, M. A., & Gupta, S. M. (2010). Environmentally conscious manufacturing and product recovery (ECMPRO): A review of the state of the art. Journal of environmental management, 91(3), 563-591.

[22] Carrell, J., Zhang, H. C., & Li, H. (2008). Review of Current End-of-life Options for Electronics and Future Automatic Disassembly Options with Shape Memory Materials with Carbon Nanotubes for Electronics. In LCE 2008: 15th CIRP International Conference on Life Cycle Engineering: Conference Proceedings (p. 470). CIRP.

[23] Jiping, Y., Dong, X., & Peng, G. (2009). Disassembly technology and disassembly process of waste printed circuit boards: A state-of-the-art. Journal of Mechanical Engineering, 45(9), 126-135.

[24] Lee, K., & Gadh, R. (1998). Destructive disassembly to support virtual prototyping. IIE transactions, 30(10), 959-972.

[25] Pak, K. G., & Sodhi, R. (2002). Destructive disassembly of bolts and screws by impact fracture. Journal of manufacturing systems, 21(4), 316-324.

[26] Gupta, S. M., & McLean, C. R. (1996). Disassembly of products. Computers & Industrial Engineering, 31(1-2), 225-228.

[27] Zhong, L., Youchao, S., Ekene Gabriel, O., & Haiqiao, W. (2011). Disassembly sequence planning for maintenance based on metaheuristic method. Aircraft Engineering and Aerospace Technology, 83(3), 138-145.

[28] Mircheski, I., T. Kandikjan, and B. Prangoski. 2012. "A Mathematical Model of Non-Destructive Disassembly Process." International Journal of Mechanical and Production Engineering Research and Development 2 (4): 61–72.

[29] Rickli, J. L., & Camelio, J. A. (2014). Partial disassembly sequencing considering acquired end-of-life product age distributions. International Journal of Production Research, 52(24), 7496-7512.

[30] Yeh, W. C. (2011). Optimization of the disassembly sequencing problem on the basis of self-adaptive simplified swarm optimization. IEEE transactions on systems, man, and cybernetics-part A: systems and humans, 42(1), 250-261.

[31] Xia, K., Gao, L., Chao, K. M., & Wang, L. (2015, October). A cloud-based disassembly planning approach towards sustainable management of WEEE. In 2015 IEEE 12th International Conference on e-Business Engineering (pp. 203-208). IEEE.

[32] Alshibli, M., El Sayed, A., Kongar, E., Sobh, T. M., & Gupta, S. M. (2016). Disassembly sequencing using tabu search. Journal of Intelligent & Robotic Systems, 82(1), 69-79.

[33] Kheder, M., Trigui, M., & Aifaoui, N. (2015). Disassembly sequence planning based on a genetic algorithm. Proceedings of the Institution of Mechanical

Engineers, Part C: Journal of Mechanical Engineering Science, 229(12), 2281-2290.

[34] ElSayed, A., Kongar, E., Gupta, S. M., & Sobh, T. (2012). A robotic-driven disassembly sequence generator for end-of-life electronic products. Journal of Intelligent & Robotic Systems, 68(1), 43-52.

[35] Hui, W., Dong, X., & Guanghong, D. (2008). A genetic algorithm for product disassembly sequence planning. Neurocomputing, 71(13-15), 2720-2726.

[36] Smith, S., Hsu, L. Y., & Smith, G. C. (2016). Partial disassembly sequence planning based on cost-benefit analysis. Journal of cleaner production, 139, 729-739.

[37] Rickli, J. L., & Camelio, J. A. (2013). Multi-objective partial disassembly optimization based on sequence feasibility. Journal of manufacturing systems, 32(1), 281-293.

[38] Yu-fei, X., & Qiang, L. (2016, May). Partial disassembly sequence planning based on Pareto ant colony algorithm. In 2016 Chinese Control and Decision Conference (CCDC) (pp. 4804-4809). IEEE.

[39] Luo, Y., Peng, Q., & Gu, P. (2016). Integrated multi-layer representation and ant colony search for product selective disassembly planning. Computers in Industry, 75, 13-26.

[40] Guo, X., Liu, S., Zhou, M., & Tian, G. (2015). Disassembly sequence optimization for large-scale products with multiresource constraints using scatter search and Petri nets. IEEE transactions on cybernetics, 46(11), 2435-2446.

[41] Jin, G. Q., Li, W. D., Wang, S., & Gao, S. M. (2019). A Systematic Selective Disassembly Approach for Waste Electrical and Electronic Equipment (WEEE). In

Sustainable Manufacturing and Remanufacturing Management (pp. 285-318). Springer, Cham.

[42] Song, X., Zhou, W., Pan, X., & Feng, K. (2014). Disassembly sequence planning for electro-mechanical products under a partial destructive mode. Assembly Automation, 34(1), 106-114.

[43] Tian, Y., Zhang, X., Liu, Z., Jiang, X., & Xue, J. (2019). Product cooperative disassembly sequence and task planning based on genetic algorithm. The International Journal of Advanced Manufacturing Technology, 1-18.

[44] Moore, K. E., Güngör, A., & Gupta, S. M. (2001). Petri net approach to disassembly process planning for products with complex AND/OR precedence relationships. European Journal of Operational Research, 135(2), 428-449.

[45] Andrés, C., Lozano, S., & Adenso-Diaz, B. (2007). Disassembly sequence planning in a disassembly cell context. Robotics and Computer-Integrated Manufacturing, 23(6), 690-695.

[46] Dong, T., Zhang, L., Tong, R., & Dong, J. (2006). A hierarchical approach to disassembly sequence planning for mechanical product. The International Journal of Advanced Manufacturing Technology, 30(5-6), 507-520.

[47] Rai, R., Rai, V., Tiwari, M. K., & Allada, V. (2002). Disassembly sequence generation: a Petri net based heuristic approach. International Journal of Production Research, 40(13), 3183-3198.

[48] Chung, C., & Peng, Q. (2005). An integrated approach to selective-disassembly sequence planning. Robotics and Computer-Integrated Manufacturing, 21(4-5), 475-485.

[49] Tian, Y., Zhang, X., Liu, Z., Jiang, X., & Xue, J. (2019). Product cooperative disassembly sequence and task planning based on genetic algorithm. The International Journal of Advanced Manufacturing Technology, 1-18.

[50] Ren, Y., Zhang, C., Zhao, F., Xiao, H., & Tian, G. (2018). An asynchronous parallel disassembly planning based on genetic algorithm. European Journal of Operational Research, 269(2), 647-660.

[51] Smith, S., & Hung, P. Y. (2015). A novel selective parallel disassembly planning method for green design. Journal of engineering design, 26(10-12), 283-301.

[52] Zhang, X. F., Yu, G., Hu, Z. Y., Pei, C. H., & Ma, G. Q. (2014). Parallel disassembly sequence planning for complex products based on fuzzy-rough sets. The International Journal of Advanced Manufacturing Technology, 72(1-4), 231-239.

[53] Pistolesi, F., & Lazzerini, B. (2019). TeMA: a Tensorial Memetic Algorithm for Many-Objective Parallel Disassembly Sequence Planning in Product Refurbishment. IEEE Transactions on Industrial Informatics.

[54] Li, J. R., Khoo, L. P., & Tor, S. B. (2002). A novel representation scheme for disassembly sequence planning. The International Journal of Advanced Manufacturing Technology, 20(8), 621-630.

[55] Hula, A., Jalali, K., Hamza, K., Skerlos, S. J., & Saitou, K. (2003). Multi-criteria decision-making for optimization of product disassembly under multiple situations. Environmental science & technology, 37(23), 5303-5313.

[56] Giudice, F., & Fargione, G. (2007). Disassembly planning of mechanical systems for service and recovery: a genetic algorithms-based approach. Journal of Intelligent Manufacturing, 18(3), 313-329.

[57] Lambert, A. J. (2007). Optimizing disassembly processes subjected to sequence-dependent cost. Computers & Operations Research, 34(2), 536-551.

[58] Tang, Y., Zhou, M., & Caudill, R. J. (2001). An integrated approach to disassembly planning and demanufacturing operation. IEEE Transactions on Robotics and Automation, 17(6), 773-784.

[59] Liu, X., Peng, G., Liu, X., & Hou, Y. (2012). Disassembly sequence planning approach for product virtual maintenance based on improved max–min ant system. The International Journal of Advanced Manufacturing Technology, 59(5-8), 829-839.

[60] Chunming, Z. (2016). Optimization for disassemble sequence planning of electromechanical products during recycling process based on genetic algorithms. International Journal of Multimedia and Ubiquitous Engineering, 11(4), 107-114.

[61] Cappelli, F., Delogu, M., Pierini, M., & Schiavone, F. (2007). Design for disassembly: a methodology for identifying the optimal disassembly sequence. Journal of Engineering Design, 18(6), 563-575.

[62] Luo, Y. (2014). Disassembly sequence planning for product maintenance.

[63] Xia, K., Gao, L., Wang, L., Li, W., & Chao, K. M. (2013, September). A simplified teaching-learning-based optimization algorithm for disassembly sequence planning. I^{n} 2013 IEEE 10th International Conference on e-Business Engineering (pp. 393-398). IEEE.

[64] Xia, K., Gao, L., Chao, K. M., & Wang, L. (2015, October). A cloud-based disassembly planning approach towards sustainable management of WEEE. I^{n} 2015 IEEE 12th International Conference on e-Business Engineering (pp. 203-208). IEEE.

[65] Percoco, G., & Diella, M. (2013). Preliminary evaluation of artificial bee colony algorithm when applied to multi objective partial disassembly planning. Research Journal of Applied Sciences, Engineering and Technology, 6(17), 3234-3243.

[66] Smith, S. S., & Chen, W. H. (2011). Rule-based recursive selective disassembly sequence planning for green design. Advanced Engineering Informatics, 25(1), 77-87.,

[67] Smith, S., & Hung, P. Y. (2015). A novel selective parallel disassembly planning method for green design. Journal of engineering design, 26(10-12), 283-301.

[68] Wang, H. (2016). Disassembly sequence planning for end-of-life products.

[69] Huang, J., Esmaeilian, B., & Behdad, S. (2015, August). Multi-purpose disassembly sequence planning. In ASME 2015 International Design Engineering Technical Conferences and Computers and Information in Engineering Conference. American Society of Mechanical Engineers Digital Collection.

[70] Lu, C., & Liu, Y. C. (2012). A disassembly sequence planning approach with an advanced immune algorithm. Proceedings of the Institution of Mechanical Engineers, Part C: Journal of Mechanical Engineering Science, 226(11), 2739-2749.

[71] Srinivasan, H., & Gadh, R. (1998, May). Complexity reduction in geometric selective disassembly using the wave propagation abstraction. In Proceedings. 1998 IEEE International Conference on Robotics and Automation (Cat. No. 98CH36146) (Vol. 2, pp. 1478-1483). IEEE.

[72] Srinivasan, H., & Gadh, R. (1999, July). Selective disassembly: representation and comparative analysis of wave propagation abstractions in sequence planning. In Proceedings of the 1999 IEEE International Symposium on Assembly and Task P'anning (ISATP'9$^{9)}$(Cat. No. 99TH8470) (pp. 129-134). IEEE.

[73] Srinivasan, H., & Gadh, R. (2000). Efficient geometric disassembly of multiple components from an assembly using wave propagation. Journal of Mechanical Design, 122(2), 179-184.

[74] Lee, K., & Gadh, R. (1998). Destructive disassembly to support virtual prototyping. IIE transactions, 30(10), 959-972.

[75] Shyamsundar, N., & Gadh, R. (1999). Geometric abstractions to support disassembly analysis. Iie Transactions, 31(10), 935-946.

[76] Yu, J., & Wang, C. (2013). Method for discriminating geometric feasibility in assembly planning based on extended and turning interference matrix. The International Journal of Advanced Manufacturing Technology, 67(5-8), 1867-1882.

[77] Ben Hadj, R., Trigui, M., & Aifaoui, N. (2015). Toward an integrated CAD assembly sequence planning solution. Proceedings of the Institution of Mechanical Engineers, Part C: Journal of Mechanical Engineering Science, 229(16), 2987-3001.

[78] Vyas, P., & Rickli, J. L. (2016, August). Automatic Extraction and Synthesis of Disassembly Information From CAD Assembly STEP File. In ASME 2016 International Design Engineering Technical Conferences and Computers and Information in Engineering Conference (pp. V004T05A042-V004T05A042). American Society of Mechanical Engineers.

[79] Zha, X. F., & Du, H. (2002). A PDES/STEP-based model and system for concurrent integrated design and assembly planning. Computer-Aided Design, 34(14), 1087-1110.

[80] Gottipolu, R. B., & Ghosh, K. (2003). A simplified and efficient representation for evaluation and selection of assembly sequences. Computers in Industry, 50(3), 251-264.

[81] Briceno, J. J., & Pochiraju, K. (2007, July). Automatic disassembly plan generation from CAD assembly models. In 2007 IEEE International Symposium on Assembly and Manufacturing (pp. 64-69). IEEE.

[82] Bedeoui, A., Benhadj, R., Trigui, M., & Aifaoui, N. (2018). Assembly plans generation of complex machines based on the stability concept. Procedia CIRP, 70(1), 66-71.

[83] Pintzos, G., Triantafyllou, C., Papakostas, N., Mourtzis, D., & Chryssolouris, G. (2016). Assembly precedence diagram generation through assembly tiers determination. International Journal of Computer Integrated Manufacturing, 29(10), 1045-1057.

[84] Tao, S., & Hu, M. (2017). A contact relation analysis approach to assembly sequence planning for assembly models. Computer-Aided Design and Applications, 14(6), 720-733.

[85] Su Q. Computer aided geometric feasible assembly sequence planning and optimizing. The International Journal of Advanced Manufacturing Technology 2007; 33(1-2), 48-57.

[86] Ou LM, Xu X. Relationship matrix based automatic assembly sequence generation from a CAD model. Computer-Aided Design 2013; 45(7), 1053-1067.

[87] Iacob R, Popescu D, Carutasu N. Development assembly/disassembly process simulation platform. Proc Manufacturing System 2013; 8: 15–24.

[88] Ben Hadj, R, Trigui M., Aifaoui N. Toward an integrated CAD assembly sequence planning solution. Proceedings of the Institution of Mechanical Engineers, Part C: Journal of Mechanical Engineering Science 2015; 229(16), 2987-3001.

[89] Su, Q. (2007). Computer aided geometric feasible assembly sequence planning and optimizing. The International Journal of Advanced Manufacturing Technology, 33(1-2), 48-57.

[90] Lambert, Alfred JD. "Disassembly sequencing: a survey." International Journal of Production Research 41.16 (2003): 3721-3759.

[91] Viganò, R., & Gómez, G. O. (2013). Automatic assembly sequence exploration without precedence definition. International Journal on Interactive Design and Manufacturing (IJIDeM), 7(2), 79-89.

[92] Zhang, H. C., & Kuo, T. C. (1997, October). A graph-based disassembly sequence planning for EOL product recycling. In Twenty First IEEE/CPMT International Electronics Manufacturing Technology Symposium Proceedings 1997 IEMT Symposium (pp. 140-151). IEEE.

[93] Go, T. F., Wahab, D. A., Rahman, M. A., Ramli, R., & Hussain, A. (2012). Genetically optimised disassembly sequence for automotive component reuse. Expert Systems with Applications, 39(5), 5409-5417.

[94] Kheder, M., Trigui, M., & Aifaoui, N. (2017). Optimization of disassembly sequence planning for preventive maintenance. The International Journal of Advanced Manufacturing Technology, 90(5), 1337-1349.

[95] Tang, Y., Zhou, M., & Caudill, R. J. (2001). An integrated approach to disassembly planning and demanufacturing operation. IEEE Transactions on Robotics and Automation, 17(6), 773-784.

[96] Belhadj, I., Trigui, M., & Benamara, A. (2016). Subassembly generation algorithm from a CAD model. The International Journal of Advanced Manufacturing Technology, 87(9), 2829-2840.

[97] Trigui, M., Belhadj, I., & Benamara, A. (2017). Disassembly plan approach based on subassembly concept. The International Journal of Advanced Manufacturing Technology, 90(1-4), 219-231.

[98] Wu, N., & Peng, Q. (2009, January). Maintainability evaluation based on the product disassembly analysis. In International Design Engineering Technical Conferences and Computers and Information in Engineering Conference (Vol. 49057, pp. 101-109).

[99] Ou, L. M., & Xu, X. (2013). Relationship matrix based automatic assembly sequence generation from a CAD model. Computer-Aided Design, 45(7), 1053-1067.

[100] Yu, J., & Wang, C. (2013). Method for discriminating geometric feasibility in assembly planning based on extended and turning interference matrix. The International Journal of Advanced Manufacturing Technology, 67(5-8), 1867-1882.

[101] Perrard, C., & Bonjour, E. (2013). Unification of the a priori inconsistencies checking among assembly constraints in assembly sequence planning. The International Journal of Advanced Manufacturing Technology, 69(1-4), 669-685.

[102] Kheder, M., Trigui, M., & Aifaoui, N. (2017). Optimization of disassembly sequence planning for preventive maintenance. The International Journal of Advanced Manufacturing Technology, 90(5-8), 1337-1349.

[103] Kuo, T. C. (2000). Disassembly sequence and cost analysis for electromechanical products. Robotics and Computer-Integrated Manufacturing, 16(1), 43-54.

[104] Ben Hadj, R., Trigui, M., & Aifaoui, N. (2015). Toward an integrated CAD assembly sequence planning solution. Proceedings of the Institution of Mechanical Engineers, Part C: Journal of Mechanical Engineering Science, 229(16), 2987-3001.

[105] Gottipolu, R. B., & Ghosh, K. (2003). A simplified and efficient representation for evaluation and selection of assembly sequences. Computers in Industry, 50(3), 251-264.

[106] Briceno, J. J., & Pochiraju, K. (2007, July). Automatic disassembly plan generation from CAD assembly models. In 2007 IEEE International Symposium on Assembly and Manufacturing (pp. 64-69). IEEE.

[107] Peng, Q., & Chung, C. (2007). Analysis of part accessibility in product disassembly. Computer-Aided Design and Applications, 4(5), 695-704.

[108] Emmanuel, S. O., & Chinedu, E. (2013). Automation of generation of models for disassembly process planning for recycling. In World Congress on Engineering (Vol. 3).

[109] Giri, R., & Kanthababu, M. (2015). Generating complete disassembly sequences by utilising two-dimensional views. International Journal of Production Research, 53(17), 5118-5138.

[110] Rashid, M. F. F., Hutabarat, W., & Tiwari, A. (2012). A review on assembly sequence planning and assembly line balancing optimisation using soft computing approaches. The International Journal of Advanced Manufacturing Technology, 59(1), 335-349.

[111] Yang, L. Y., Zhao, G., Wu, B. B., & Yan, G. R. (2011). Assembly Sequence Planning for Aircraft Component Based on Improved Clashes Matrix. In Applied Mechanics and Materials (Vol. 88, pp. 22-28). Trans Tech Publications Ltd.

[112] Wilson, R. H., & Latombe, J. C. (1994). Geometric reasoning about mechanical assembly. Artificial Intelligence, 71(2), 371-396.

[113] Yan, E., Ding, Y., & Zhu, Q. (2010). Mapping library and information science in China: A coauthorship network analysis. Scientometrics, 83(1), 115-131.

[114] Leydesdorff, L., & Schank, T. (2008). Dynamic animations of journal maps: Indicators of structural changes and interdisciplinary developments. Journal of the American Society for Information Science and Technology, 59(11), 1810-1818.

[115] Tizghadam, A., & Leon-Garcia, A. (2010). Betweenness centrality and resistance distance in communication networks. IEEE network, 24(6), 10-16.

[116] Espejo González, R., Lumbreras Sancho, S., Ramos Galán, A., Huang, T., & Bompard, E. (2019). An extended metric for the analysis of power-network vulnerability: the line electrical centrality.

[117] Agathokleous, A., Christodoulou, C., & Christodoulou, S. E. (2017). Robustness and vulnerability assessment of water networks by use of centrality metrics. European Water Resources Association, 58, 489-495.

[118] Giustolisi, O., Ridolfi, L., & Simone, A. (2020). Embedding the intrinsic relevance of vertices in network analysis: the case of centrality metrics. Scientific reports, 10(1), 1-11.

[119] Lambert AJD, Gupta SM. Methods for optimum and near optimum disassembly sequencing. International Journal of Production Research 2008; 46(11), 2845-2865.

[120] Yi J, Yu B, Du L, Li C, Hu D. Research on the selectable disassembly strategy of mechanical parts based on the generalized CAD model. The International Journal of Advanced Manufacturing Technology 2008; 37(5-6), 599-604.

[121] Chang, MML, Ong SK, Nee AYC. Approaches and Challenges in Product Disassembly Planning for Sustainability. Procedia CIRP 2017; 60, 506-511.

[122] ISO 10303-21:2002 Industrial automation systems and integration -- Product data representation and exchange -- Part 21: Implementation methods: Clear text encoding of the exchange structure

[123] Ungerer, M., & Buchanan, K. (2002). Usage Guide for the STEP PDM Schema Release 4.3. In PDM Implementor Forum.

[124] Pan, C. (2005). Integrating CAD files and automatic assembly sequence planning.

[125] Riggs, R. J., & Hu, S. J. (2013). Disassembly liaison graphs inspired by word clouds. Procedia CIRP, 7, 521-526.

[126] MOYER, L. K., & GUPTA, S. M. (1997). Environmental concerns and recycling/disassembly efforts in the electronics industry. Journal of Electronics Manufacturing, 7(01), 1-22.

[127] Gungor, A., & Gupta, S. M. (1998). Disassembly sequence planning for products with defective parts in product recovery. Computers & Industrial Engineering, 35(1-2), 161-164.

[128] Favi, C., Germani, M., Mandolini, M., & Marconi, M. (2012). LeanDfd: a design for disassembly approach to evaluate the feasibility of different end-of-life scenarios for industrial products. In Leveraging technology for a sustainable world (pp. 215-220). Springer, Berlin, Heidelberg.

[129] Tang, Y., Zhou, M., Zussman, E., & Caudill, R. (2002). Disassembly modeling, planning, and application. Journal of Manufacturing Systems, 21(3), 200.

[131] Li, W. D., Xia, K., Gao, L., & Chao, K. M. (2013). Selective disassembly planning for waste electrical and electronic equipment with case studies on liquid crystaldisplays. Robotics and Computer-Integrated Manufacturing, 29(4), 248-260.

[133] Joshi, A. D. (2017). Optimal end-of-life decision-making strategies for products with design alternatives (Doctoral dissertation, Northeastern University Boston).

[134] Kuo, T. C., Huang, S. H., & Zhang, H. C. (2001). Design for manufacture and design for 'X': concepts, applications, and perspectives. Computers & industrial engineering, 41(3), 241-260.

[135] Vinodh, S., Kumar, R. P., & Nachiappan, N. (2012). Disassembly modeling, planning, and leveling for a cam-operated rotary switch assembly: a case study. The International Journal of Advanced Manufacturing Technology, 62(5-8), 789-800.

[136] Kang, C. M., Kwak, M. J., Cho, N. W., & Hong, Y. S. (2010). Automatic derivation of transition matrix for end-of-life decision making. International journal of production research, 48(11), 3269-3298.

[137] Gungor, A., & Gupta, S. M. (1999). Issues in environmentally conscious manufacturing and product recovery: a survey. Computers & Industrial Engineering, 36(4), 811-853.

[138] Rose, C. M., Beiter, K. A., & Ishii, K. (1999, May). Determining end-of-life strategies as a part of product definition. In Proceedings of the 1999 IEEE International Symposium on Electronics and the Environment (Cat. No. 99CH36357) (pp. 219-224). IEEE.

[139] Bhasin, J. (2019, August 19). Graph Analytics — Introduction and Concepts of Centrality. Medium. https://towardsdatascience.com/graph-analytics-introduction-and-concepts-of-centrality-8f5543b55de3.

[140] Disney, A. (2021, February 8). Social network analysis: Centrality measures. Cambridge Intelligence. https://cambridge-intelligence.com/keylines-faqs-social-network-analysis.

[141] Bastian, M., Heymann, S., & Jacomy, M. (2009, March). Gephi: an open source software for exploring and manipulating networks. In Proceedings of the International AAAI Conference on Web and Social Media (Vol. 3, No. 1).

ABSTRACT

PREDICTING THE GEOMETRICAL DISASSEMBLY FEASIBILITY OF MECHANICAL ASSEMBLIES IN DESIGN PHASE

by

HEADER M. ALRUFAIFI

May 2021

Advisor: Dr. Jeremy L. Rickli

Major: Industrial Engineering

Degree: Doctor of Philosophy

Disassembly of products has gained more and more attention due to the economic, environmental, and social benefits and the contribution to the protection of natural resources [1]. Where, disassembly is the first and usually the most critical and challenging process in most recovery processes (i.e. remanufacturing, reuse, maintenance, and recycling processes) which are essential reverse flows in circular economy systems. As policies, regulations, products, and systems move towards and strive for a circular economy, it is increasingly vital that disassembly analysis, models, and methods are feasible during development and manufacturing life-cycle stages. However, checking disassembly feasibility is considered a critical step [2, 3] in determining the geometrical feasible disassembly sequence. Thus, today's designers need new tools allowing them in the early stage of assembly's life (i.e. design phase) generating, evaluating, and verifying the feasibility of disassembling an assembly, determining disassembly sequence feasible in geometrical aspects , and predicting the change happens in the geometrical disassemble feasibility in the assembly's lifetime due to corrosion. In this dissertation, I worked on determining geometrical feasible disassembly sequences by checking the disassemble feasibility of components of an assembly by considering the types of relationships among components and

summarizing all these disassembly sequences in one precedence matrix. Then, using the developed precedence matrix in predicting the change in geometrical disassemble feasibility that may happen due to corrosion between assembly's' parts in active lifetime of the assembly.

In Chapter 2, we focused on using component interaction data from CAD design models to automatically extract critical disassembly information for contact and non-contact assembly's parts. In Chapter 3, we focused on construct a precedence matrix from proven collision tests of contact, non-contact constraints. In Chapter 4, we focused on predicting changes in the geometrical disassemble feasibility of an assembly during its lifetime in early design phase. The success of this work improves the design of disassembly while it provides tools for designers to know the geometrical feasible disassembly sequences and know make the do a recommendation for the best time in assemblies' lifetime to disassemble it and get the most of its part in tact to reused the assemblies parts in future recovery processes.

AUTOBIOGRAPHICAL STATEMENT

Header M. Alrufaifi is currently a doctoral candidate in the department of The Industrial and Systems Engineering at Wayne State University. He received an M.Sc. degree in Mechanical Engineering from the University of Baghdad - Baghdad, Iraq in 2012. Before that, he received a B.Sc. degree in Production Engineering from the University of Technology - Baghdad, Iraq in 2006. His primary research interests include studying the geometrical disassembly feasibility in the early design phase of mechanical assemblies to improve disassembly design. His research has been published at 26th CIRP Life Cycle Engineering (LCE) Conference. He has participated in many conferences at WSU. He also received an NSF travel award to attend the CIRP conference. Header will start as an assistant professor in the department of Mechanical engineering at Wasit University - Kut, Iraq in Fall 2021.